COAL GASIFICATION IN AN EXPERIMENTAL FLUIDIZED-BED REACTOR

by

DEBASHIS NEOGI

B. Tech. ChE. Indian Institute of Technology, Kharagpur, India, 1981

A MASTER'S THESIS

submitted in partial fulfillment of the

requirements for the degree

MASTER OF SCIENCE

Department of Chemical Engineering

KANSAS STATE UNIVERSITY
Manhattan, Kansas

1984

Approved by

Walter P. Walawender

Major Professor

TABLE OF CONTENTS

LIST OF TABLES

LIST OF FIGURES

ACKNOWLEDGEMENT

I should like to express my sincerest thanks to Dr.W.P.Walawender and Dr.L.T.Fan for their invaluable guidance, encouragement and advice during the entire course of this work. I sincerely thank Dr.L.E.Erickson for consenting to sit on my committee.

I also wish to thank my colleagues Mr.Snehal A.Patel, Mr.S.K.Singh and Mr.C.C.Chang for their help, suggestions and criticisms. I should like to express my appreciation to Mr.D.Morey, Mr.Mike Grady and Mr.Mike Lafebere for their assistance in the experimentation. A special thanks goes to my roommate Mr.Millend K.Gupta for helping me with my drawings.

I should like to express my sincere gratitude to my parents who provided me with continuous encouragements and advices during my stay in U.S.A.

The financial support has been provided by the Engineering Experiment Station (Hydrogen Project) of Kansas State University. All experimental work has been performed at the Department of Chemical Engineering, Kansas State University, Manhattan, Kansas.

Lastly, I wish to thank Pat Morris and Janet Vinduska for their help in typing this manuscript.

THE ENERGY PARABLE

Long before time began, we had problems with energy shortages. You will recall that according to Freud's Oedipus Legend, the Primeval Father slept late, got all the choice cuts and did a little hunting and fishing when he felt like it. The Primeval Mother serviced the Father and did all the cooking and cleaning. The Brother Clan mostly laid around camp all day drinking and shooting craps. One day the Primeval Father returned from shooting and fishing and found that his supper was not ready. When he demanded an explanation, the Primeval Mother said, "There ain't no supper because there ain't no fire because ain't no wood." So the Father confronted the Brother Clan and they said, "That ain't our job. Besides all the close-in wood is gone, burnt up, we got to move camp to a new wood supply." At that the Father grew wroth and told them, "I have just appointed myself Energy Czar. You lazy louts get out there and get some wood right now, you get no supper 'til it's done." Well, you know what happened. The Brother clan revolted, killed the Primeval Father, confiscated the Primeval Mother, moved camp out of the Garden of Eden, and we have been looking for a new energy supply ever since.

CHAPTER I

INTRODUCTION

The decline in the availability of domestic reserves of petroleum and natural gas fuels, coupled with the increasing reliability problems in the supply of imported fuels has generated a renewed interest in the utilization of U.S. coal reserves. The concept of coal conversions to produce a more useful or convenient form of energy has been known for many years, and various processes have been explored to accomplish this task. Thermal gasification has been proposed as one technical options for the conversion of coal to gaseous fuels and/or chemicals. Although many contacting devices have been proposed for coal gasification, fluidized beds are widely used because of their advantageous characteristics, such as high rates of heat transfer and excellent gas solid contacting.

The objectives of this thesis are, 1) to experimentally study the gasification of Kansas coal in a bench scale fluidized-bed reactor, and 2) to develop a mathematical model to describe the steady-state and transient behavior of the experimental reactor.

Chapter II reviews the literature on the gasification of coal. The review discusses coal gasification technology, the various steps in coal gasification processes, and the advantages of using a fluidized-bed reactor for the gasification of coal.

Chapter III presents the results of the experimental study on the gasification of Kansas coal. The effect of the reactor temperature on the product gas composition, mass and volumetric yields, gas heating value, energy recovery and carbon conversion were determined. A mechanism was postulated to identify the dominant chemical reactions in different temperature regimes.

Chapter IV presents a model to describe the experimental fluidized-bed coal gasification process. The model assumed a reaction mechanism which

took into account the devolatization of coal, char gasification, and water-gas shift reaction. Both the dynamic behavior and steady-state performance of the gasifier were simulated based on the model. The results of the simulations were compared with the experimental data.

Chapter V summarizes the major conclusions of this thesis and outlines the recommendation for extension of this work.

CHAPTER II

LITERATURE REVIEW

Coal as an Alternative Energy resource.

Owing to the dwindling supply of energy and raw materials since mid-seventies, everyone is aware that a rational and economic use of resources, particularly energy resources, is the real challenge facing the world economy. As the price of our petroleum and natural gas resources increase and supplies diminish, increased emphasis will be placed upon the development of alternative sources of energy. Today, petroleum and natural gas account for 75% of the total energy consumption of the United States. Furthermore, about 50% of our petroleum is imported. It is, therefore, essential that alternative sources of energy be developed in order that the country's economic growth of energy consumption, can be maintained. As much there is a pressing need to conserve known supplies of crude oil and establish processes for the production of synthetic liquid fuels and gases.

Coal is clearly our most abundant fossil resource and must play a key role in supplying energy and chemicals for the remainder of this and all of the next century. As such the conversion of the nation's vast resources of coal to liquid and gaseous fuels has been envisioned as a major contributor to the energy picture in the near future. There is an urgent need for a strong, balanced energy program involving the direct combustion of coal and the conversion of coal to gaseous and liquid fuels. In addition, new and improved technology in these areas must assure environmental protection. For coal to play a significant role in our energy future, utilization cannot be restricted to the use of only premium coal; that is, the types of coal with low sulfur, low ash, and non-caking characteristics. Research must be pursued into the utilization of our total coal reserves.

Various processing options are being explored to convert coal into fuels and useful chemicals. The most important factor concerning the

potential utilization of coal is its conversion flexibility. Although coal is relatively stable as a storehouse of energy and chemicals, it can be treated in a few different but basically simple ways in order to release these values usefully. Coal has been available to man for a long time; it is natural that it should have been used in many different ways and also that the balance of usage has changed from time to time as needs varied and technology developed. The evolutionary process of changing pattern of use is probably now a critical point; the next decades are likely to see a more rapid adoption of the role of coal than ever before. In general most of the coal conversion technologies can be classified into the thermochemical category. The main approaches for converting coal into an improved non-polluting energy source are:

(1) Coal combustion to produce heat, steam, and/or electricity;

(2) Coal pyrolysis to produce gas, pyrolytic liquids, char, and chemicals;

(3) Coal gasification to produce low or intermediate BTU gas; and

(4) Coal liquefaction to produce liquid fuels. The different ways of converting solid coal into liquid are e. g. non-catalytic liquid phase dissolution or solvent extraction, direct catalytic hydrogenation, pyrolysis, etc.

In this work, the gasification of coal is considered. The term gasification signifies the thermal reaction of solid fuels with air, oxygen, steam, carbon dioxide, or mixture of these, to yield a gaseous product that is suitable for use either as a source of energy or as a raw material for the synthesis of chemicals, liquid fuels, or other gaseous fuels. Thus, gasification yields a product that can be handled with maximum convenience and minimum cost, and in addition, greatly extends the uses to which solid fuels may be put. For both technical and economic reasons, most gasification

processes for synthesis gas production or for the production of energy as gaseous fuel, strive for total gasification of the solid fuel.

The science and technology of the complete gasification of coal have advanced significantly due to the considerable expansion in basic research on the fundamental chemistry and physics of gasification reactions, and on gasification and purification processes. This expansion effort stems in part from increased interest in the use of gas as a raw material for the synthesis of chemicals and liquid fuels and in part from the need to develop methods for gasifying coal and other solid fossil fuels to ensure the long-range supply of energy in the form of gaseous fuel.

Coal gasification technology.

The gasification of coal is not a new technology. However, interest in the United States has increased significantly over the last fifteen years. von Fredersdorff and Elliot (1963) reviewed a variety of gasification processes in great detail. More recent reviews include those of Howard-Smith and Werner (1976), Simeons (1978), Massey (1979), Howell (1979), and Grainger et al. (1981). Figure 1 (Grainger et al., 1981) illustrates the different stages and uses of coal gasification.

While the basic concept in all coal gasification processes is to decompose the coal by exposure to heat with subsequent reaction of the residual char with the oxidative environment, considerable variations in operating conditions and contacting paterns exists. These variations stem primarily from the form and nature of the product desired from the gasification process. There are scores of proposed processes in the literature. Some of them are for producing high-heating-value gas suitable for introduction into pipelines; some for producing low- to medium-heating-value gas which can be used locally and there are those processes in which liquids or solids are the major end product.

Coal gasification processes are comprised of four steps (Howell, 1979). The importance of each step depends upon the nature of the coal feed-stock, the contracting patern employed, and the desired forms of end product. The four steps are:

(1) Coal Pretreatment

(2) Primary Gasification

(3) Secondary Gasification

(4) Purification and Product Gas Alteration

Pretreatment

Pretreatment involves alteration of coal into a feedstock which is amenable to the conversion process employed. Most bituminous coals exhibit swelling and softening tendencies when exposed to elevated temperatures (Van Krevelen, 1956). This tendency is called caking, and is usually characterized by the coal's free swelling index (FSI). Many processes using fluidized beds or moving bed reactors are unable to accommodate caking behavior without experiencing bed agglomeration problems. Fresh coal suddenly injected into an active fluidized bed gasifier becomes heated to reactor temperature almost instantaneously. Pyrolysis reactions and steam-coal reactions are much too slow to maintain that thermal pace; hence the particle melts and upon touching others of like kind, agglomerate to form larger particles (Massey, 1979). Defluidization and collapse of the bed follow rapidly, with severe caking of the collapsed material to form hard, difficult-to-remove deposits and an inoperable system.

Much effort has been expended to combat this tendancy, largely by preoxidation of the coal to destroy its caking tendency. Gasior et al. (1967) reported success with a 20 ft of free fall through steam containing 5.5 mol % nf oxygen at coal temperatures of 583-703 K and at 1.82-2.38 MPa. They were

successful in converting Pittsburg seam coal (0.635-0.9525 cm) from an initial free swelling index (FSI) of 8.0 to final values of 1.5-2.0; the product remained uncaked when exposed to hydrogen at 873 K. Pretreatment reduced the volatile content from 35.6% to 24.9% and particle density by about 50%. Kavlic and Lee (1967) reported success with fluidized bed pretreatment of coal at 660-680 K, 0.1 MPa pressure, and about 1-2 hours residence time, consuming 0.0624-0.0937 scm oxygen per kg coal treated. Their work showed a similar decrease of volatile content. For the pretreatment to be practical, the correct combination of temperature, coal residence time and oxygen concentration must be used to accomplish decaking without an excessive loss of coal's volatile matter.

There are several processes in which it is possible to handle various types of caking coal without pretreatment. In the Hydrane process, developed by the U.S. Bureau of Mines (Feldman, 1972), crushed raw coal is fed to a two-zone hydrogenation reactor operated at 7 MPa and 1173 K. In the first zone, the coal falls freely as a dilute cloud of particles through hydrogen-rich gas. As the coal is heated in this zone, it loses its volatile matter and agglomerating characteristics. The remaining char falls into a fluidized bed reactor and undergoes futher gasification. There are also liquid medium gasifiers which can treat caking coal. These fall into two general categories, operating at distinctly different temperatures. Molten salt-reactors, generally employing molten sodium carbonate, operate at about 1755 K. Such temperature levels permit no hydrocarbons to survive long enough to appear in the product gas, especially in the molten iron system. The atgas process injects the dried crushed coal into a molten iron bath at a temperature of 1643 K and a pressure of 5 MPa (Karnavas et al., 1972). The coal is dissolved by the molten iron where the volatile matter cracks in the presence

of oxygen and steam to produce a gas composed of hydrogen and CO. One great advantage of this process is the removal of sulfur from the raw gas product by the molten iron. Similar to the Atgas process, the Molten Salt process (Cover, 1973) injects coal, steam and oxygen into a molten bath of sodium carbonate at 1273 K and 3 MPa. The Char Oil Energy Development (COED) process treats caking coals in a different manner from the processes mentioned earlier. In this process, coal passes through a series of progressively hotter fluidized bed reactors. In each reactor, a fraction of the coal's volatile matter is released, and the temperature of each bed is chosen just below the maximum temperature to which the coal can be heated without softening sufficiently to agglomerate. The number of stages and the operating temperature of each stage are determined by the caking properties of the coal used. Unlike the other gasification processes, fuel gas is not the major product from the COED process. The product distribution from an Illinois No. 6-Seam Bituminous coal was 57.1% char, 23.6% oil, 13.2% gas, and 6.1% liquid (Eddinger, 1965).

Another common problem associated with the use of coal in gasification processes is that many types of coal are high in sulfur content. To a significant extent the need for conversion of coal to gas is dictated by the desire for relief from noxious sulfur oxide emissions accompanying direct coal combustion. The case for conversion to gas is further supported by the need for abatement of particulate solids emissions to the atmosphere. All coals contain some sulfur in all three forms: combined with the organic coal substance ("organic sulfur"), combined with iron as pyrite or marcasite ("pyrite sulfur"), and combined as calcium and iron sulfates ("sulfate sulfur"). During primary gasification, studies have shown that about 70% of the coal's original sulfur content is gasified at 1273 K (Suuberg, 1978) and 85% is gasified at

2073 K (Kobayashi, 1977). In a recent survey of coal conversion technology (Howard and Smith, 1976) it was suggested that it would be more efficient and less expensive to desulfurize high-sulfur coal before use rather than to resort to stack gas cleaners to reduce sulfur pollutants to acceptable levels.

Quite a few techniques are available for the desulfurization of coal. Removal of pyritic sulfur has been accomplished using physical processes such as magnetic separation (Howard et al., 1975) and by chemical leaching techniques, such as the Ledgemont oxygen leaching process (Agarwal et al., 1975). For the removal of the organic sulfur it is necessary to have hydrogenation to produce hydrogen sulfide. However, a process, known as the Battele Hydrothermal Coal Process (BHCP), has been reported to remove 99% of the pyrite sulfur and 70% of the organic sulfur from coal using a process based on the heating of a water-coal slurry and a CaOH leaching agent at moderate temperatures and pressures (Stambaugh, 1977).

Even though many techniques are available for sulfur removal prior to the coal conversion process, the majority of the proposed gasification processes for producing pipeline quality fuel gas rely upon the removal of the sulfur pollutants from the product gas stream. It is necessary for such processes to remove carbon dioxide produced during the gasification as well. The acid gas removal measures needed for CO_2 also helps in the removal of the principal sulfur pollutant, hydrogen sulfide.

Primary Gasification

Primary gasification is also known as devolatization, carbonization, and pyrolysis. This phenomenon results from the exposure of coal to an elevated temperature. Under this condition, the coal liberates a hydrogen-rich volatile fraction which contains CO, CO_2, H_2O, CH_4, H_2S, other light

hydrocarbons, as well as tars, oils, phenols and a solid residue. This decomposition of the gaseous environment. The order of appearance of the volatile species when coal is heated at a constant rate is discussed by Howard (1963). After drying, the sequence is chemical water, CO_2, higher hydrocarbons (tars, etc.), ethane, methane, and finally H_2. The order is not precise and substantially overlapping occurs. However, a much improved picture emerges when such evidence is linked with information on the chemical structure of coal. The solid residue formed during devolatization (char) has a very high carbon content and is extremely unreactive to further thermal decomposition. The volatiles formed within a coal particle include unreacter species and species which are extremely reactive (Anthony and Howard, 1976). The unreactive volatiles escape from the particle to the surrounding environment, but only a fraction of the reactive volatiles usually escape. The volatiles that do not escape sometimes consists of highly reactive free radicals which are subjected to a variety of secondary reactions such as cracking and repolymerization. This can happen on the hot coal surface to form more stable and less reactive char and thus reduce the actual volatile yield. Since these secondary reactions are undesirable in practice, their extent can be reduced by enhancing the transport of volatile fragments away from the reactive environment, such as by operating at reduced pressures with smaller and widely dispersed particles. Yields of volatiles depend on the coal type and the conditions under which heating takes place. Proximate analysis, in which coal is slowly heated in an inert environment under precisely defined conditions, has shown the volatile matter of coal to range from less than 10% for anthracites to over 50% for lignites (Averitt, 1961). Investigations, performed using extremely rapid heating techniques under less precisely defined conditions, have shown yields of volatiles which

are substantially greater than those found by proximate analysis (Anthony and Howard, 1976).

An extensive review of the available fundamental information on devolatization of coal has been given by Anthony and Howard (1976). This phenomenon is not yet completely understood. The mechanism involved in devolatization depends on operating conditions such as temperature, pressure, particle size, constituents of the carrier gas, and the type of coal (Wen et al., 1967; Friedman et al., 1968; Anthony and Howard, 1976), as well as the heating rate (Junten and Van Heek, 1968). There are even conflicting views as to whether the net process is endothermic or exothermic.

An important part of coal science and technology has been concerned with the yields and compositions of the products formed and the rates and mechanisms of the physical and chemical changes taking place during devolatization. Depending on the rank of the coal, devolatization typically begins between 623 K and 723 K (Anthony and Howard, 1976) and forms a carbon rich residue and hydrogen rich volatile fraction. The decomposition continues until a temperature of about 1223 K is reached, which, if maintained for an extended time, results in a residue of nearly pure carbon possessing a structure approaching that of graphite. The accumulated volatiles are comprised of various gases and liquids, the relative proportions of which depend on the coal type and the manner and rate of heating. The extent of devolatization and the factors that influence it are of primary importance to gasification processes. The char resulting from this step will determine the extent of secondary gasification needed to obtain acceptable product gas yields, and the extent of gas methanation necessary to obtain pipeline quality gas.

Secondary Gasification

Secondary gasification usually concerns the gasification of the residual char from the devolatization step. The char-gas reactions may be classified into two distinct categories, namely, volumetric reactions and surface reactions (Wen and Dutta, 1979). These reactions, whether of the volumetric or surface type, take place on the external or internal surface of the char. Thus diffusion is an important step in heterogeneous char-gas reactions. The main reactions occurring are:

(a) Steam-carbon reaction

$$C+H_2O \longrightarrow CO+H_2$$

(b) Carbon-CO_2 reaction

$$C+CO_2 \longrightarrow 2CO$$

(c) Methane forming reaction

$$C+2H_2 \longrightarrow CH_4$$

(d) Water-gas shift reaction

$$CO+H_2O \rightleftharpoons CO_2+H_2$$

Reaction (a) is endothermic and does not occur unless the required heat is supplied. The methane forming reaction (c) is exothermic and is relatively slower than reaction (a) at high temperature. The water-gas shift reaction (d) is considered to be primarily heterogeneous phenomenon which occurs on the fuel surface, with very little reaction in the gas phase. It approaches thermodynamic equilibrium generally as a function of steam conversion or fuel-bed depth at a given temperature, although other important factors, such as fuel ash constituents, must be considered.

Most proposed processes employ some combination of hydrogen, steam, and oxygen to accomplish the secondary gasification reactions. When a high heating value gas is the desired end product, it is desirable to

produce as much methane as possible during the primary and the secondary gasification steps to reduce the need for downstream water-gas shift and methanation reactions. The residual fixed carbon in the char reacts with hydrogen to produce methane, but the reported rates for this reaction are relatively slow (Feldkirchner and Linden, 1963). Studies have shown that the use of high hydrogen partial pressures during primary and secondary gasification leads to a greatly increased methane production (Anthony and Howard, 1976). Also the hydrogen reacts with the reactive volatiles formed during primary devolatization to produce light hydrocarbons capable of escaping from the coal particles without further reaction. The existance of such a phenomenon occurring is supported by evidence of an increased volatile evolution in the presence of hydrogen with rates similar to that of devolatization, and by a decrease in the tars formed as the pressure of hydrogen is increased (Anthony and Howard, 1976). Inspite of the fact that hydrogen has been shown to promote the production of methane, most of the coal gasification processes make use of steam and oxygen as the gasification agents (Howard-Smith and Werner, 1976). Two notable exceptions are the Hydrane and Hygas processes which generate their needed hydrogen from the steam-oxygen gasification of residual char. The major differences between high-Btu gas producing processes and those producing low-Btu gas are as follows: the latter processes employ air in the place of oxygen, perform no downstream methanation, and operate at lower pressures.

Purification and Product Gas Alteration

Hot gas leaving the gasifier is laden with dust, gas impurities, and condensable tars, phenols, light hydrocarbons, etc. In general, most gasification processes have a gas cleaning step. This step usually involves direct water quenching or scrubbing the raw gas, followed by the use of

cyclones, sand filters, or electrostatic precipitators. The bulk removal of oils and water is accomplished by quenching or cooling, during which heavy oils are completely removed along with a large fraction of the light oils. The remaining light oil fractions in the gases are absorbed by solid absorbents.

Cool, clean, humid gases are then reheated and "shifted", if necessary to adjust the H_2/CO ratio to 3:1 for methanation. The shift conversion is normally done by the passage of part of the gas stream over a catalyst at about 290-400 K to effect the mildly exothermic reaction.

$$CO+H_2O \longrightarrow H_2+CO_2$$

The product of the converter is then blended with the unshifted portion of the total gas product to obtain the desired 3:1 ratio of H_2/CO. This process conventionally uses an iron-chromium catalyst.

Purification of the gas coming from the shift converter is essential, not only from the pollution point of view, but it also enhances the calorific value required for pipe-line quality gas. Carbon dioxide adds nothing to the heating value of the final gas and should be removed before methanation. The methanation catalysts, usually containing nickel compounds, are extremely sensitive to any contaminating sulfur. Many processes are available for the removal of CO_2 and H_2S, namely, the Benfield process, and the Selexol process (Massey, 1979).

Methanation is the final synthesis step used to upgrade the syngas to pipe-line quality gas. It accomplishes two things: First, it converts a mixture of gases of relatively low heating value into methane, which is compatible in physical properties and heating value with natural gas, and second, the methanation step reduces the CO content to nontoxic level. Details of this process is given in Massey, 1979 and ERDA review 76-67.

Fluidized-Bed Gasification of Coal

Several types of reactors have been used to gasify coal. They include fixed beds, entrained beds, moving beds, molten bath beds, and fluidized beds. Extensive reviews of each type of reactors can be found in the Energy Review No. 70 (Noyes Data Corp., 1981). The present review will mainly deal with the fluidized-bed reactor.

A stationary bed of coal becomes fluidized when the force of the gasifying agents moving through the bed is sufficient to suspend the coal particles. This requires smaller coal sizes than the fixed bed units, normally the particle size range should be 0.1 to 2 mm. Sometimes sand and/or other materials are used as the bed material. While the bed is kept in the state of fluidization coal particles are fed into the bed either from the top or side. The fluidizing action causes thorough mixing of the coal, bed materials and the gases, and the bed exhibits almost isothermal conditions.

There are several reasons why fluidization has come into wide use in the development of new gasification technology. These reasons are much the same as those which lead to the extensive use of fluidization in fluid catalytic cracking in the petroleum industry and for gas solids contacting in the nuclear area. Without such technology the petroleum industry would not have achieved the flexibility it has today in handling and refining crude oil. The principal reasons for use of fluidization are:

(1) Excellent Gas-Solid Contacting -- Since the gasification of coal necessitates intimate gas-solids mixing wherein oxygen and/or steam react with coal, fluidization is a preferred technique in which excellent gas-solids contacting is achieved in a minimum volume.

(2) Attainment of Uniform Temperature -- The uniform temperature provided by a well fluidized bed of solids enables one to operate at a variety

of temperatures. A gasifier can be operated at lower temperature to reduce thermal losses or to investigate the pyrolysis of coal. It can be operated at a higher temperature to investigate the char gasification reactions.

(3) Excellent Heat Transfer -- In addition to uniform temperature, a fluidized bed provides excellent heat transfer throughout the bed. This is especially important in processes such as CO-Gas and CO_2 Acceptor Processes where a hot circulating material is used to provide heat in the fluidized gasifier stage.

(4) Handling of Feed, type and size -- It can handle a wide variety of fuels and particle sizes. This enables one to use coal fines, as produced in modern mining operations, in gasification of coal.

(5) Solids Transfer -- While keeping coal solids fluidized in a reactor bed, the ability to move solids in and out of reactors and between reactors is excellent. By proper design, fluidized solids can be handled in transfer lines in much the same manner as a free flowing liquids.

(6) Complexity -- It is less complex than the fixed bed and has no internal moving parts.

(7) Capacity -- A fluidized bed can handle a continuous flow solids in large quantity.

(8) Safety -- Probably the greatest importance in the area of developing a new coal technology is the inherent safety involved in fluidized bed type operations. Fluidized-beds normally contain coal or char material in large amounts. This inventory of carbon in the system tends to prevent a rapid change from a reducing to an oxidizing environment within the gasifier. Interruption in the feed to fluidized-bed gasifiers can be tolerated for extended periods without any concern for a

process upset or a safety problem. Also, because of the high heat capacity of the fluidized bed of solids, even the withdrawal of heat input into the bed over minutes or even hours can be accommodated with the ability to go back on line quickly without the hazard of late combustion or any other instability as is possible with suspension type gasifiers.

(9) Product Gas -- There is less tar and phenol in the product gas. Due to uniform conditions in the bed the composition of the gas remains reasonably constant.

(10) Turndown Capability -- Should it be necessary or desirable, a fluidized bed system provides a simple means by which gasifier output can be reduced (or later increased) over fairly wide levels while maintaining uniform composition in product gas.

(11) Ash Removal -- Ash removal is quite simple in a fluidized-bed reactor and may be done either from the side or from the bottom.

Limitations. The fluidized bed is less developed than fixed bed and till now has a poorer commercial market. Proper design of the distributor plate is very important for successful operation of the fluidized bed. The capacity of the gasifier is sometimes limited because of entrainment at high gas velocities. Caking coal sometimes requires pretreatment because of agglomeration problems. But recent studies at Kansas State University (Walawender et al., 1981) shows that agglomeration can be eliminated by using a mixture of limestone and sand for the bed material. The operating range is limited by the gas velocity required to maintain fluidization and an acceptable rate of ellutriation. In spite of these limitations, fluidization is still preferable because of its flexibility and many advantages.

To successfully design a commercial fluidized system which is economically viable, a vast amount of research and development is needed. While the technology of gasification had been available for quite sometime, its development was superceded by the growth in importance of petroleum. Only in the last fifteen years have some studies on gasification of coal, particularly in fluidized beds, beed done. Most of the research done in coal conversion using a fluidized bed was related to coal combustion. For gasification, generally pilot-scale experiments were conducted, and bench or laboratory scale experiments be carried out in small bench-scale reactors in order to provide information for the design of commercial fluidized-bed reactors. Matsui et al. (1984), Yeboah et al. (1980), Wen et al. (1973), Caram et al. (1979), and Dobner et al. (1975) are some of the researchers who conducted theoretical and experimental studies related to gasification of coal and/or char in fluidized-bed reactors.

Researchers at Kansas State University have conducted extensive studies on the gasification of carbonaceous materials in fluidized-bed reactors. Walawender and Fan (1978) reported preliminary results on the gasification of feedlot manure in a 0.23 m I.D. fluidized-bed reactor. One of the problems discussed in this work was agglomeration of the bed when the system was operated in a reducing atmosphere for more than 7 to 8 hours. Others who reported similar problems were Burton (1972) for municipal sewage sludge and Smith et al. (1982) for Australian coal. Walawender et al. (1981) found that limestone if used as bed additive prevents agglomeration and subsequent choking of the bed.

Work at Kansas State University included a study on the generation of fuel gas by gasification of Kansas bituminous coal (Howell, 1979). The gasification experiment was carried out in a 0.0508 m I.D. fluidized-bed

reactor at atmospheric pressure over a temperature range of 973 K to 1373 K. Using a feedstoch which consisted of 90% sand and 10% coal, and a superficial velocity of 36.7 cm/sec, it was found that caking problems of the coal could be eliminated. Steam was used as the fluidizing medium. The heating value of the gaseous product ranged from 18 MJ/m^3 at 973 K to 11.9 MJ/m^3 at 1373 K. Gas yields were 0.221 m^3/kg at 973 K and 0.99 m^3/kg at 1373 K. A typical gas composition reported at a temperature of 1000 K was 48 mole % H_2, 15 mole % CO_2, 12 mole % CO, 17 mole % CH_4, 2-3 mole % C_2H_4. ;=2 mole % C_2H_6, and traces of hydrogen sulphide.

REFERENCES CITED

Agarwal, J. C., R. A. Gilberti, P. F. Irminger, L. J. Petrovic, and S. S. Sareen, Mining Congress Journal, pp. 40, March (1975).

Anthony, D. B. and J. B. Howard, "Coal Devolatization and Hydrogasification," AIChE Journal, Vol. 22, No. 4 (1976).

Averitt, P., "Coal Reserves of the United States," U.S. Geological Survey Bulletin 1136 (1961).

Burton, R. S., "Fluid Bed Gasification of Solid Waste Materials," M.S. Thesis, West Virginia University (1972).

Caram, H. S. and N. R. Amundson, "Fluidized Bed Gasification Reactor Modeling. 1. Model Description and Numberical Results for a Single Bed," Ind. Eng. Chem. Process Des. Dev., Vol. 18, 1 (1979).

Cover, A. E., "The Kellog Coal Gasification Process," Synthetic Gas Production Symposium, AIChE, New York (1973).

Dobner, S., R. A. Graff, and A. M. Squires, "Analysis of Trials of Synthane Steam Oxygen Fluid Bed Gasification Process," Presented at 68th Annual AIChE Meeting, Los Angeles, Nov. 16-20 (1975).

Eddinger, R. T., "Char Oil Energy Development," FMC Technical Report PCR-469 (1965).

Energy Technology Review No. 70, "Coal Gasification Process," Ed. P. Nowacki, Noyes Data Corporation, Park Ridge, N.J. (1981).

ERDA Review 76-67, "Energy from Coal: A State-of-the-Art Review," Prepared for: Office of Fossil Energy, U.S. Energy Research and Development Administration, Under Contract No. E(49-18)-2225 (----).

Fan, L. T. and W. P. Walawender, "Pyrolytic Conversion of Carbonaceous Solids to Fuel Gas in Quartz Sand Fluidized Bed," U.S. Patent 4,448,589 (1984).

Feldkirchner, H. L. and H. R. Linden, "Reactivity of Coals in High Pressure Gasification," Ind. Eng. Process Des. Dev., Vol. 2, 153 (1963).

Feldman, H. F., "Supplemental Pipeline Gas from Coal by Hydrane Process," Presented at 71st AIChE National Meeting, Dallas, Texas (1972).

Friedman, L. D., E. Rau, and R. T. Eddinger, "Maximizing Tar Yields in Transport Reactors," Fuel, Vol. 47, 149 (1968).

Gasior, S. J., A. J. Forney, and J. H. Field, "Decaking of Coal in Free Fall," in Fuel Gasification, pp. 1, Advances in Chemistry Series, No. 69, Am. Chem. Soc. Washington, D.C. (1967).

Grainger, L. and J. Gibson, "Coal Utilization: Technology Economics, and Policy," Pub. Grahan and Trotman, London, U.K. (1981).

Howard, H. C., "Pyrolytic Reaction of Coal," in Chemistry of Coal Utilization, pp. 340, Supplementary Volume, Ed. H. H. Lowry, Wiley, N.Y. (1963).

Howard-Smith, I. and G. J. Werner, "Coal Conversion Technology," Chemical Technology Review No. 66, Noyes Data Corp., Park Ridge, N.J. (1976).

Howard, P., A. Hanchett, and R. G. Aldrich, "Chemical Cumination for Cleaning Bituminous Coal," Presented at the Institute of Gas Technology Symposium, Chicago, Illinois, June 26 (1975).

Howell, J. A., "Kansas Coal Gasification," M.S. Thesis, Kansas State University (1979).

Juntgen, H. and K. H. Van Heek, "Gas Release from Coal as a Function of Rate of Heating," Fuel, Vol. 47, 103 (1968).

Karnavas, J. A., and others, "Atgas-Molten Iron Coal Gasification," AGA Fourth Synthetic Pipeline Gas Symposium, Chicago, Illinois (1972).

Kavlic, V. J. and B. S. Lee, "Coal Pretreatment in Fluidized Bed," in Fuel Gasifiation, Advances in Chemistry Series, No. 69, Am. Chem. Soc., Washington, D.C. (1967).

Kobayashi, H., J. B. Howard, and A. F. Sarofim, "Sixteenth Symposium (International) on Combustion," pp. 411, The Combustion Institute, Pittsburgh, PA (1977).

Massey, L. G., "Coal Gasification for High and Low Btu Fuels," in Coal Conversion Technology, Ed. C. Y. Wen and E. S. Lee, pp. 313, Addison-Wesley Publishing Company, Reading, Massachusetts (1979).

Matsui, I., T. Kojima, T. Furusawa, and D. Kunii, "Gasification of Coal Char by Steam in a Continuous Fluidized Bed Reactor," Proceedings of Fourth International Conference on Fluidization, Ed. D. Kunii and R. Toei, pp. 655-662, Pub. Engineering Foundation, N.Y. (1984).

Simeons, C., "Coal: Its Role in Tomorrow's Technology," A sourcebook on Global Coal Resources, Pergamon Press, Oxford, U.K. (1978).

Smith, I. W., "Australian Research on Flash Pyrolysis," Presented at The AIChE Winter Meeting, Orlando, Florida, Feb. 28 (1982).

Stambaugh, E. P., and others, "Environmentally Acceptable Solid Fuels by the Battelle Hydrothermal Coal Process," Battelle Columbus Laboratories, Columbus, Ohio, June 19 (1977).

Suuberg, E. M., W. A. Peters, and J. B. Howard, "Product Composition and Kinetics of Lignite Pyrolysis," Ind. Eng. Chem. Process Des. and Dev., Vol. 17, No. 1 (1978).

Van Krevlen, D. W., F. J. Huntgens, and H. N. M. Dormans, "Chemical Structure and Properties of Coal XVI-Plastic Behavior on Heating," Fuel, Vol. 35, 462 (1956).

von Fredersdorff, C. G. and M. A. Elliot, "Coal Gasification," Chemistry of Coal Utilization, Supplementary Volume, Ed. H. H. Lowry, Wiley, N.Y. (1963).

Walawender, W. P. and L. T. Fan, "Gasification of Dried Feedlot Manure in a Fluidized Bed - Preliminary Pilot Plant Tests," Presented at the 84th AIChE National Meeting, Atlanta, Georgia (1978).

Walawender, W. P., S. Ganesan, and L. T. Fan, "Steam Gasification of Manure in a Fluid Bed: Influence of Limestone as a Bed Additive," Symposium Paper: Energy from Biomass and Wastes V., Institute of Gas Technology, pp. 517-527 (1981).

Wen, C. Y., R. C. Bailie, C. Y. Lin, and W. S. Obrien, "Production of Low Btu Gas Involving Coal Pyrolysis and Gasification," Presented at the Symposium on Coal Gasification, Division of Fuel Chemistry, 165th National Meeting, Am. Chem. Soc., Dallas, Texas, April 8 (1973).

Wen, C. Y. and S. Dutta, "Rates of Coal Pyrolysis and Gasification Reactions," Chapter 2, Coal Conversion Technology, Ed. C. Y. Wen and E. S. Lee, Addison-Wesley Publishing Company, Massachusetts (1979).

Yeboah, Y. D., J. P. Longwell, J. B. Howard, and W. A. Peters, "Effect of Calcined Dolomite on the Fluidized BEd Pyrolysis of Coal," Ind. Engg. Chem. Process Des. and Dev., Vol. 19, 4 (1980).

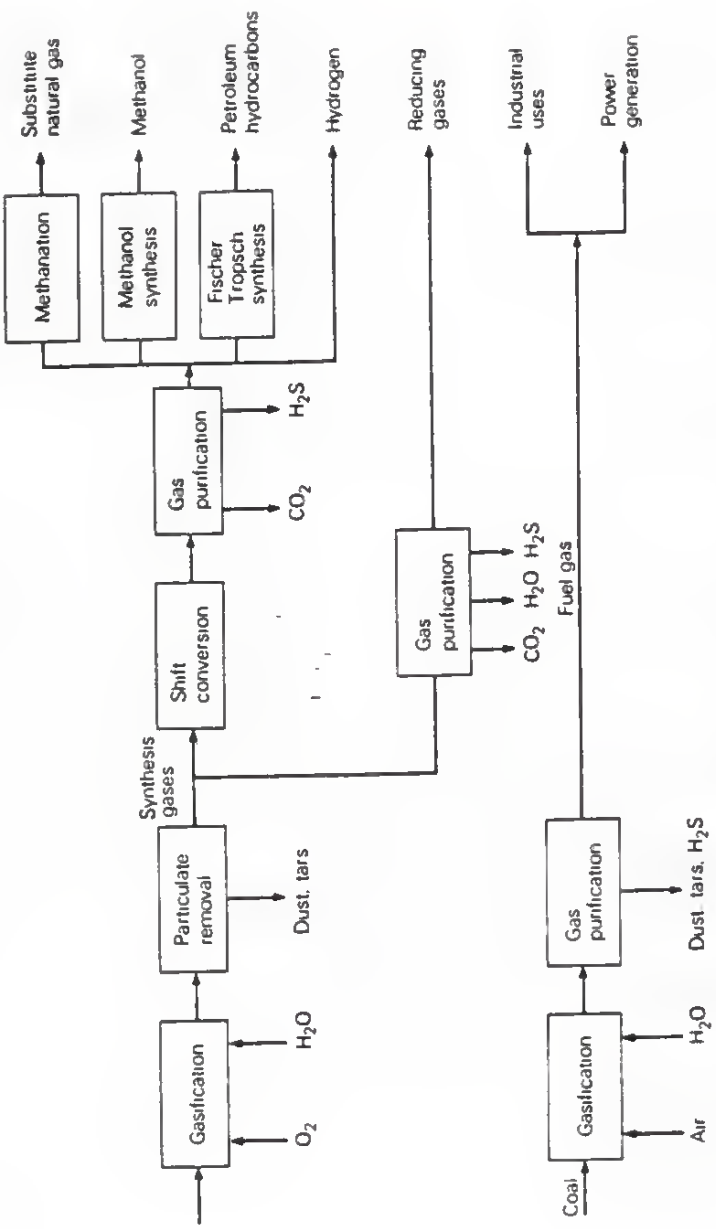

Figure 1. Different stages and uses of coal gasification.

CHAPTER III

GASIFICATION OF KANSAS COAL

INTRODUCTION

Gasification is one alternative for converting coal into a gaseous product that is suitable for use either as a source of energy or as a starting material for the synthesis of chemicals and liquid fuels. Gasification yields a product that can be handled with of convenience and minimum cost. Coal represents approximately 70% of the recoverable fossil fuel resources in the United States (Averitt, 1975). Total coal reserves in the USA amounts to 3.2×10^{12} tons as estimated by the US Department of Energy. Thus the potential for the utilization of coal to ensure a continuous supply of liquid and gaseous fuels and chemicals is undeniable. To achieve this potential, a major research effort is needed to develop economical methods to convert our most abundant fossil fuel into pollution free and more useable forms.

The gasification of coal is not a new technology. Von Fredersdorff and Elliot (1963) reviewed gasification technology up to 1963. More recent reviews include those of Howard-Smith and Werner (1976), Simeons (1978), Masey (1979), Howell (1979), and Grainger *et al*. (1981). Various processes have been conceived to convert coal to a more useful or convenient form of energy. The majority of these processes rely on the gasification of coal char with various mixtures of steam, hydrogen, and oxygen. Although many contacting devices have been proposed, fluidized beds are widely used in gasification processes because of their advantageous characteristics, such as high heat transfer rate and excellent gas-solid contacting. However, difficulties arise in operating a fluidized bed when the coal has strong caking properties and tends to agglomerate in the bed.

Thorough characterization of the feedstock is necessary for a successful reactor design. Many of the important coal properties can be

determined in the laboratory, i.e. elemental composition, porosity, density, and swelling index. Thermal analysis techniques can provide initial estimates of the behavior of coal as it undergoes heating, as a function of temperature, pressure, and the surrounding atmosphere.

Most processes for coal gasification use reactors which have large gas to solid ratios, such as moving, entrained and fluidized beds. This not only promotes the gas-solid contacting necessary for char-gas reactions, but also tends to reduce the likelihood of agglomeration when using caking coals. The Hydrane process, (Feldman, 1972), developed by the U.S. Bureau of Mines, is an example of a process which can directly use a caking coal. In the first stage of this two stage process, coal is reacted with hydrogen in a free fall zone where the dilute phase particle dispersion prevents agglomeration of the coal. In the second stage, the residual char is either consumed in synthesis gas production or used as a fuel for the process. Another advantage of this process is that only light methanation is required to remove the small amount of carbon monoxide formed during the hydrogasification step for the final product to meet the pipeline specifications. Caking coals can not be used directly in many processes; they must be pretreated by mild oxidation in order to destroy their caking tendencies (Kavlick and Lee, 1967). Some of these processes include the Hygas, Lurgi, Synthane and CO_2 Acceptor processes (Howard-Smith and Werner, 1976).

In this study a bench scale fluidized-bed reactor was used to investigate the steam gasification of a caking bituminous coal mined in Kansas. Specifically, the effect of the reactor temperature on the product gas composition and yield, heating value, carbon conversion, and energy recovery were studied. Experiments were conducted with an uniform

axial tempreature profile in the reactor and an attempt was made to maintain a constant gas phase residence time.

QUALITATIVE MECHANISM AND CHEMISTRY OF COAL GASIFICATION

The first step in coal gasification is devolatization or pyrolysis. This phenomenon results from the exposure of the coal to an elevated temperature. The devolatization typically begins at 623 K to 723 K and results in a volatile fraction containing hydrogen, CO, CO_2, H_2, CH_4, H_2S, and other light hydrocarbons, as well as tars, oils, phenols, and a highly carbonaceous solid residue. This decomposition is due to heat alone and will occur regardless of the surrounding gaseous environment. The yield composition of the volatiles and depends on the coal type, and manner and rate heating. Proximate analysis indicates that the volatile matter ranges from less than 10% for anthracites to over 50% for lignites (Averitt, 1961). However, captive sample techniques with small coal particles using rapid heating have shown that volatile yields higher than those observed by proximate analysis can be obtained (Anthony and Howard, 1976).

When heated, many types of coal undergo physical changes such as swelling and softening (Van Krevelen, 1956). As devolatization proceeds, the softening process reaches a peak and subsequently the coal resolidifies (Overturf et al., 1978). This swelling tendency is normally characterized by the coal's free swelling index (FSI). The FSI ranges in value from unity for non-caking coal, to 9 for severely caking coals. A process which utilizes a caking coal must account for this property to prevent possible agglomeration in the reactor system.

When coal is heated in a reactive gas environment, e.g., steam, devo-

latization is followed by the char gasification reactions and secondary gas phase reactions. The gas yield, product distribution, and problems associated with the swelling phenomenon are largely dependent on the type of reactor and the operating conditions.

The second step in any coal gasification process involves gasification of the char formed during the devolatization step. Air, oxygen, steam, carbon dioxide, or mixtures of these are used to increase the yield of gaseous products at the expense of the char produced in the first step. The intended use of the product gas, dictates the particular gaseous environment required. For example, combinations of oxygen and steam are used for producing low to medium heating value gases and hydrogen is used when pipeline quality gas is desired (Anthony et al., 1974). Steam gasification is convenient because steam is easily produced and readily removed from the product gas.

The following are some of the principal reactions that need to be considered in the design of a coal gasifier (Wen and Dutta, 1979):

Solid-Gas Reactions

(1) $C(s) + H_2O\ (g) \longrightarrow CO\ (g) + H_2\ (g)$

(2) $C(s) + CO_2\ (g) \longrightarrow 2CO\ (g)$

(3) $C(s) + 2H_2\ (g) \longrightarrow CH_4\ (g)$

Gas-Gas Reactions

(4) $CO(g) + H_2\ (g) \rightleftharpoons CO_2\ (g) + H_2\ (g)$

(5) Higher Hydrocarbons (g) ---> Lower hydrocarbons (g)

While these are in no way the only possible reactions in which steam can participate, they provide a basis for studying the effects of steam on the product gas.

EXPERIMENTAL

Facilities

The fluidized bed reactor used in this work was designed to study the pyrolysis and gasification of various carbonaceous materials, e.g., coal, at atmospheric pressure and over a temperature range from 650 K to 1450 K. The experimental system consisted of three sections (Figure 1); the reactor section, the gas clean-up section and the gas sampling and analysis section. The reactor consisted of four zones (Figure 2); the disengaging, the fluidized bed, packed bed and gas inlet zones. Inconel 600 alloy was used to construct the reactor because of its high temperature resistance and capacity to withstand rapid heating and cooling.

The reactor was constructed from a 10.16 cm (4-inch) I.D. by 55 cm (21.6 inch) length schedule 40 pipe. It was fitted with a pipe, 15.24 cm (6-inch) I.D. by 20 cm (7.9 inch) length, of the same material. This upper 20 cm section of the reactor served as the disengaging zone (freeboard) of the reactor. The bottom 25 cm (9.84 inch) served as the gas distribution and gas preheater zone. The top 15 cm (5.9 inch) of this zone was packed with aluminum oxide pellets (0.5 cm in diameter). The packed bed section allowed the fluidizing gas to uniformly enter the fluidized bed zone. A thermocouple was placed in the inlet zone to monitor the fluidizing gas temperature. The inlet zone was separated from the packed bed zone by a 60 mesh 316 SS screen (Opening width = 0.23 mm, open area = 30.5%) as mentioned earlier. The packed bed zone and the fluidized bed zone was also separated by an identical screen in the form of an inverted cup. The screen was held in place, from the top, by six metal studs, about 0.635 cm long welded at equal distance on the inner

wall of the reactor, from above, and by the packed bed from below. This screen prevented the percolation of the bed material into the packed bed zone. A heat resisting sealant was used, instead of gaskets, between all the flanges.

The inert matrix which made up the bed was composed of a mixture of 25% by weight of limestone and 75% by weight of silica sand. The limestone was used to eliminate bed agglomeration which typically occurred in a bed composed only of sand (Walawender et al., 1981). The limestone particle size was -7 to +50 mesh (2.82 mm - 0.287 mm), and the sand particle size was -30 to +50 mesh (0.59 mm to 0.287 mm). The static bed height was 8 - 10 cm, and the expanded bed height was 12 - 14 cm.

The reactor was heated by means of ten quarter cylindrical electrical resistance heaters, each capable of delivering up to 1200 Watts of power with a maximum sustained operating temperature of 1550 K. Five heaters were used for heating the upper part of the reactor and five for the bottom part, thus forming two distinct sets of heaters. Voltage to each set of heaters was controlled by two, three-mode, PID controllers (Omega model 49K-814). There were five thermocouples installed in the reactor. The thermocouples were of the chromel alumel type with 1/8 inch inconel sheaths. One of them was a sliding thermocouple for measuring the axial temperature profile in the reactor. The others were located at the freeboard, fluidized bed section, preheating zone, and one in the middle of the reactor inserted from the side. The controllers activated the heaters, in response to the temperatures sensed by the thermocouples, to maintain the temperature inside the reactor at a preset value. A pressure probe, connected to a manometer, indicated the bed pressure and the state of fluidization as revealed through the fluctuation of the manome-

ter level.

The feed was introduced into the reactor by gravity flow through a vertical feedpipe (3 cm I.D.) which discharged at a location about 8 cm above the static bed. A Vibra Screw Feeder (Model SCR-20), with a solid core flight screw, fed the coal particles at an uniform volumetric flowrate. The screw drive was designed with a closed loop feedback system, which immediately compensated for any variations between the actual speed and the set point. A purge flow of N_2 aided solid flow through the feedpipe and prevented gas backflow and subsequent condensation of vapor in the feeder. To prevent the feed materials from prematurely devolatizing before it reached the bed, the feedpipe was equipped with a water jacket which maintained the temperature inside the feedpipe below 400 K.

Steam served as the fluidizing medium, and was produced externally in the Sussman Hot Shot electric boiler (Model MB-6) and was supplied to the gas preheater section at a temperature around 400 K and 202.6 kPa pressure. The gas exiting from the reactor was passed through a cyclone to remove the fine solid particles, e.g., char, from the gas steam. The cyclone was well insulated and maintained itself at 500-600 K. After leaving the cyclone the gas stream was passed through two water cooled single pipe heat exchangers in series. This resulted in condensation of steam and tar, which was collected in a condensate receiver. Further gas cleaning was accomplished by means of a dry scrubber packed with glass wool. The scrubber was effective in removing the fine condensible mist traveling with the gas, without creating any appreciable pressure drop. A wet test meter connected to a strip chart recorder was used to measure the flow rate of the gas. A side draw of the off-gas was passed through

a column packed with drierite ($CaSO_4$) and then sent to an on-line process gas chromatograph for analysis. The nitrogen purge through the feed pipe was measured by a wet-test meter. The concentration of the nitrogen in the product gas along with its rate allowed computation of the product gas rate.

Procedure

To start up each experimental run, the heaters and steam generators were turned on and the controllers were set at the desired operating temperatures. During the heat-up period, air was used as the fluidizing agent and as the feed pipe purge gas. The water flow to the jacketed feed pipe was also initiated; the water maintained the feed pipe cool. The steam generator was operated in such a way that its supplied steam at constant pressure. Once steam was available, the fluidizing air flow was gradually replaced by steam. The volumetric flow rate of steam required to maintain fluidization was determined by collecting condensate, downstream from the heat exchangers and was controlled by a needle valve on the steam line.

When the bed and the freeboard reached the selected operating temperature, the axial temperature profile was measured and minor corrections made with the controllers to ensure a uniform profile. The exit-gas from the system was analyzed to ensure it was free of air. At this point, the system was ready for the feeding to begin. The total start-up time from a cold start was about two hours and about one hour from a warm start. Normally at the end of each run, the heaters were not turned off but just turned down so that the system stayed warm overnight.

A slight drop in the temperature of the reactor occurred when feeding

was initiated, but was corrected automatically by the controllers. A gas sample was taken about 5 minutes after feeding began and every 11 minutes thereafter. Condensate and nitrogen flow rates were measured every 10 minutes throughout the run. A typical experiment at a given temperature lasted 100 to 120 minutes with the last 50 and 60 minutes yielding steady gas chromatograph readings. The feed rate was evaluated by disconnecting the lower section of the feed pipe and weighing the effluent collected over three 3-minute time intervals. This was done at the start and end of run.

It was not possible to measure the total char produced in the experiment because of the hold-up of char in the bed and connecting pipes. It was also not possible to measure the total tar produced due to lack of adequate separation facilities. Also, significant quantities of tar were held up in the heat-exchangers. Consequently, overall material balances were not attempted.

Chemical Analyses

Analyses of the dry off-gas were conducted by an Applied Automation (Optichrom 2100) on-line process gas chromatograph. The components of interest were H_2, CO, CO_2, CH_4. C_2H_4, C_2H_6, C_3H_6, C_3H_8, O_2, and N_2. The chromatograph had a cycle time of 11 minutes. Moisture and ash analyses of feed material were performed according to standard ASTM procedures in a ventilated oven and muffle furnace respectively. Elemental analyses of the feed were carried out with a Perkin-Elmer model 240b elemental analyzer.

Operating Conditions

The operating conditions for all the experimental runs are summarized

in Table 1. By adjusting the steam rate according to the temperature of the run, an attempt was made to maintain a fairly constant gas phase mean residence time over all the runs. The gas phase mean residence time ranged from 4 to 7 seconds and was estimated on the basis of the reactor temperature, total dry gas flowrate, and steam rate. The steam rate was varied from 15.33 g/min. to 11.0 g/min. The average feed rate varied between 4.4 g/min. and 5.8 g/min., even though the screw-feeder setting was the same for all the experimental runs. The principal experimental variable was the reactor temperature. All the experiments were performed with an uniform axial temperature profile in the reactor and freeboard.

Feed Material

The feed material used for the experiments was Bituminous coal from Rowe coal bed located in southeast Kansas. Pretreatment of the coal included hammer milling and size classification. The proximate and ultimate analyses of the coal used are given in Table 2. The powder density of the coal was 1580 kg/cu. m. The Higher Heating Value of the coal was 30.62 MJ/kg (calculated by the Dulong formula). The coal had a Free Swelling Index of 5.5. The particle size distribution of the feed material is also given in Table 2.

METHOD OF DATA ANALYSIS

The data obtained during the last 50-60 min. of each run when the reactor was operating under steady-state condition were used for all the calculations. Each gas chromatograph cycle was treated as an individual data point. The GC readings were corrected for the nitrogen purge to give the produced gas composition. The dry produced gas analysis was used to calculate the higher heating value (HHV) of the gas using the standard heat of combustion for each component. The volumetric flowrate of the dry produced gas (nitrogen free) was determined from the difference between the rates measured by the wet-testmeter with and without coal feeding. The volumetric gas yield of the dry produced gas at 288 K and 101.3 kPa per unit mass of the DAF feed was calculated by dividing the produced gas volume flowrate by the mass flowrate of the dry ash free feed. The energy recovery was calculated as the ratio (expressed as percentage) of the product of the volumetric gas yield per unit mass of DAF feed and the gas heating value (HHV) to the heat of combustion of a unit mass of DAF feed. It represents the percentage of the energy content of the feed that appears as to combustible gas. The carbon conversion was determined as the ratio (expressed as percentage) of the atoms of carbon in the gas produced from a unit mass of DAF feed to the atoms of carbon in a unit mass of DAF feed. It represents the percentage of carbon in the feed that is converted to gaseous form. Finally, the mass yields of the gas and the mass yields of the individual gas components were calculated by converting the volumetric gas yields to a mass basis to give the masses of the gas produced per unit mass of DAF feed.

Statistical Analysis

Effect of temperature. The regression analysis was employed to determine the "best fit" polynomial relationships between the independent variable, the reactor temperature and the dependent variables, namely, the produced gas composition, produced gas heating value, volumetric yield, mass yield of the produced gas and its individual components, energy recovery and carbon conversion. First, second and third order polynomial models were fitted to the data points. An analysis of variance was also performed and this determined the significance of the regression models. The parameters determined by the regression analysis were accepted as being significant on the basis of the F-test at 5% significance level.

The criteria used for selecting the best fitting model were F-test (significance probability, PR>F), parameter significance level, and R-Square values. F - Test is used to test how well the model as a whole (after adjusting for the mean) accounts for the dependent variable's behavior. If the significance probability, labeled PR>F, is small, it indicates significance. R-Square measures how much variation in the dependent variable can be accounted for by the model. R-Square value can range from 0 to 1. In general, the larger the value of R-Square, the better is the model's fit.

Simultaneous effect of temperature and steam-to-feed ratio. In the experiments the steam rate was adjusted with the temperature in an effort to maintain a constant gas phase residence time in the reactor. Nonetheless, the results show that the residence time did vary a little from one temperature to another. Due to the adjustments made in the steam rate at

different temperatures, the steam-to-feed ratio varied (since the feed rate was maintained almost constant) with the temperature. The stepwise procedure was used for testing whether the steam-to-feed ratio along with the temperature had significant effect on the dependent variables. First, second, and third order polynomial models with temperature and steam-to-feed ratio as the independent variables, were fitted to the data points. Also the interaction term was included to test the joint effect of the two independent variables.

The stepwise procedure is useful to examine a collection of independent variables and find which of the variables should be included in the regression models. It provides five methods for stepwise regression. In the present analysis four methods were used for selecting the best model. They were,

(1) Forward Selection

(2) Backward Elimination

(3) Stepwise

(4) Maximum R-Square improvement

The details of these methods can be found in SAS User's Guide (1979).

The criteria used for selecting the best fitting model were F-test, parameter significance level, and R-Square values.

RESULTS

Effect of Temperature

The results of the regression analyses with temperature as the independent variable are summarized in Table 3. In this table, the dependent variables are denoted as y, the number of data points used for the analysis as n, the square of the correlation coefficient as R, and the F-test statistical value as F-value. Also tabulated in this table are the probability of falsely rejecting the proposed regression model, PR > F, and the estimates of the significant regression model parameters (the intercepts and the model coefficients) All the dependent variables have been shown to be functions of temperature. The R-Square values range from 0.58 to 0.96.

Produced gas composition. The variations in the concentrations of H_2, CO, CO_2, CH_4, C_2H_4, C_2H_6, C_3H_6, and C_3H_8 are shown in Figures 3 and 4. The solid lines represent the best fit polynomial regression lines. The mole percentages of H_2, C_2H_4, and C_3H_6 are best described by second order polynomial models and the rest of the gas component molar percentages by third order polynomials. The parameters of the models are given in Table 3.

The concentration of H_2 increased with an increase in temperature from 49.1% at 850 K to 60.2% at 1050 K and then decreased slightly to 59.0% at 1125 K. The concentration of CO_2 increased from 18.5% at 850 K to a maximum of 30.5% at 925 K and then decreased to 18.1% at 1125 K. The CO concentration showed the reverse trend as compared to CO_2. The mole % of CO decreased from 14.2 % at 850 K to 6.0% at 925 K and then increased to 20.9% at 1125 K. Methane decreased from 5.1% at 850 K to

2.0% at 1125 K. The minor components, C_2H_4, C_2H_6, C_3H_6, and C_3H_8, all decreased with an increase in the temperature (see Figure 5). The minor components collectively comprised only 3% of the total gas composition.

Produced gas heating value. The higher heating value (HHV) of the gas as a function of temperature is shown in Figure 5. The solid line represents the best fit regression model. The HHV is best described by a third order polynomial, the coefficients of which are given in Table 3. The HHV decreased with temperature from 16.5 MJ/m at 850 K to 10.5 MJ/m at 975 K and then increased slightly to 12.5 MJ/m at 1125 K. It should be noted that the variation of HHV of the gas was quite small; it was between 975 K and 1125 K.

Produced gas yield. The variation in the volumetric yield of the produced gas (on a dry-ash free basis) as a function of temperature is shown in Figure 6. The solid line, which is obtained from a third order polynomial, represents the regression result. The gas yield increased from 0.15 m^3/kg DAF feed at 850 K to 2.82 m^3/kg DAF feed at 1125 K.

Energy recovery. The energy recovery represents the percentage of the energy content of the feed that appears as combustible gas. Figure 7 plots the energy recovery against temperature. The data are fitted by a third order polynomial (solid line). The energy recovery increased from 8% at 850 K to 94% at 1125 K.

Carbon conversion. The carbon conversion shown in Figure 8 is the percentage of carbon in the feed converted to gas. A third order polynomial (solid line) describes the data. The carbon conversion increased with the temperature from 7% at 850 K to 82% at 1125 K.

Product gas mass yield. The mass yield of gas as a function of temperature is shown in Figure 9. The polynomial regression is represented by the solid line. The mass yield increased from 0.12 kg gas/kg DAF feed at 850 K to 1.88 kg gas/kg DAF feed at 1125 K. The mass yields of the individual components of the product gas are plotted as functions of temperature (Figures 10 and 11). The mass yield of the major components of the gas (CO, CO_2, H_2, CH_4) all increased with increasing temperature, with CO_2 and CO showing a considerable increase over the temperature range studied. The mass yields of the minor components (C_2H_4, C_2H_6, C_3H_6, and C_3H_8) remained relatively invariant with temperature.

Condensate to steam ratio. The ratio of the mass of condensate collected as the mass of steam fed to the reactor is shown in Figure 12 as a function of temperature. Note that steam was consumed in an increasing amount as the temperature increased. The condensate-to-steam ratio decreased from 1.01 at 873 K to 0.6 at 1125 K.

Simultaneous Effects of Temperature and Steam-to-Feed Ratio

The results of the statistical analysis with the temperature and steam-to-feed ratio as the independent variables are presented in Table 4. It is evident from Table 4 that the steam-to-feed ratio and temperature have significant effects on all the dependent variables. The F-test has been applied to the data at a significance level of 10%. By comparing Tables 3 and 4, we can see that the R-Square value improves when both the temperature and steam-to-feed ratio are used as the independent variables instead of the temperature alone.

The gas composition, HHV, gas yield, energy recovery, carbon

conversion, and mass yields are plotted as functions of temperature in Figures 13 through 19 for three steam-to-feed ratios of 2, 2.5, and 3.0. These figures reveal that all the dependent variables are influenced significantly by the steam-to-feed ratio. The best fit regression line equations with the temperature and steam-to-feed ratio as independent variables are presented in Table 4. It should be mentioned that the experiment was not specifically designed to determine the effect of the steam-to-feed ratio; thus, these plots are not valid representations of gasification results over the entire temperature range. Nevertheless, they would aid us to discern the resultant trend if a particular steam-to-feed ratio is maintained throughout the temperature range. Also it should be noted that even though the temperature significantly affected all the dependent variables, inclusion of the steam-to-feed ratio in the model always improved the fit.

DISCUSSION

The first step in coal gasification, devolatization or pyrolysis, is an extremely rapid process, occurring almost instantaneously when small coal particles are fed to a fluidized bed and heated rapidly to the gasification temperature. Anthony and Howard (1976) investigated this phenomenon in great detail. They have concluded that temperature is the dominant factor influencing the extent of devolatizing in the reactor and that more than 90% of the devolatization will be complete in less than 1 second for the temperature range of 850 to 1150 K and for small particle size (around 0.2 mm). This observation implies that the secondary gas phase reactions and char gasification reactions determine the composition and yield of the gas product.

The secondary gas phase reactions have been speculated as consisting of both the tar cracking and water-gas shift reactions. Wen et al. (1973) have found that synthesis gas production is maximized if the volatiles are held at a relatively high temperature. The exposure to the high temperature results in cracking of tar and other condensible molecules to lower chain aliphatics.

Howell (1979) and Matsui et al. (1984) have indicated that above 973 K, the char gasification and water-gas shift reactions are extensive if excess steam is used. The molar ratio of steam to carbon (R) is an important factor controlling the char gasification reactions. Masey (1979) has suggested that when R=1.0, raising the temperature tends to enhance gasification of carbon but raising the system pressure tends to retard it. His propositions are based on the equilibrium composition in the system of graphite and steam at 1 Atm.

All the experiments in the present study were conducted under steady-

state conditions with a well-defined axial temperature profile and gas phase residence time. The feed particles were small (average particle size being 0.297 mm) resulting in essentially instantaneous devolatization. Examination of the experimental data has given rise to a hypothesis of the two temperature regimes, one below 940 K and the other above 940 K. The major reactions in the former ($T < 940$ K) are the tar cracking and water-gas shift reactions, and those in the latter ($T > 940$ K) and the char gasification reactions (1) and (2) along with the water-gas shift reaction.

The experimental evidence supporting the proposed hypothesis of the simultaneous tar cracking and water-gas shift reactions in the first regime ($T < 940$ K) is delineated below.

Figure 8 shows that the carbon conversion increases with an increase in temperature below 940 K. Based on numerous gasification studies, Wen and Dutta (1979) have suggested that no significant char gasification reactions take place below 940 K. Since the water-gas shift reaction does not affect the carbon conversion, significant tar cracking must occur in this low temperature regime. This is also supported by the fact that the mass yield of the gas increases in the same temperature range.

Note that the gas phase residence time in the reactor was found to be of the order of 4 ~ 7 seconds. Our previous result indicated that a residence time of this order is sufficient for the cracking reaction to reach completion at a given temperature (Singh, 1983). Visual observation of the color of the condensate obtained in the experiments also suggested that the tar production decreases with increasing temperature and becomes almost insignificant at 930 ~ 950 K.

Yeboah et al. (1980) studied the pyrolysis of Illinois No. 6 coal

whose characteristics are very similar to those of the coal under investigation. They found that the initial devolatization product distribution for Illinois No. 6 coal at 923 K was 14.2 wt. % DAF feed of dry gas, 17.0 wt. % DAF feed of tar, and 6.2 wt. % DAF feed of water. Assuming that the coal under investigation had the same devolatlization product distribution and that all of the volatile matter in the feed (44% wt. % of DAF feed by proximate analysis) had been devolatilized, the devolatization product distribution would be 16.7 wt. % DAF feed of dry gas, 20.0 wt. % DAF feed of tar, and 7.3 wt. % DAF feed of water. If all the devolatilized tar underwent the cracking reactions, produced gas mass yield would increase by 0.2 kg gas/kg DAF feed. Addition of the devolatization product gas to this gives an estimated overall mass yield of 0.36 kg gas/kg DAF feed. This level of the mass yield is significantly below that observed as shown in Figure 9. Since the possibility of significant char gasification reactions have been eliminated below 940 K, the only other reaction that can increase the mass yield is the water-gas shift-reaction, indicating that this reaction occurs to a significant extent below 940 K; the mass yield observed experimentally was 0.8 kg gas/kg DAF feed at 940 K.

Figure 12 shows that the condensate-to-steam ratio between 833 K and 880 K is almost constant and has a value of 1.01. The experimentally observed steam feed rate and water production in the devolatization step had yielded the corresponding estimate of 1.07, indicating that the water-gas shift reaction occurs only slightly between 833 K and 880 K. The steam consumption rate above of 880 K increases drastically, indicating the enhancement of the rate of water-gas shift reaction. Occurrence of the water-gas shift reaction at low temperatures is due to the exis-

tence of excess steam in the system, driving the reaction towards the right. Thus, it appears that ample experimental evidence exists to support the hypothesis that the tar cracking and water-gas shift reactions occur simultaneously throughout the first regime (833 K to 940 K).

Wen and Dutta (1979) have suggested that char gasification reactions become significant at temperatures above 940 K, and the extent of such reactions is enhanced if excess steam is present in the system. Experimental data indicate that the molar concentration of CO_2 decreases and that of CO increases in the second regime (T > 940 K). This trend is expected if both the water-gas shift and char gasification reactions occur simultaneously.

Figure 9 shows that carbon conversion increases from 33% at 940 K to 82% at 1125 K. The char obtained in the experiments was analyzed and found to contain 83 wt. % DAF carbon. Ultimate analysis of the coal indicated a carbon content of 72 wt. % DAF feed. Assuming that no char gasification occurs and tar cracking is complete, the maximum carbon conversion will be 37.5%. Figure 8 shows that the observed carbon conversions are much higher than 37.5% at the higher temperatures indicating significant char gasification in the second regime.

The carbon conversion was estimated to be 80% from the steady-state char output (due to elutriation). This value of 80% is probably excessive in the light of char hold-up in the connecting pipes. Nevertheless, it indicates significant char gasification in the reactor system.

Provided that the proposed hypothesis is valid the following reactions are expected to occur to significant extent in the second regime.

(1) $C + H_2O \rightarrow CO + H_2$

(2) $C + CO_2 \rightarrow 2CO$

(3) $CO + H_2O \rightleftharpoons CO_2 + H_2$

Figure 10 shows that the mass yields of CO, CO_2, and H_2 increase with an increase in temperature when it is greater than 940 K. The increase in the mass yield of CO indicates that the char gasification reactions, (1) and (2), must occur. But if only reactions (1) and (2), occur we should see a decrease in the mass yield of CO_2. Figure 10 shows that the mass yield of CO_2 increases significantly for T > 940 K, thus, indicating the simultaneous occurrence of the water-gas shift and char gasification reactions. The increase in the mass yield of H_2 with the increase in the temperature was relatively small due to its low molecular weight. The increase in the mass yield of CO_2 was much greater than those of other species because of its high molecular weight. Carbon monoxide is both produced and consumed when reactions (1), (2), and (3) occur simultaneously. Since the mass yield of CO increased, it was evident that the char gasification reactions were faster than the shift reaction (overall effect). The mass yield of gas continues increase to significantly in the second regime (see Figure 9) due to gasification of char through the shift reaction.

Figure 12 shows that the condensate to steam ratio decreases significantly as the temperature increases, indicating increasing steam consumption. Visual observation of the color of the condensate indicated evidence of negligible presence of tar.

CONCLUSIONS

Steam gasification experiments were conducted with Kansas Bituminous coal in a bench-scale fluidized-bed reactor over a temperature range of 833 K to 1133 K. The volumetric and mass yields of the produced gas increased with increasing temperature. The major components of the produced gas were CO, CO_2, H_2, and CH_4 which comprised over 95% of the gas. The other gas components detected were C_2H_4, C_2H_6, C_3H_6, and C_3H_8. The higher heating value (HHV) of the gas decreased from 16.5 J/m at 850 K to about 11.2 MJ/m at 1125 K. Variations in the HHV of the product gas were small between 975 K and 1125 K. Both the carbon conversion and energy recovery increased substantially with an increase in the temperature.

The gas composition and mass yield data have led us to postulate that two regimes exist in the secondary gasification reactions. The first regime ($T < 940$ K) is dominated by the tar cracking and water-gas shift reaction. Char gasification and the water-gas shift reactions are the major reactions taking place in the second regime ($T > 940$ K).

The use of excess steam in the system was found to have a significant effect on the gasification process. It probably enhanced both the water-gas shift and char gasification reactions. The postulation is supported by the experimentally measured mass yield, HHV, carbon conversion, and energy recovery data. The steam to feed ratio was found to have a significant effect on the gasification process.

REFERENCES CITED

Anthony, D. B. and J. B. Howard, "Coal Devolatization and Hydrogasification," AIChE Journal, 22, 625-656 (1976).

Anthony, D. B., J. B. Howard, H. C. Hottel, and H. P. Meissner, "Rapid Devolatization of Pulverized Coal," Fifteenth Symposium (International) on Combustion, pp. 1303, The Combustion Institute, Pittsburg, PA. (1974).

Averitt, P., "Coal Reserves of the United States," U.S. Geological Survey Bulletin 1136 (1961).

Averitt, P., "Coal Resources of the United States, January 1, 1974," Geological Survey Bulletin 1412, pp. 100, U.s. Department of the Interior, Washington, D.C. (1975).

Grainger, L. and J. Gibson, "Coal Utilization: Technology Economics and Policy, "Pub. Grahan and Trotman, London, U.K. (1981).

Howard-Smith, I. and G. J. Werner, "Coal Conversion Technology, "Noyes Data Corp., Park Ridge, N.J. (1976).

Howell, J. A., "Kansas Coal Gasification," M.S. Thesis, Kansas State University (1979).

Kavlick, V. J., and B. S. Lee, "Coal Pretreatment in Fluidized Bed," in Fuel Gasifiation, Advances in Chemistry Series, No. 69., Am. Chem. Soc., Washington, D.C. (1967).

Masey, L. G., "Coal Gasification for High and Low Btu Fuels," in Coal Conversion Technology, Edited by C. Y. Wen and E. Stanley Lee, pp. 313, Addison-Wesley Publishing Company, Reading, Massachusetts (1979).

Matsui, I., T. Kojima, T. Furusawa, and D. Kunii, "Gasification of Coal Char by steam in a continuous fluidized bed reactor", Proceedings of the Fourth International Conference on Fluidization, Edited by D. Kunii and R. Toei, pp. 655 - 662, Pub. by Engineering Foundation, New York (1984).

Overtuf, B. W., F. Kayihan, and G. V. Reklaitis, "Modeling and Analysis of an Integrated Coal Pyrolysis, Gasification, and Combustion Reactor System," presented at the 71st Annual Meeting of AIChE, Miami Beach, Nov. 16 (1978).

SAS User's Guide, 1979 Edition, SAS Institute Inc., Box 8000, Cary, NC 27511 (1979).

Simeons, C., "Coal: Its Role in Tomorrow's Technology," A Sourcebook on Global Coal Resources, Pergamon Press, Oxford, U.K. (1978).

Singh, S., "The Gasification of Biomass in a Fluidized Bed Reactor", M.S. Thesis, Kansas State University (1983).

Van Krevelen, D. W., F. J. Huntjens, and H. N. M. Dormans, "Chemical Structure and Properties of Coal XVI - Plastic Behavior on Heating, "Fuel, 35, 462 (1956).

von Fredersdorff, C. G. and M. A. Elliot, "Coal Gasification," Chemistry of Coal Utilization, Supplementary Volume, H. H. Lowry, ed., Wiley, New York (1963).

Walawender, W. P., S. Ganesan, and L. T. Fan, "Steam Gasification of Manure in a Fluid Bed: Influence of Limestone as a Bed Additive" Symposium Papers: Energy from Biomass and Wastes V., Institute of Gas Technology, pp. 517-527 (1981a).

Wen, C. Y., R. C. Bailie, C. Y. Lin, and w. S. O'Brien, "Production of Low Btu Gas Involving Coal Pyrolysis and Gasification", Presented at Symposium on Coal Gasification, Divison of Fuel Chemistry, 165th National Meeting, American Chemical Society, Dallas, Texas, April 8-12 (1973).

Yeboah, Y. D., J. P. Longwell, J. B. Howard and W. A. Peters, "Effect of Calcined Dolomite on the Fluidized Bed Pyrolysis of Coal," Ind. and Eng. Chem. Process Des. and Dev., 19, 646-653 (1980).

Table 1.

Reactor Operating Parameters

Reactor Temperature Range	833-1133 K
Fluidizing Gas	Steam
Superficial velocity	0.18 - 0.14 m/s
Minimim Fluidization Velocity	0.12 - 0.09 m/s
Steam Rate	15.33 - 11.0 g/min
Feed	Kansas Bituminous Coal
Feed Rate	4.4 - 5.8 g/min
Mean Particle Size (Feed)	0.297 mm
Particle Size (Bed)	
Sand (75 weight %)	-30 +50 mesh
Limestone (25 weight %)	-7 +50 mesh
Volatile Residence Time	4 - 7 s

Table 2.

Analysis of Feed - Kansas Bituminous Coal

Proximate Analysis (%)		Ultimate Analysis (% DAF basis)	
Fixed Carbon (DAF)	55.4	C	72.0
V.M. (DAF)	44.6	H	5.33
Ash (Dry)	8.4	N	1.4
Moisture	7.8	O (by diff.)	13.7
		S	7.5

ASTM Free Swelling Index 5.5

High Heating Value (MJ/kg As Received) 30.62

Particle Size

Tyler Mesh	Cut Size mm	Weight Fraction (%)
+14	1.19	4.52
+20	0.841	25.98
+30	0.59	21.14
+40	0.42	17.58
+50	0.297	11.83
+60	0.25	9.81
+80	0.177	4.22
+100	0.149	4.20
-100	< 0.149	0.72

Mean Particle Size, mm 0.297

True Powder density, kg/m^3 1580.0

Table 3. Statistical Analysis: Temperature as Independent Variable.

Dependent Verieble y	Semple Size n	R^2	F-velue	PR > F	Significent Regression Model $y = A + BT + CT^2 + OT^3$			
					A	B	C	O
mole % H_2	67	0.93	476.76	0.0001	- 217.916	0.525	- 0.000248	0.0
mole % CO_2	67	0.78	91.34	0.0001	-1713.158	5.063	- 0.004856	1.5337×10^{-6}
mole % CO	67	0.87	169.12	0.0001	1772.408	- 5.146	0.004944	-15606×10^{-6}
mole % CH_4	67	0.95	485.01	0.0001	845.017	- 2.267	0.002038	-6.1239×10^{-7}
mole % C_2H_4	67	0.82	178.39	0.0001	18.295	- 0.032	1.457×10^{-5}	0.0
mole % C_2H_6	67	0.92	299.09	0.0001	43.404	- 0.1078	8.880×10^{-5}	-2.4186×10^{-8}
mole % C_3H_6	67	0.92	446.65	0.0001	11.611	- 0.0202	8.8054×10^{-6}	0.0
mole % C_3H_8	67	0.70	58.87	0.0001	- 5.046	0.01717	$- 1.8667 \times 10^{-5}$	6.5586×10^{-8}
Higher Heating Value (MJ/m^3)	67	0.93	331.18	0.0001	492.907	- 1.3208	0.00119	-3.6144×10^{-7}
Gee yield (m^3/kg)	67	0.95	517.11	0.0001	119.410	- 0.3902	0.000415	-1.4282×10^{-7}
Energy Recovery (%)	67	0.96	625.50	0.0001	3503.885	-11.4278	0.01214	-4.1563×10^{-6}
Cerbon Conversion (%)	67	0.96	623.52	0.0001	2832.087	- 9.264	0.00986	-3.3765×10^{-6}
Mass Yield (kg gas/kg OAF Feed)	67	0.95	503.23	0.0001	78.519	- 0.2578	0.000276	-9.5381×10^{-8}

T = Temperature

Table 3. Continued.

Dependent Variable y	Sample Size n	R^2	F-value	PR > F	Significant Regression Model $y = A + BT + CT^2 + DT^3$			
					A	B	C	D
Mass Yield Individual components (kg gas/kg DAF Feed)								
H_2	67	0.95	454.64	0.0001	641.321	- 2.1011	0.00224	-7.7746×10^{-7}
CO_2	67	0.92	293.99	0.0001	4256.146	-14.4217	0.01588	-5.6333×10^{-6}
CO	67	0.95	445.46	0.0001	2575.329	- 8.0207	0.00812	-2.6525×10^{-6}
CH_4	67	0.88	180.23	0.0001	334.984	- 1.0867	0.00117	-4.1427×10^{-7}
C_2H_4	67	0.83	119.79	0.0001	61.658	- 0.2008	0.000214	-7.4219×10^{-8}
C_2H_6	67	0.80	101.91	0.0001	17.323	- 0.0561	6.1558×10^{-5}	-2.2407×10^{-8}
C_3H_6	67	0.62	41.12	0.0001	- 25.808	0.07804	-7.5245×10^{-5}	2.3402×10^{-8}
C_3H_8	67	0.58	34.78	0.0001	- 9.037	0.02835	-2.8984×10^{-5}	9.6959×10^{-9}

T = Temperature

Table 4. Statistical Analysis; Temperature and Steam-to-Feed Ratio as Independent Variables.

Oependent Verieble y	R^2	PR > F	Significent Regreseion Model $y = A + BT + CT^2 + DT^3 + E\eta + F\eta^3 + G\eta^3 + HT\eta$							
			A	B	C	D	E	F	G	H
mole % H_2	0.95	0.0001	668.953	0.0	0.0	-0.5×10^{-7}	-756.968	267.776	-34.565	0.0795
mole % CO_2	0.85	0.0001	-358.079	2.125	-0.263×10^{-2}	0.89×10^{-6}	-191.429	0.0	0.0	0.1947
mole % CO	0.91	0.0001	773.43	-2.946	0.325×10^{-2}	-0.107×10^{-5}	137.585	0.0	0.0	-0.1418
mole % CH_4	0.97	0.0001	-781.50	0.0	0.366×10^{-3}	-0.13×10^{-6}	841.289	-269.617	35.344	-0.1699
Higher Heating Velue (MJ/m^3)	0.95	0.0001	107.545	-0.481	0.562×10^{-3}	-0.175×10^{-6}	54.013	0.0	0.0	-0.0552
Ges Yield (m^3/kg)	0.96	0.0001	84.491	-0.437	0.462×10^{-3}	-0.158×10^{-6}	60.242	- 23.738	3.0866	0.0
Energy Recovery (%)	0.97	0.0001	2508.487	-12.771	0.135×10^{-1}	-0.459×10^{-5}	1721.541	-678.035	88.098	0.0
Cerbon Conversion (%)	0.97	0.0001	1776.437	-10.704	0.113×10^{-1}	-0.384×10^{-5}	1834.470	-721.562	93.523	0.0
Mase Yield (kg gee/kg OAF Feed)	0.97	0.0001	51.132	-0.294	0.312×10^{-3}	-0.107×10^{-6}	47.183	-18.585	2.413	0.0

T = Temperature
η = Steam-to-Feed Ratio

Table 4. Continued.

Dependent Variable y	R^2	PR > F	Significant Regression Model $y = A + BT + CT^2 + OT^3 + E\eta + F\eta^3 + G\eta^3 + HT\eta$							
			A	B	C	O	E	F	G	H
Mass Yield of Individual Components										
H_2	0.96	0.0001	472.793	- 2.321	0.246×10^{-2}	-0.845×10^{-6}	288.658	- 113.918	14.849	0.0
CO_2	0.95	0.0001	1747.855	-17.075	0.185×10^{-1}	-0.646×10^{-5}	4097.106	-1625.705	212.735	0.0
CO	0.95	0.0001	2683.952	- 8.643	0.877×10^{-2}	-0.287×10^{-5}	70.013	- 14.052	0.0	0.0
CH_4	0.93	0.0001	-247.977	- 0.641	0.865×10^{-3}	477.027	-173.027	22.806	-0.0427	0.0

T = Temperature
η = Steam-to-Feed Ratio

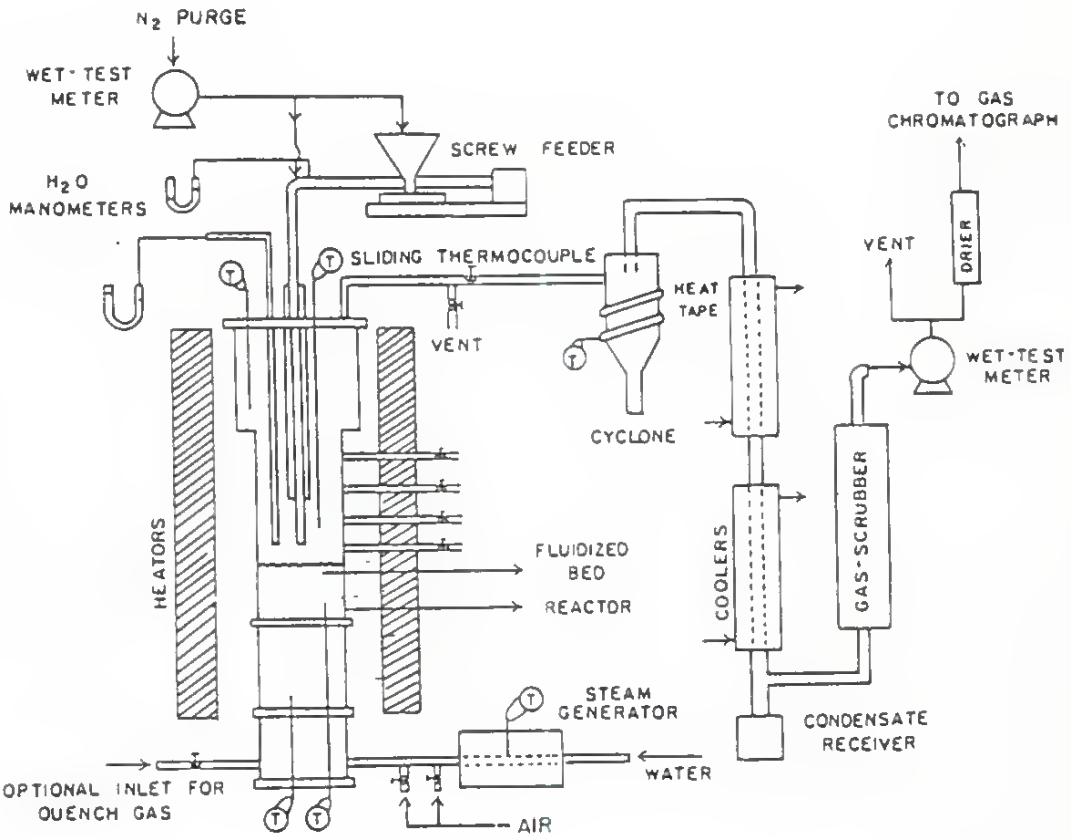

Fig. 1. Bench-scale fluidized-bed coal gasification system.

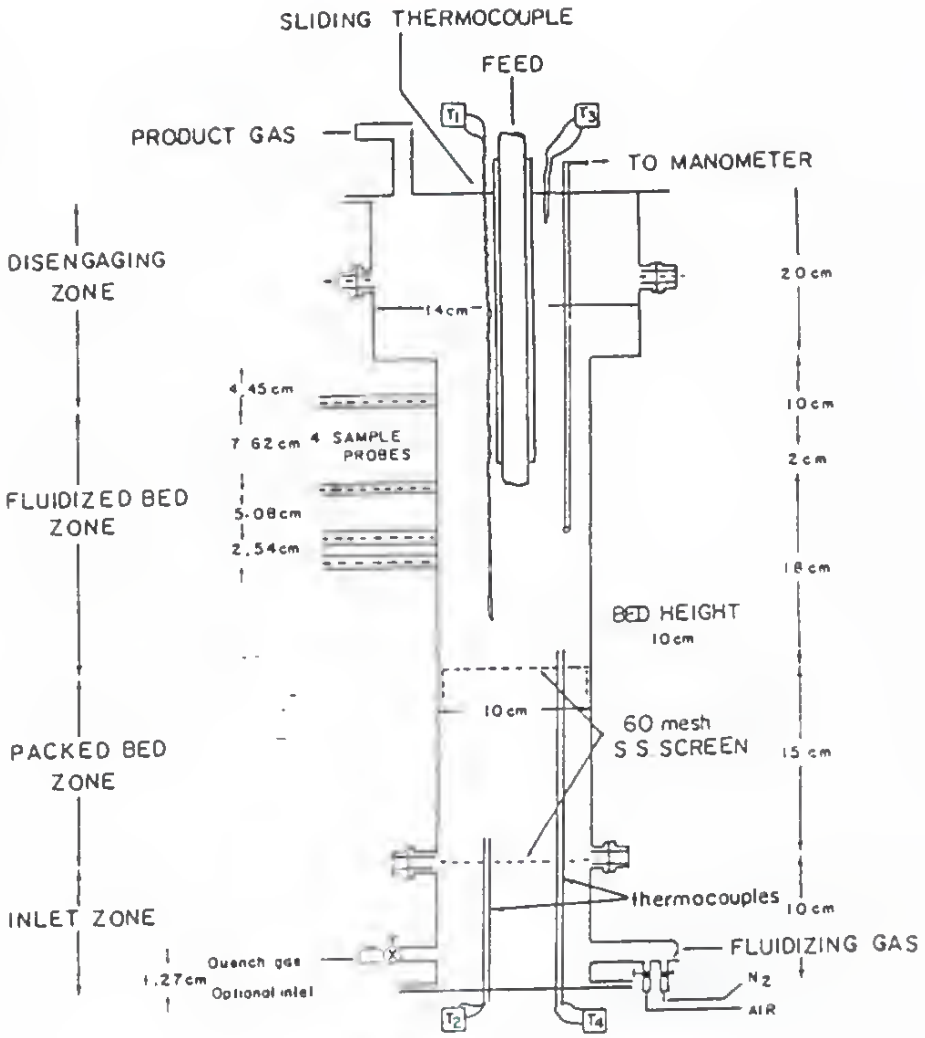

Fig. 2. Fluidized-bed Reactor.

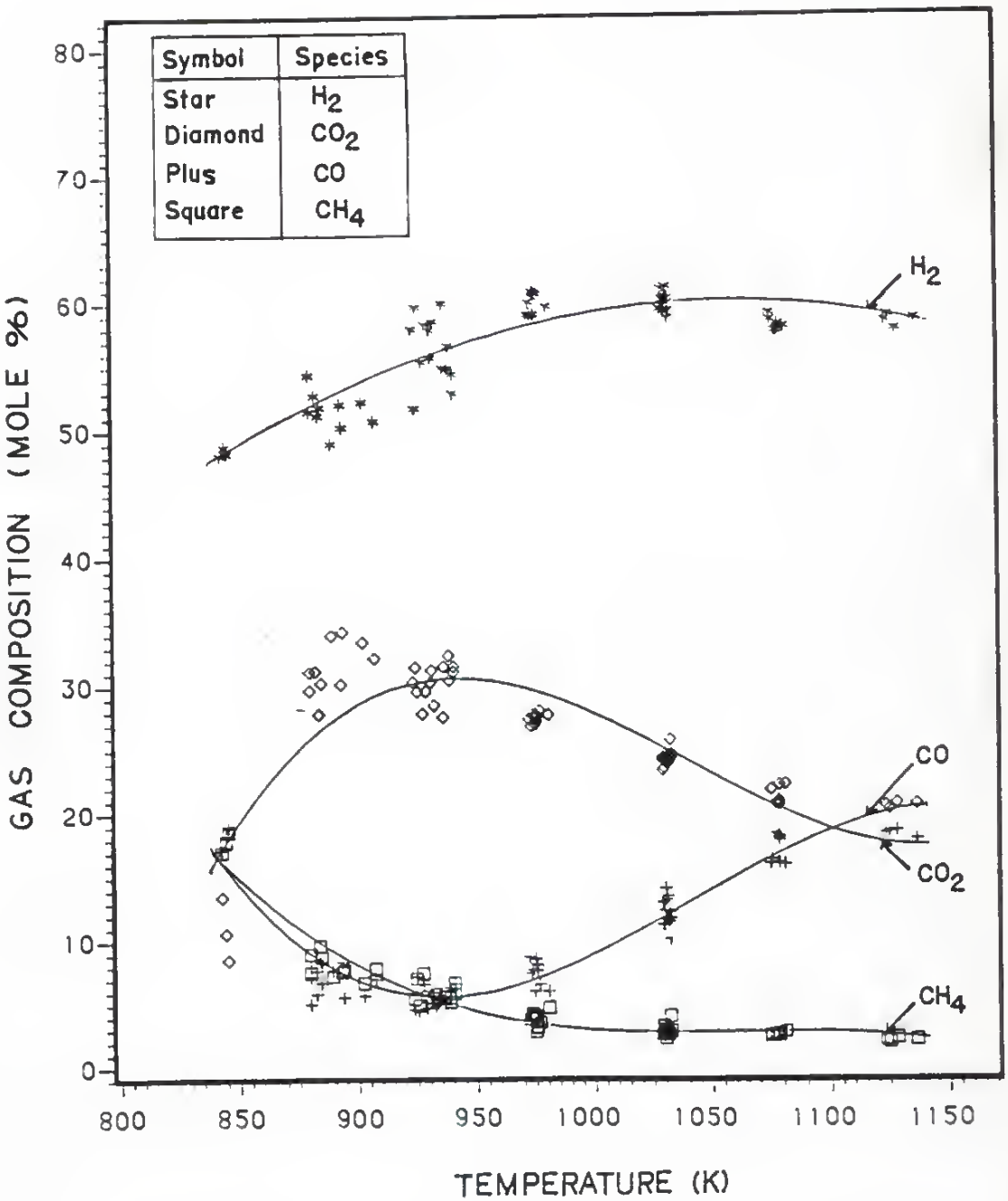

Fig. 3. Gas composition of major components vs. temperature.

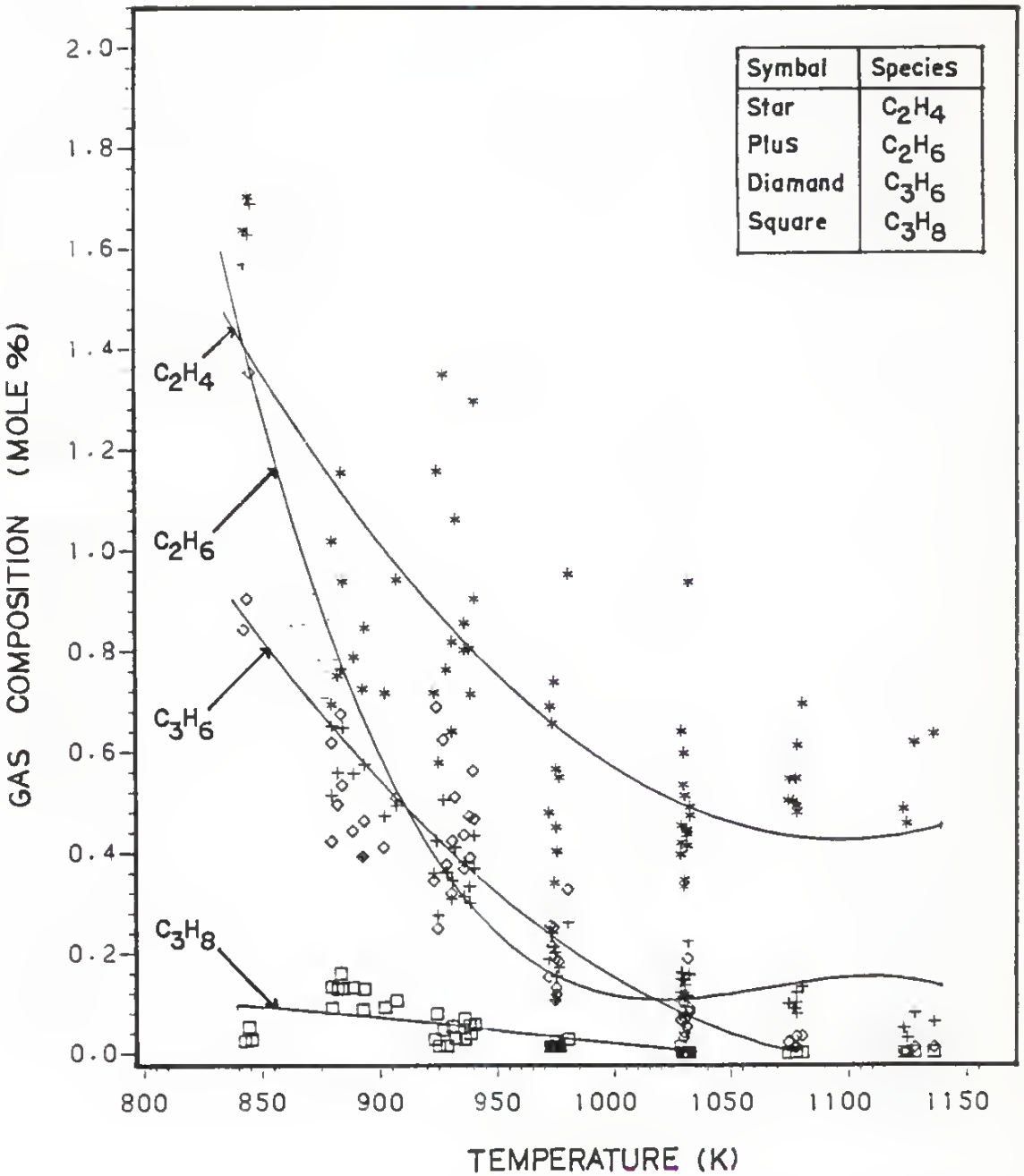

Fig. 4. Gas composition of minor components vs. temperature.

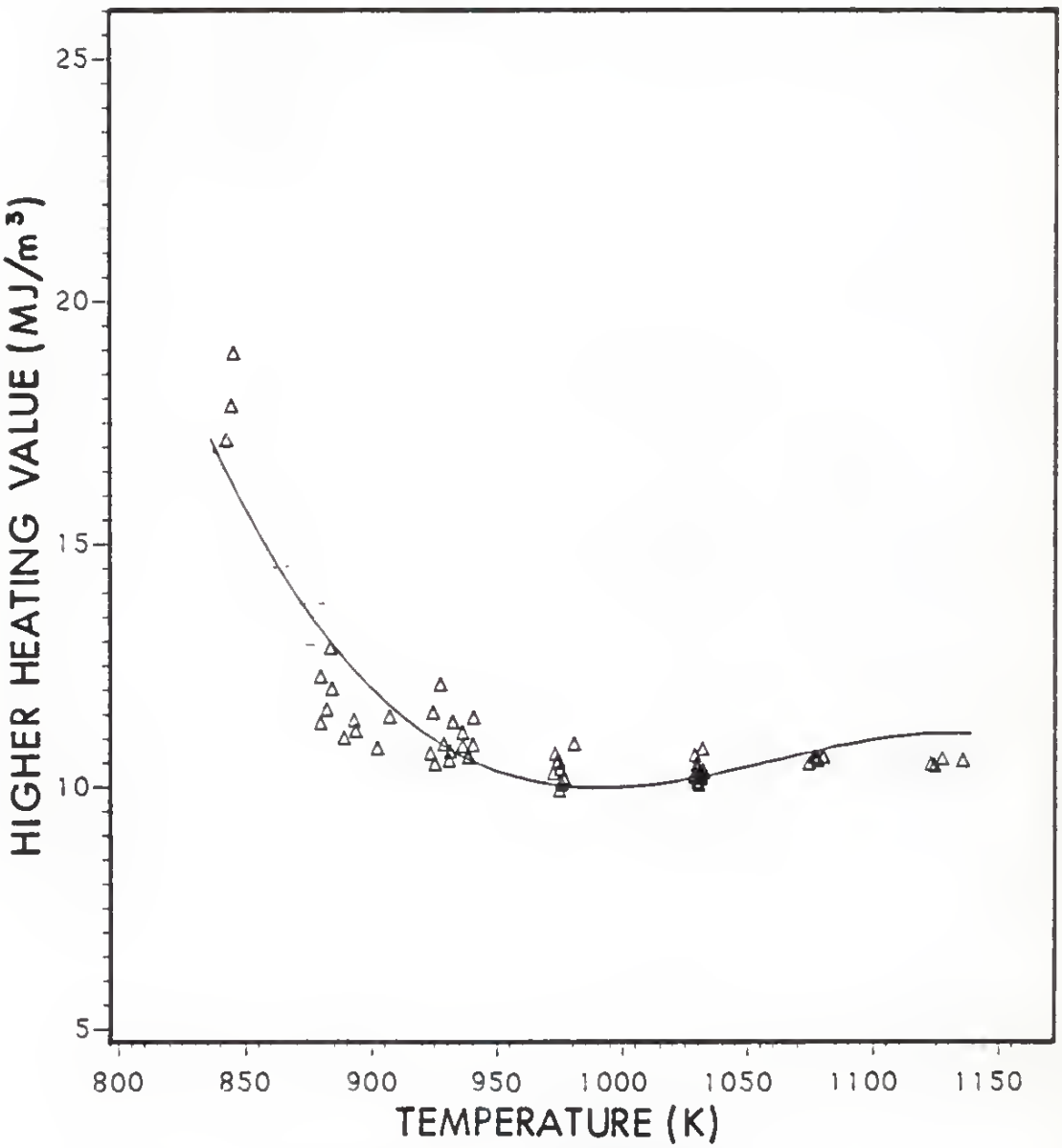

Fig. 5. Gas heating value vs. temperature.

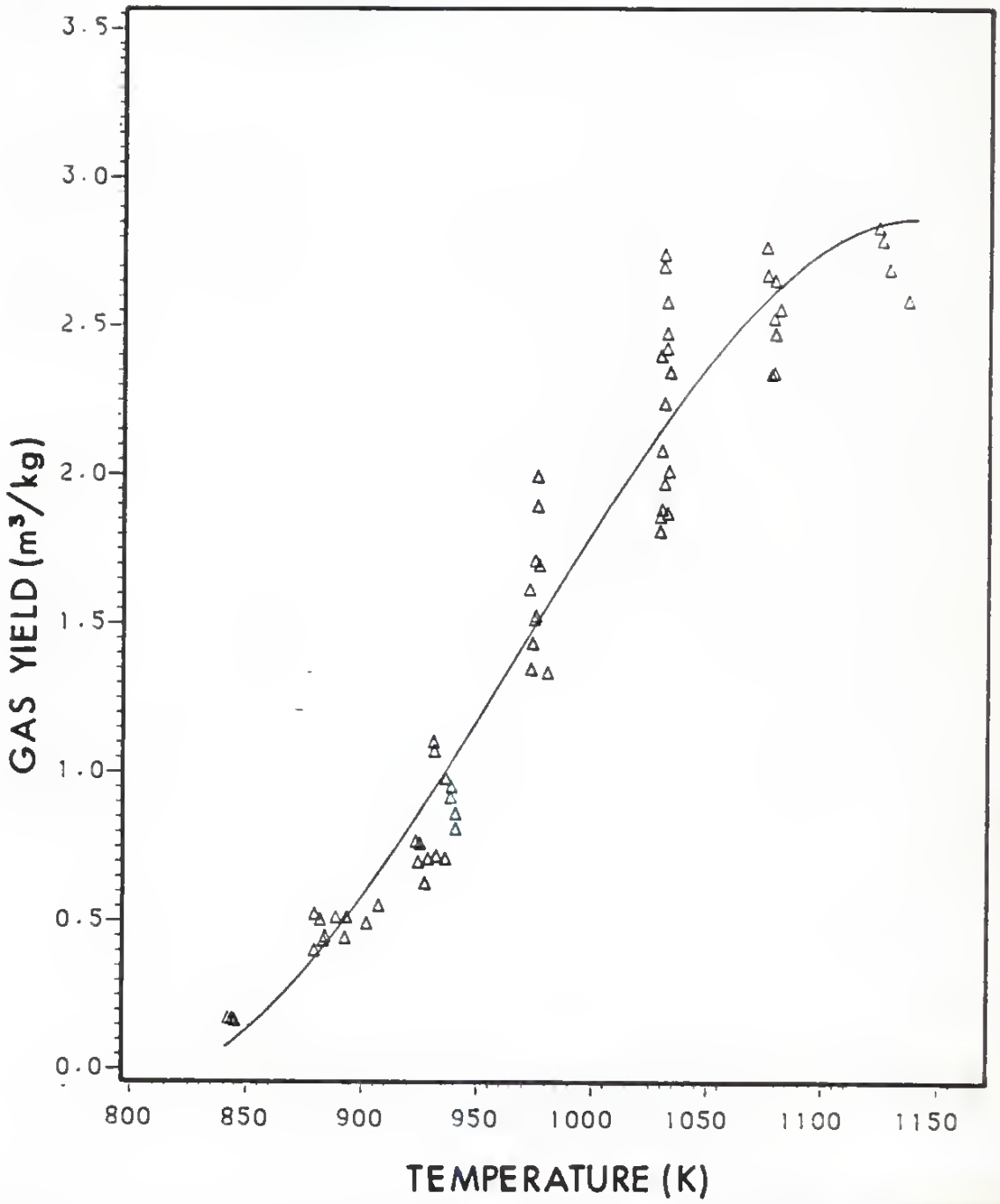

Fig. 6. Gas yield vs. temperature

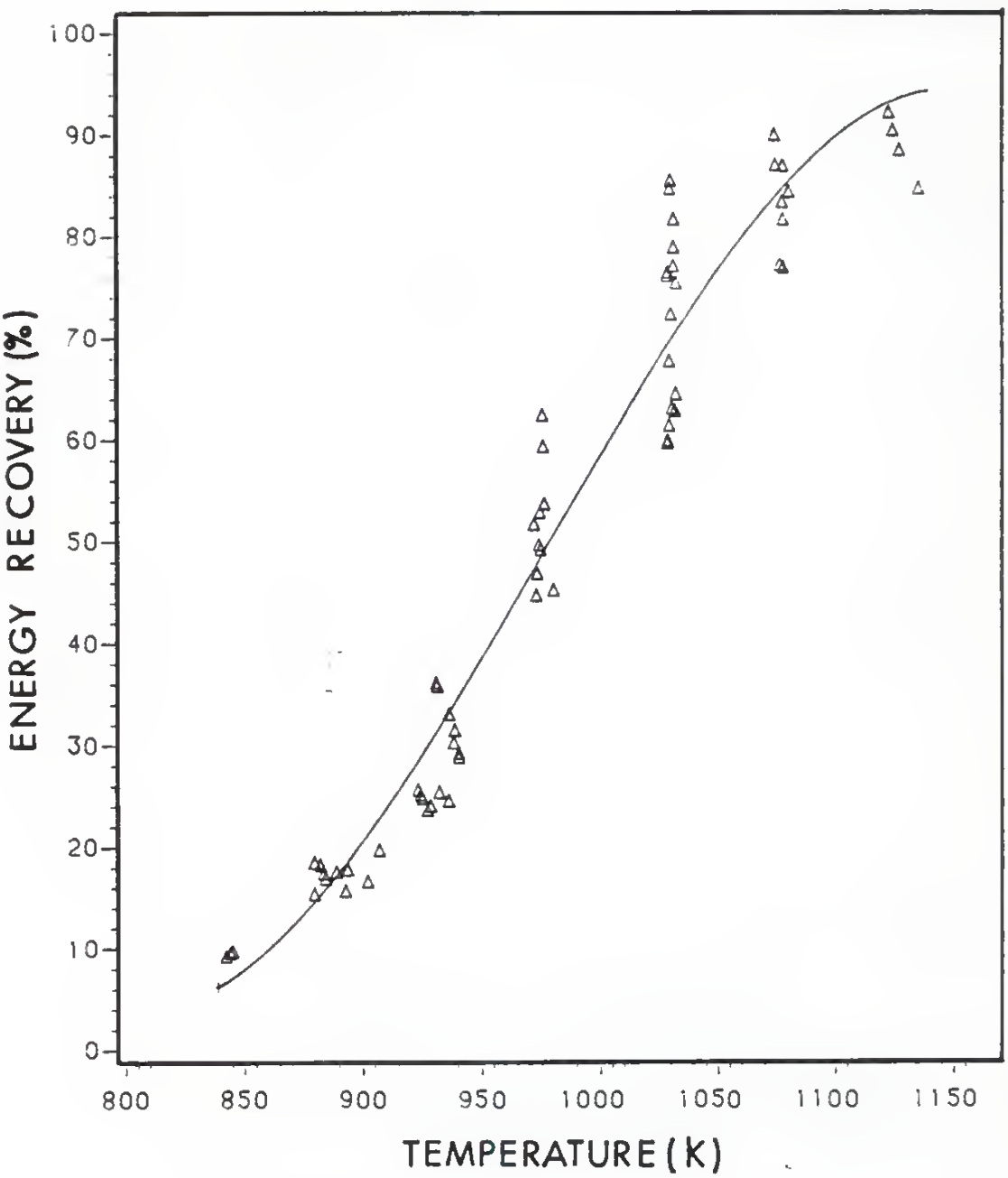

Fig. 7. Energy recovery vs. temperature.

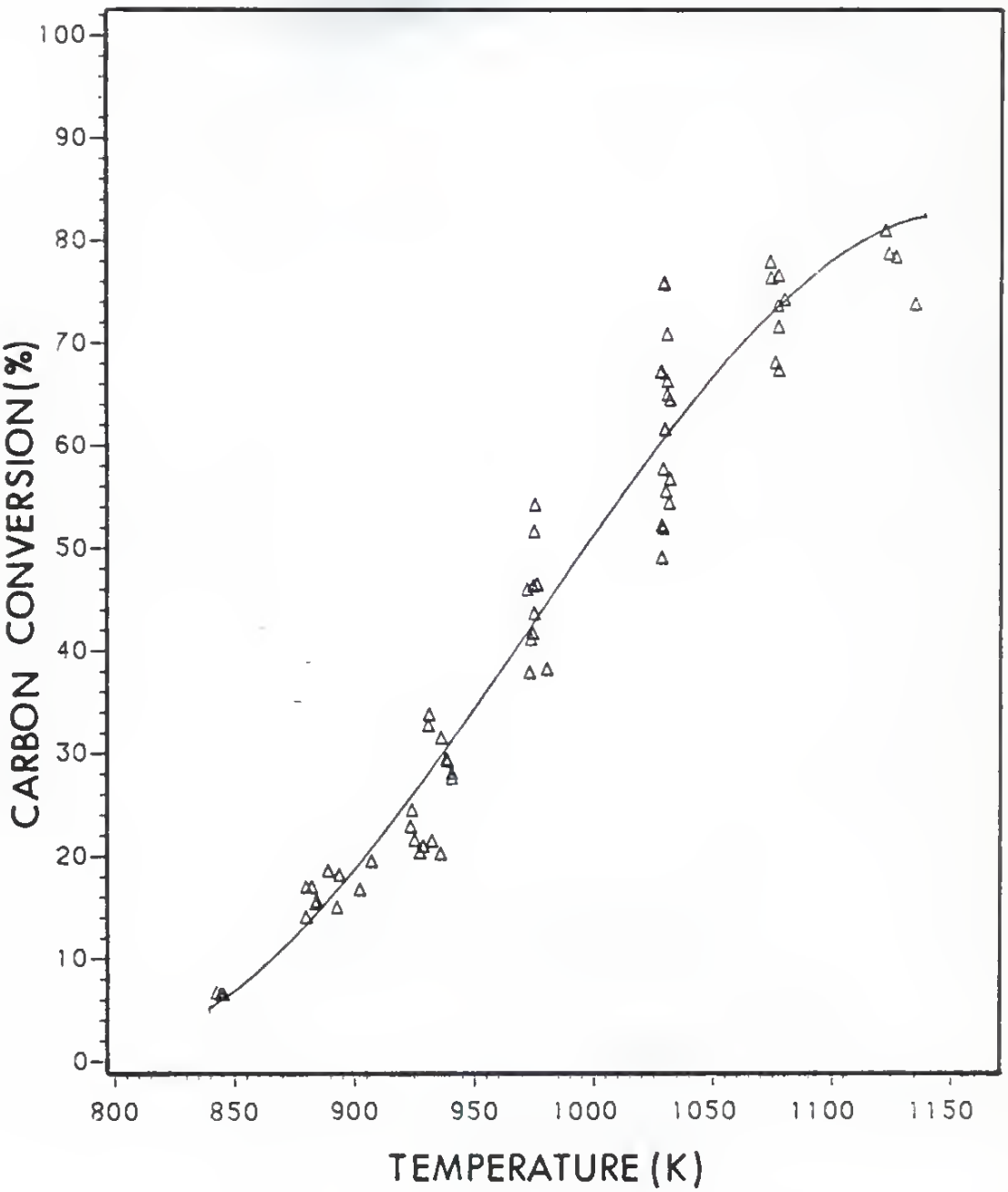

Fig. 8. Carbon conversion vs. temperature.

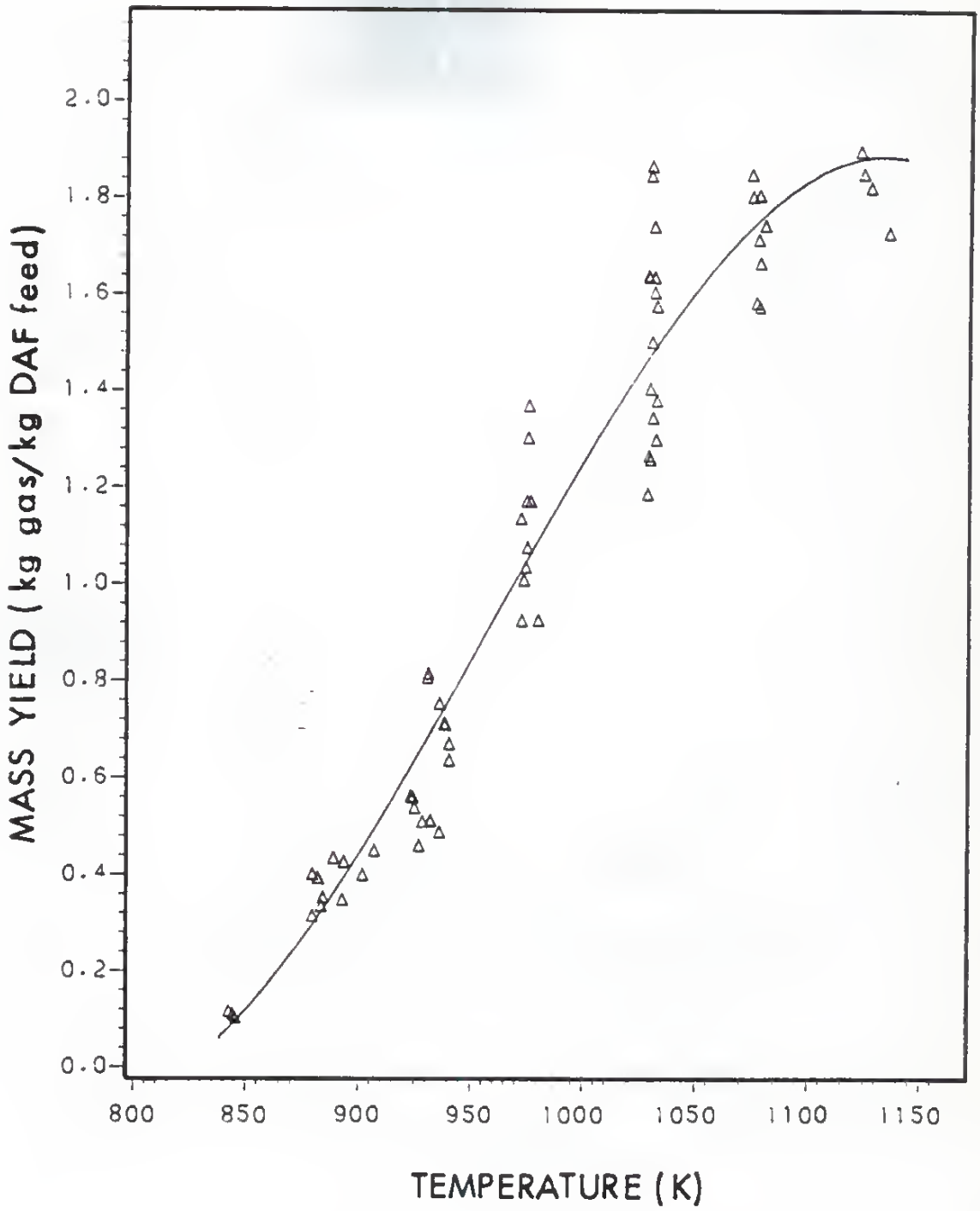

Fig. 9. Mass yield vs. temperature.

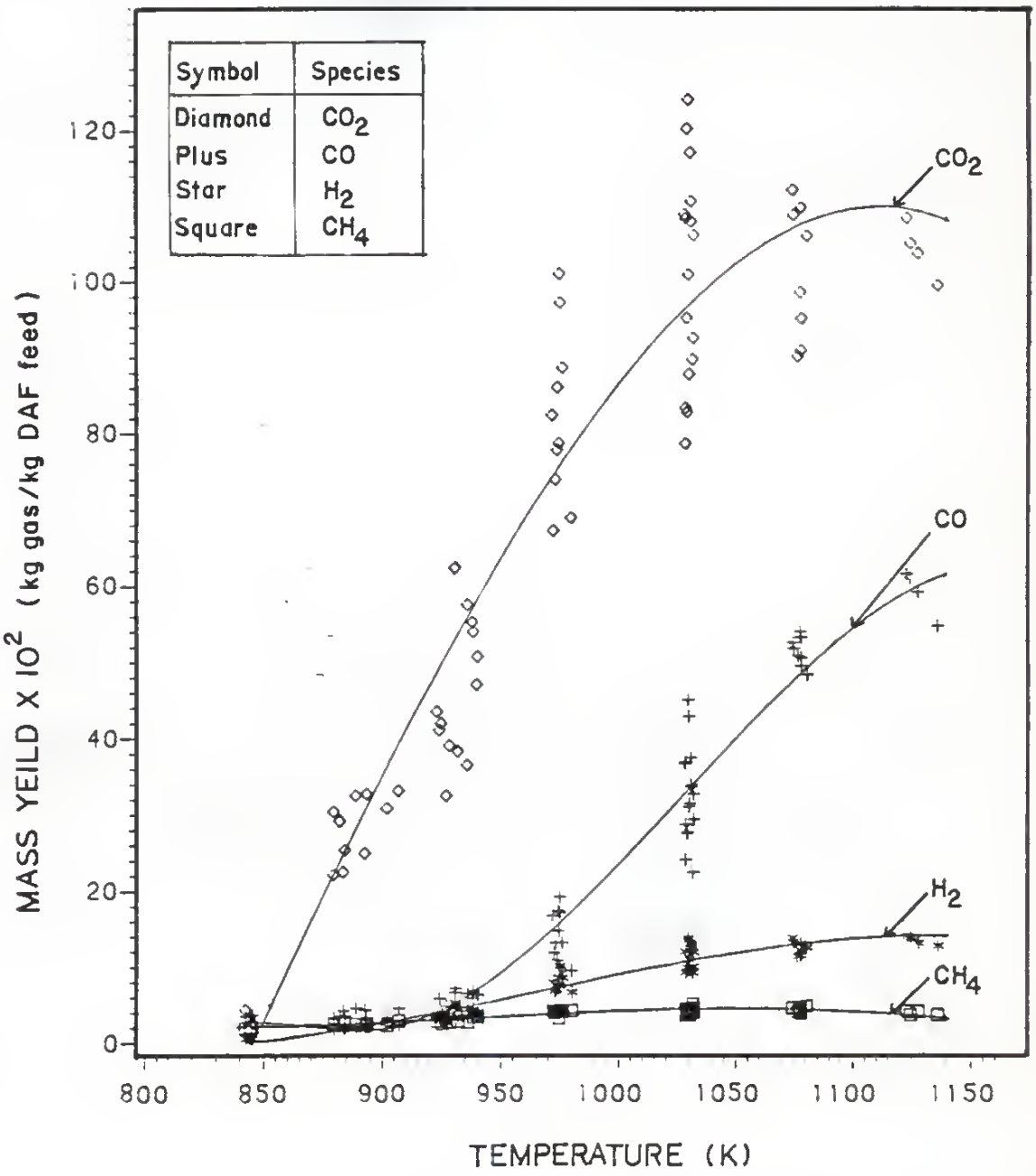

Fig. 10. Mass yields of major components vs. temperature.

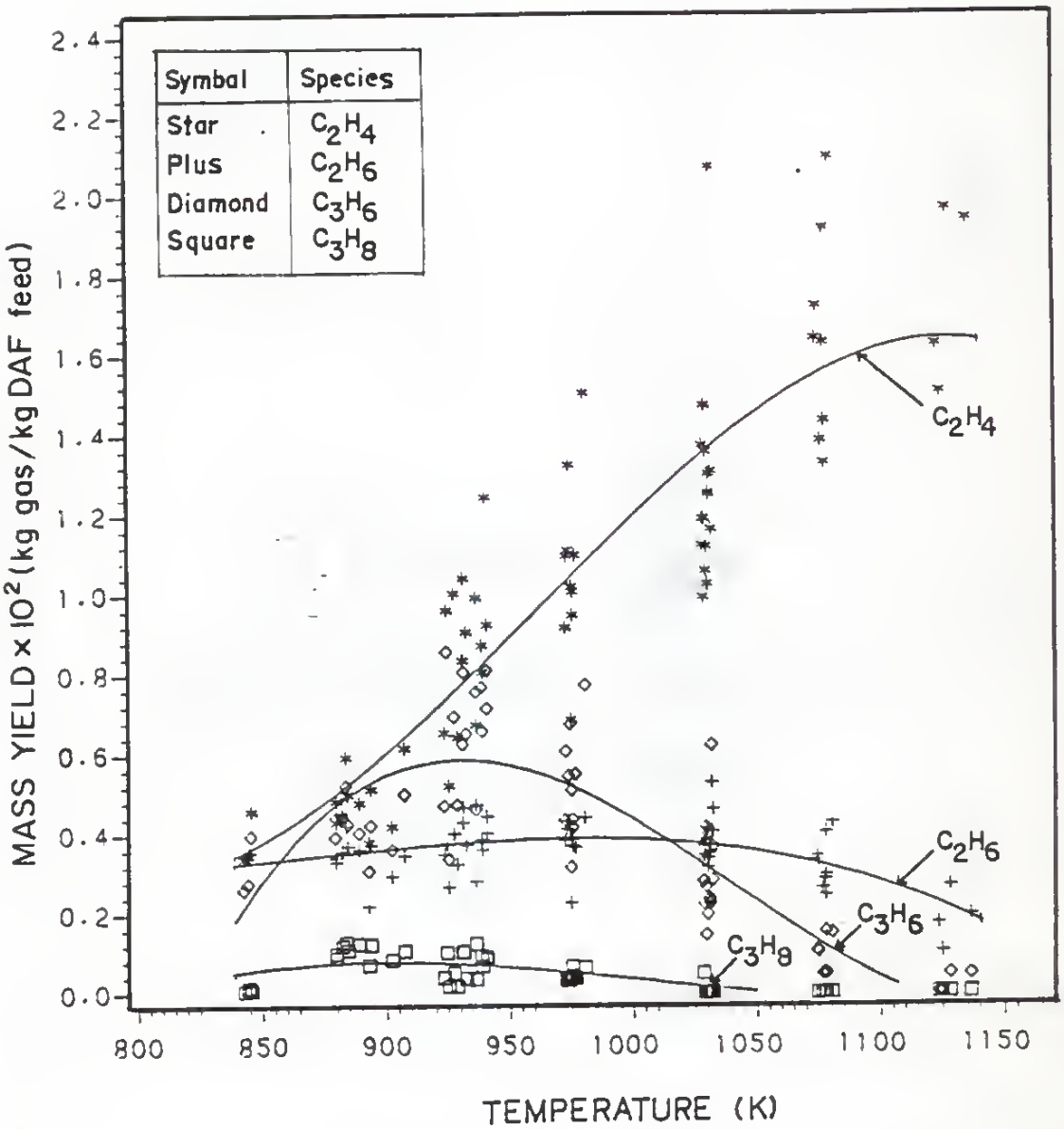

Fig. 11. Mass yields of minor components vs. temperature.

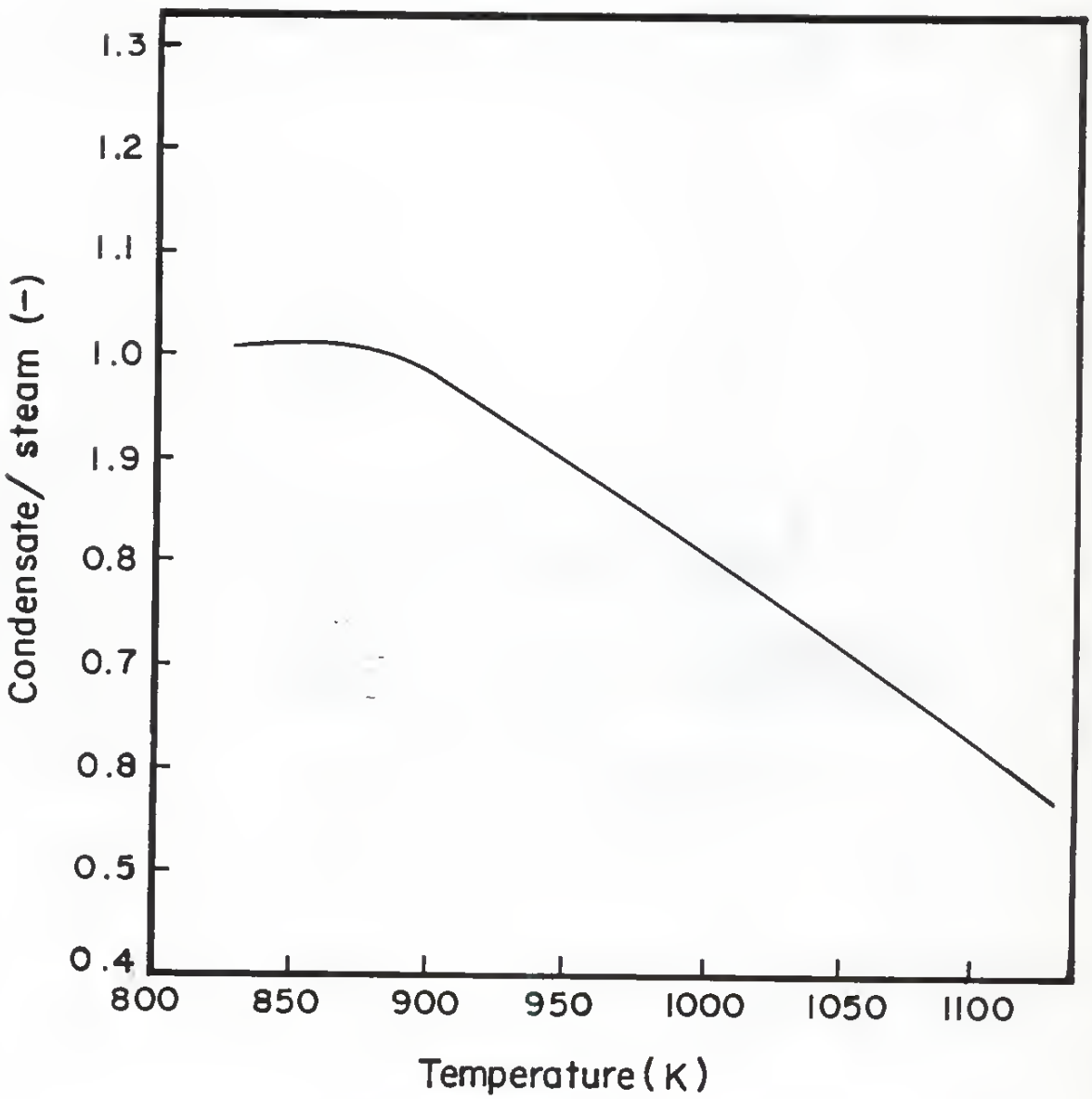

Fig. 12. condensate/steam ratio vs. temperature.

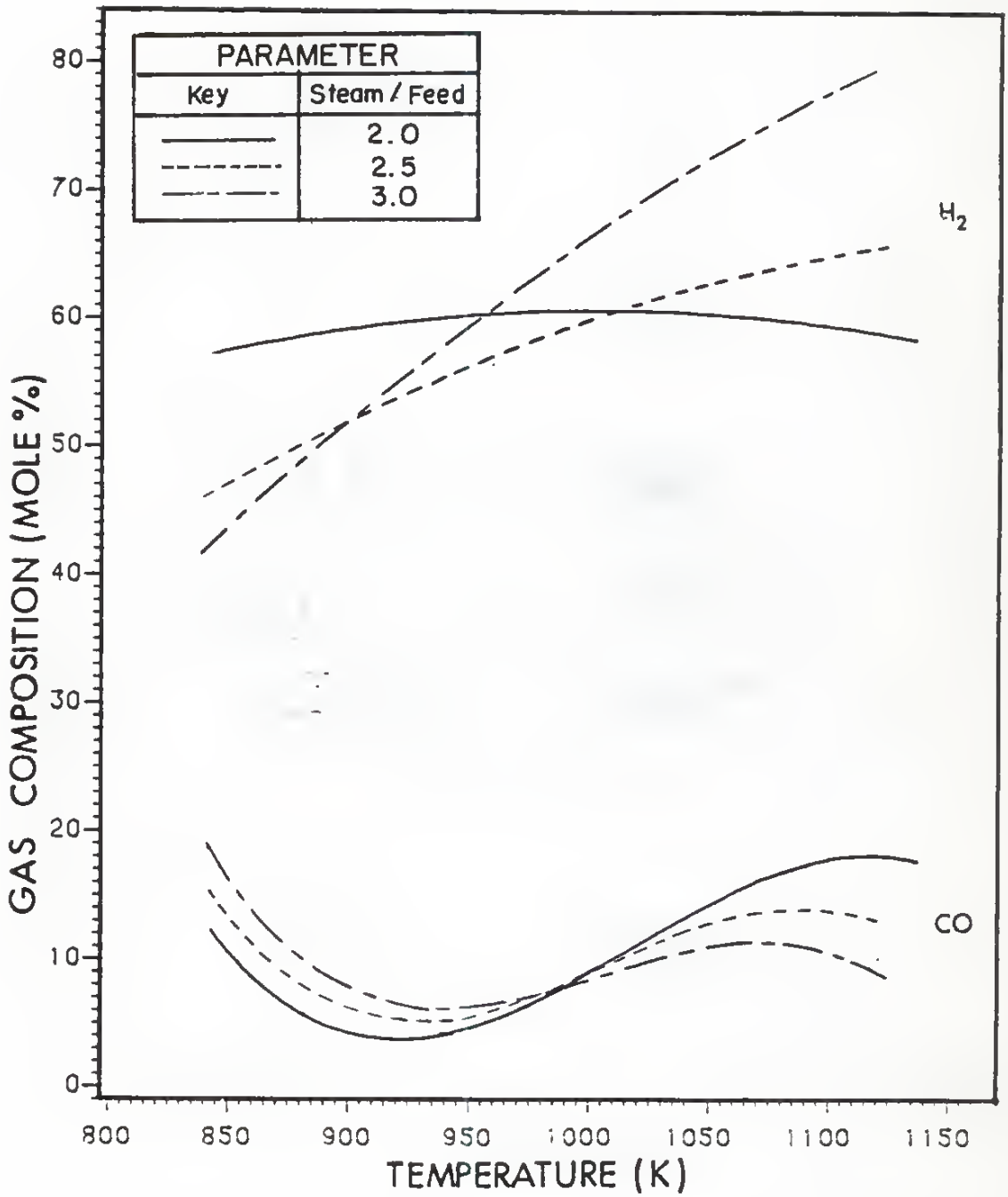

Fig. 13. Effect of steam-to-feed ratio and temperature on gas composition.

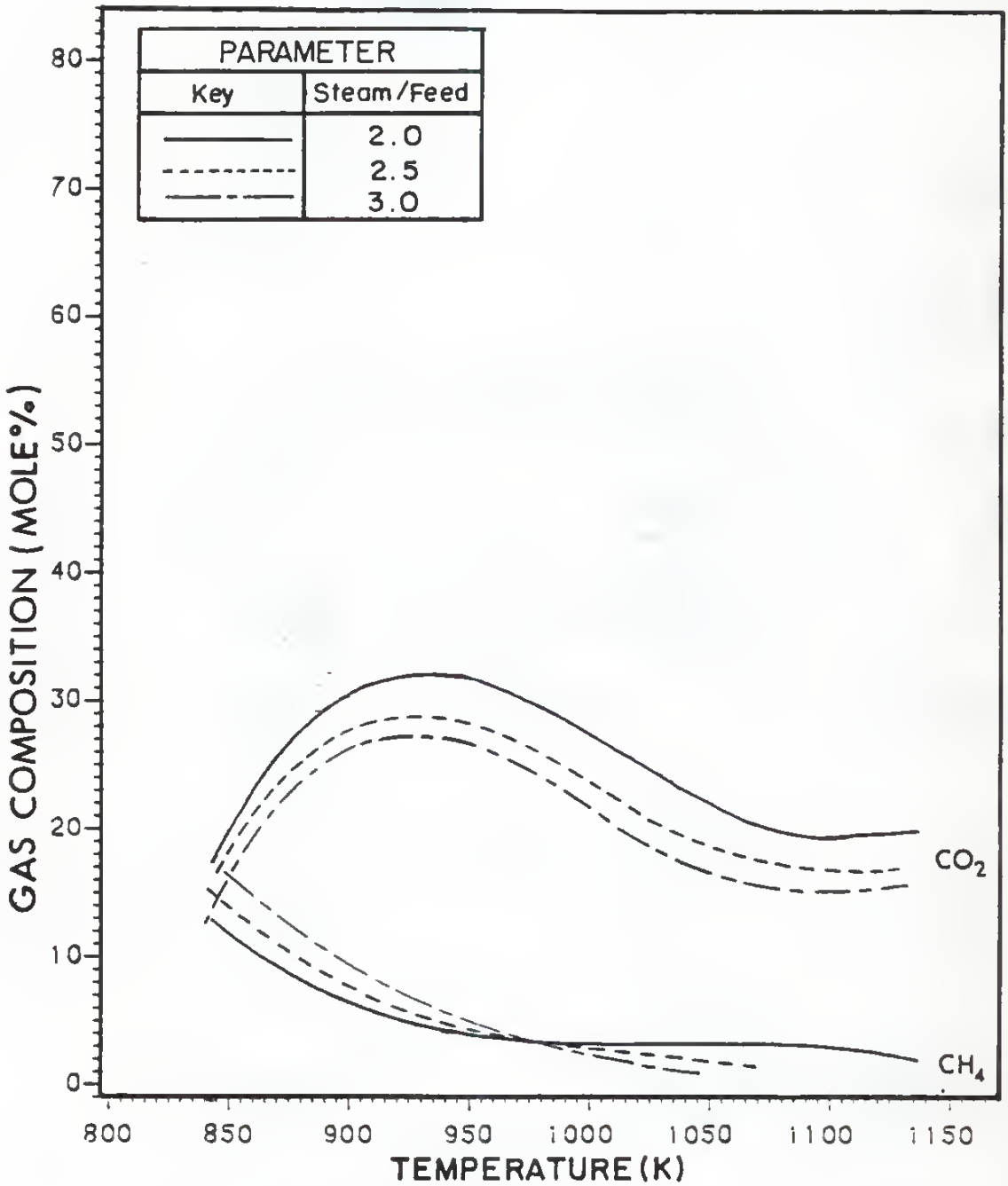

Fig. 14. Effect of steam-to-feed ratio and temperature on gas compositions.

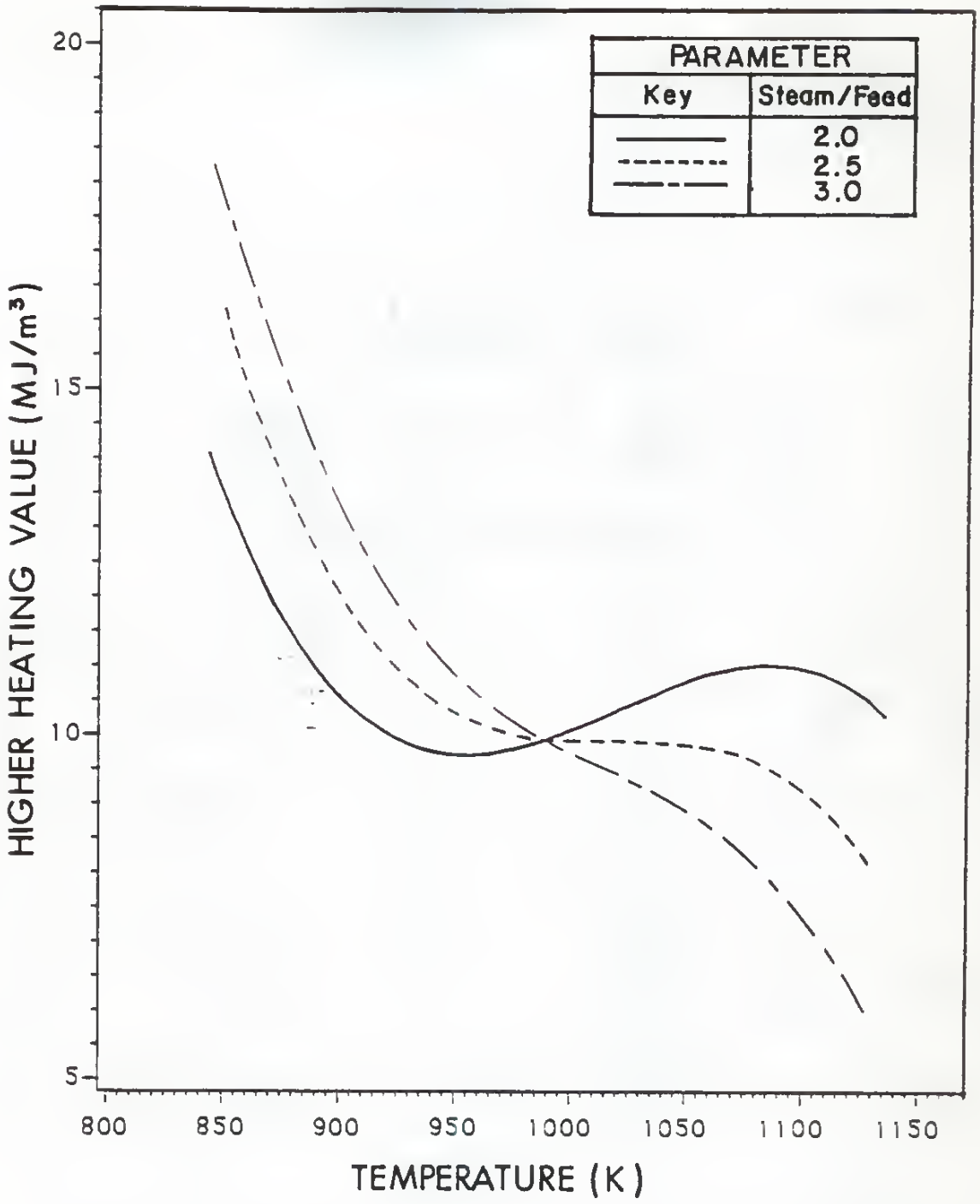

Fig. 15. Effect of steam-to-feed ratio and temperature on gas heating value.

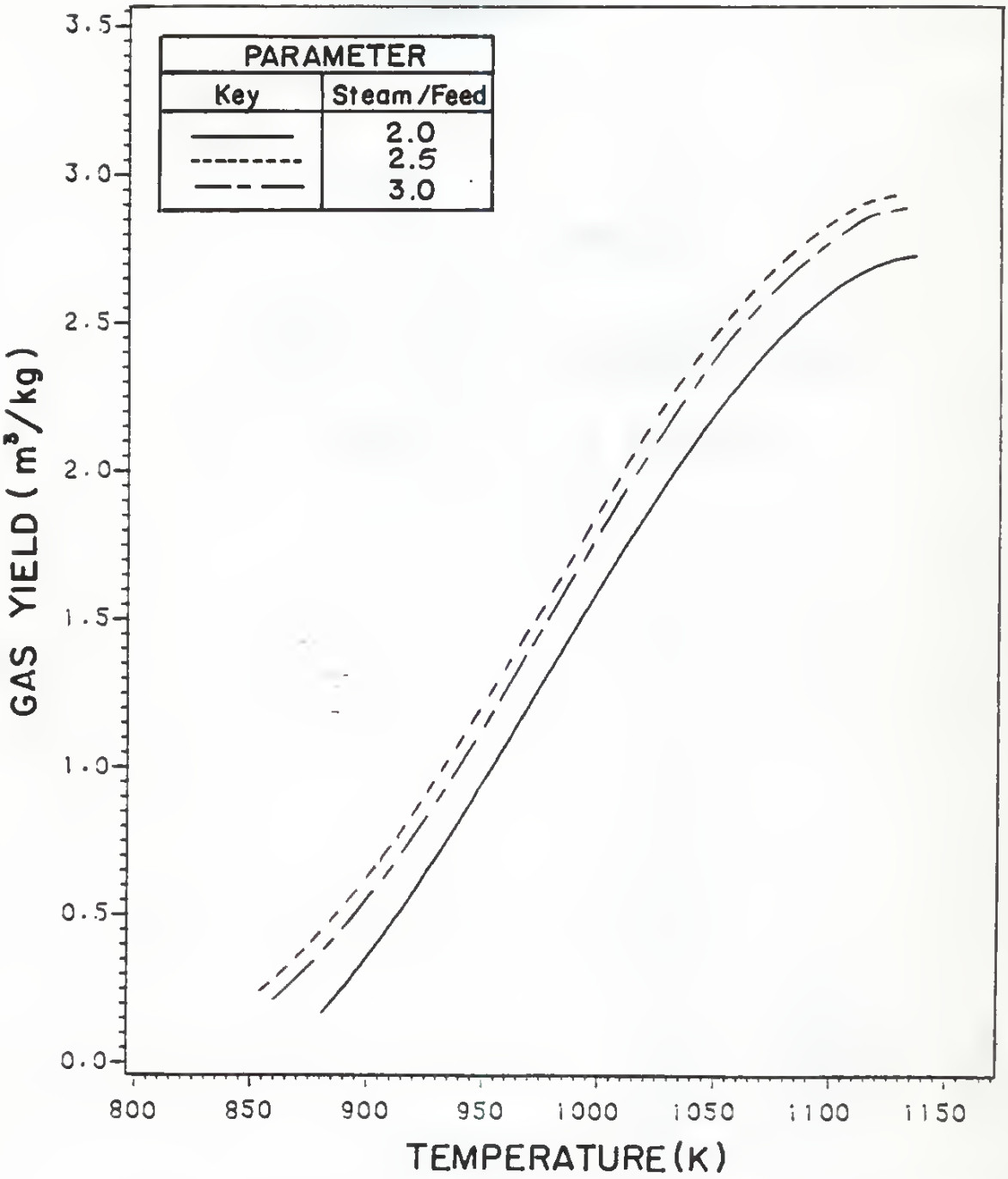

Fig. 16. Effect of steam-to-feed ratio and temperature on the gas yield.

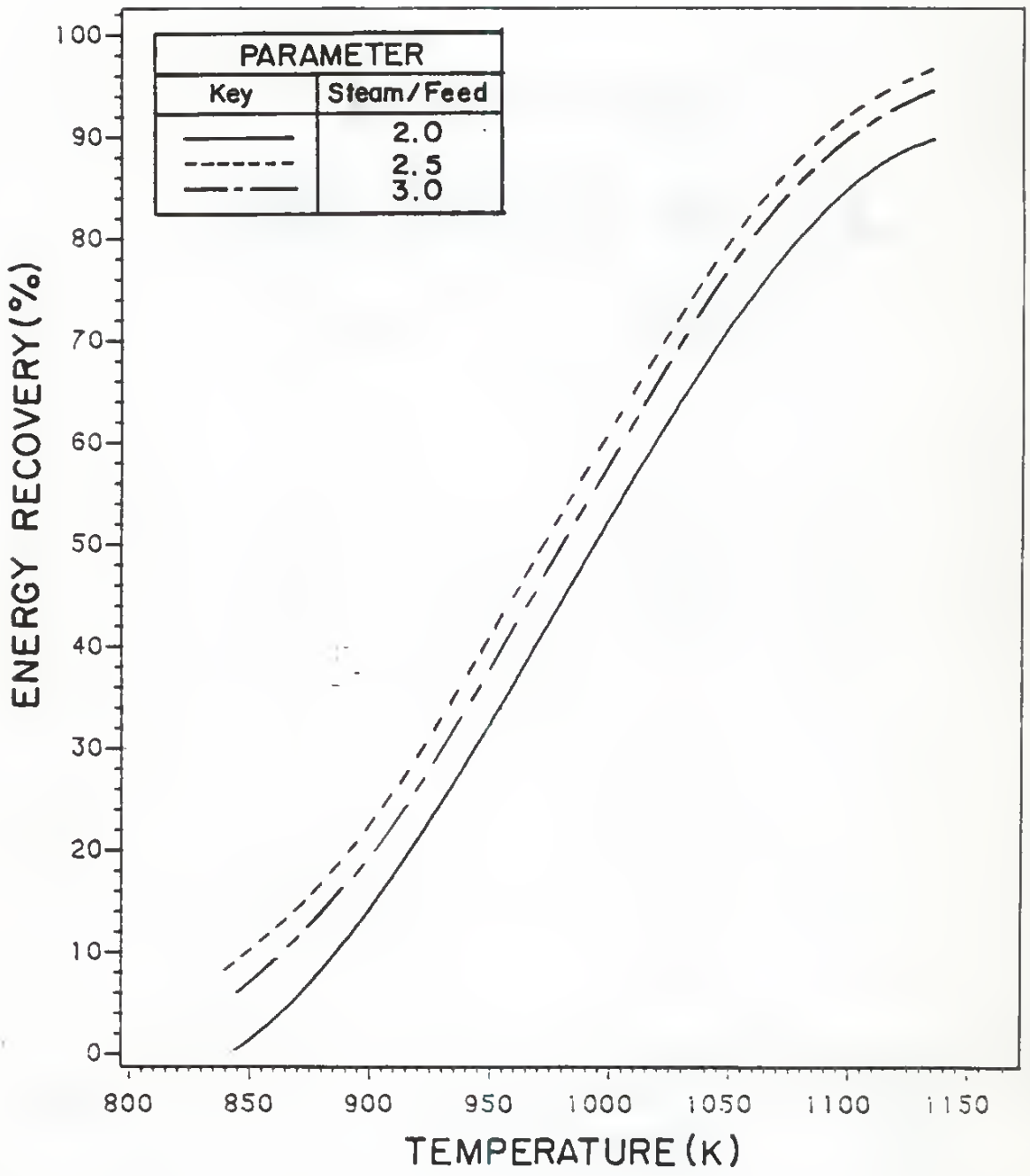

Fig. 17. Effect of steam-to-feed ratio and temperature on the energy recovery.

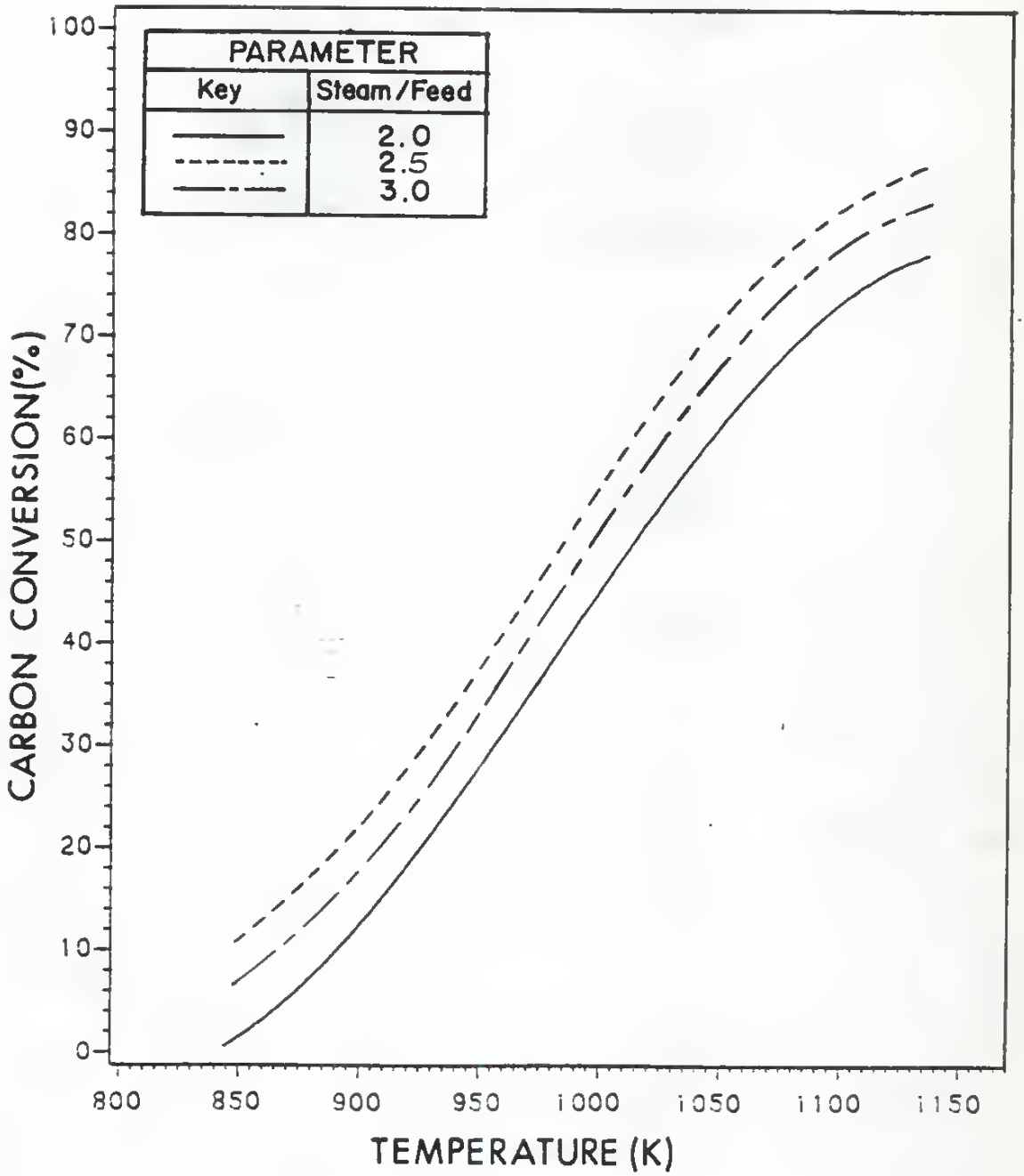

Fig. 18. Effect of steam-to-feed ratio and temperature on carbon conversion.

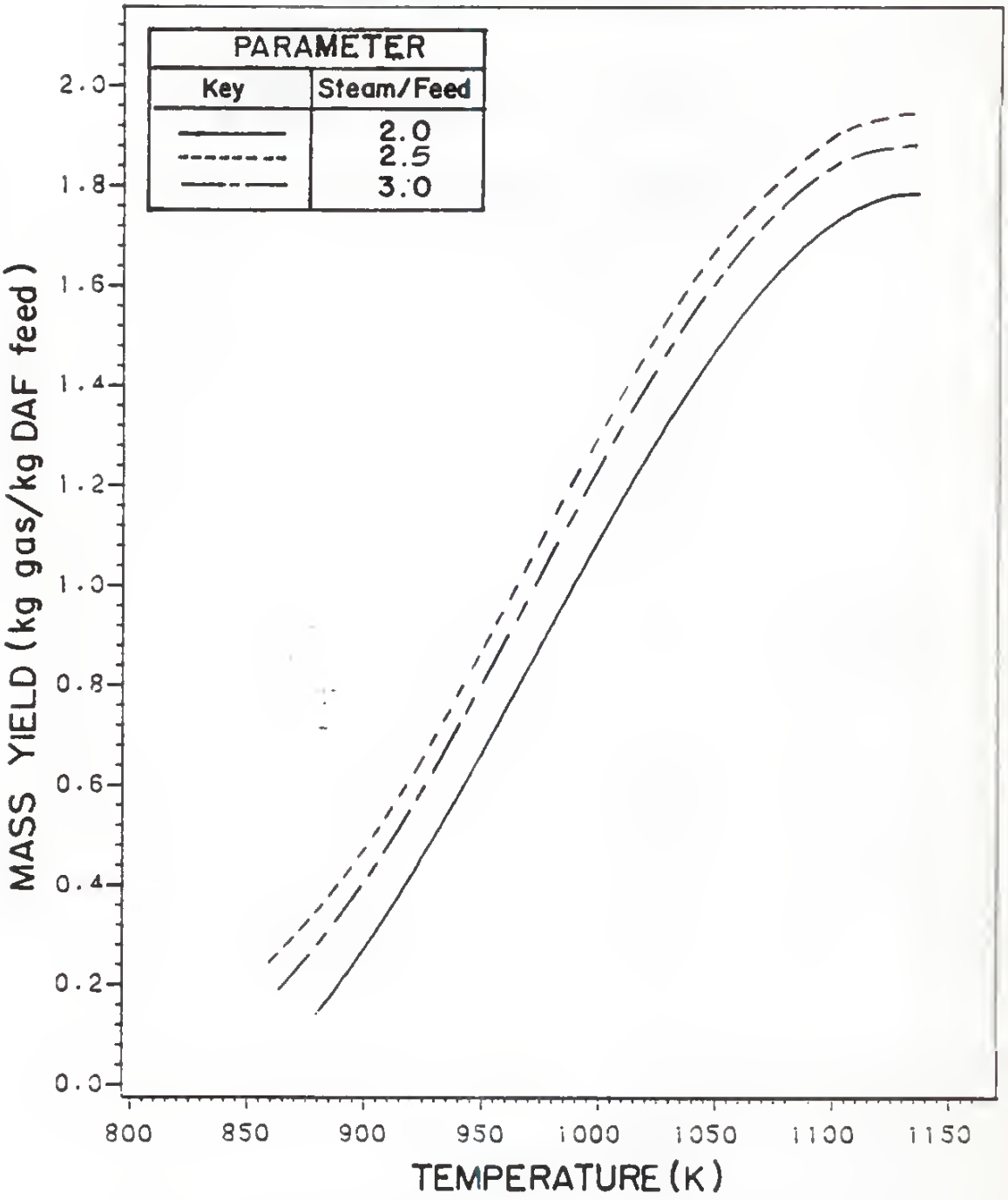

Fig. 19. Effect of steam-to-feed ratio and temperature on the gas mass yield.

CHAPTER IV

MATHEMATICAL MODELING OF COAL GASIFICATION IN A FLUIDIZED-BED REACTOR

INTRODUCTION

Conversion of the nation's vast resources of coal to liquid and gaseous fuels has been envisioned as a major contributor to the energy picture in the near future. Several feasible processes have been proposed; among them is fluidized-bed gasification. Although many contacting devices have been proposed for coal gasification, fluidized beds are widely used because of their advantageous characteristics, such as high rates of heat transfer and excellent gas-solid contacting. Even though numerous experimental studies on coal gasification were undertaken, relatively little has been done to model it.

It is well known that the scale-up, design, operation and control of any process are vastly facilitated by the availability of a mathematical model; fluidized-bed gasification is no exception. Modeling this process requires a knowledge of the hydrodynamics and chemical phenomena that take place in the bed. Also, any mathematical model developed must be verified experimentally before it can be implemented in practice.

Zeles (1978) presented a mathematical model for the simulation of steam-oxygen gasification of coal in a fluidized bed. A modification of the Bubble Assemblage Model was used to model the fluidized bed. Kinetic expressions for the reactions of carbon with O_2, H_2O (steam), H_2 and CO_2 were used for the emulsion and cloud phases. Simulated results based on the model compared favorably with the experimental data obtained by the Institute of Gas Technology (Zeles, 1978). The experiments were conducted in a 15.24 cm (6 inch) diameter fluidized-bed reactor at pressures from 25 to 40 atm. Elutriation and entrainment of char were not incorporated in this model. Lack of data on the rate of formation of individual volatile species made treatment of devolatization difficult. The model assumes that

gas composition is independent of temperature, thus simplifying it substantially. Dynamic characteristics of the gasification reactor were not studied; only steady-state results were presented.

Biba et al. (1978) modeled the gasification of coal under pressure in a fixed-bed reactor. Their paper focused on the parameters of reaction kinetics and on the transfer of material and energy which are necessary for developing the model of the fixed-bed reactor. The resultant system of differential equations were solved in order to calculate the concentration and temperature profiles in the solid and gas phases as a function of the bed height. The modified Euler method was employed for the solution in their work; however; only the steady-state behavior of the reactor was considered in their work.

A model for the fluidized-bed combustion of coal was presented by Becker et al. (1975). The material and energy balances for coal combustion were considered and models were developed for various terms in these balances. Both steady-state and transient operations were studied; however the governing equations of the model were not solved, and thus no comparison was made with experimental data to prove its validity.

A steady-state model of the moving bed coal gasifier was developed by Yoon et al. (1977), based on kinetics and transport rate processes, thermodynamic relations, and mass and energy balances. Model predictions were in good agreement with published plant data for the Lurgi gasifier.

Recently, Raman et al. (1981) presented a model to describe the fluidized-bed gasification of biomass and applied it to the gasification of feedlot manure. Several simplifying assumptions were imposed in deriving the model, and only steady-state solutions were obtained. Chang et al. (1983) extended this work and considered the dynamic modeling of biomass

gasification.

The objectives of this work were; 1) to gasify coal in an experimental fluidized-bed reactor, 2) to develop a mathematical model to describe the coal gasification in such a reactor, 3) to simulate the dynamic characteristics of the reactor, 4) to obtain experimentally steady-state performance data, and 5) to compare the experimental steady-state results with the simlulated data.

MODEL DEVELOPMENT

Gasification of coal in a fluidized-bed reactor involves chemical reactions as well as mass transport which are profoundly affected by hydrodynamics in the reactor. The present model is based on the two-phase theory of fluidization with the following assumptions (Davidson and Harrison, 1963).

1. The fluidized bed consists of two phases, namely, bubble and emulsion phases, which are homogeneously distributed statistically.
2. The flow of gas in excess of the minimum fluidization velocity passes through the bed in the form of bubbles, which are free of solids.
3. The voidage of the emulsion phase remains constant and is equal to that at incipient fluidization.
4. The bed can be characterized by an equivalent bubble size, and the flow of gas in the bubbles is in plug flow.
5. The emulsion phase is well mixed.
6. The bed is under isothermal condition.
7. No reaction takes place in the freeboard of the reactor.

Derivation of the Governing Equations

In deriving the governing equations, the flow of gases have been approximated by a despersive term. This has been done to facilitate the numerical solution of the resulting parabolic equations. The numerical values of the axial dispersion coefficients, D_{ib} and D_{ie}, have been chosen such that they represent nearly plug flow conditions

in the bubble phase and nearly completely mixed conditions in the emulsion phase. A schematic representation of the model is shown in Figure 1.

(a) Bubble phase: A mass balance on species i over an elemental volume of $A_b \Delta x$ in the bubble phase gives

(Accumulation of i)

= (rate of species i in by convection)- (rate of species i out by convection)

+ (rate of species i in by dispersion) - (rate of species i out by dispersion)

- (rate of species i out by exchange with the emulsion phase)

+ (rate of production of species i by chemical reaction)

or

$$\frac{\partial}{\partial t}(A_b \Delta x\, C_{ib}) = U_b A_b C_{ib}\Big|_x - U_b A_b C_{ib}\Big|_{x+\Delta x} - D_{ib} A_b \frac{\partial C_{ib}}{\partial x}\Big|_x + D_{ib} A_b \frac{\partial C_{ib}}{\partial x}\Big|_{x+\Delta x} - A_b \Delta x F_{be}(C_{ib}-C_{ie}) + A_b \Delta x\, R_{ib} \qquad (1)$$

Dividing both sides by $A_b \Delta x$ and letting $\Delta x \to 0$, we obtain

$$\frac{\partial C_{ib}}{\partial t} = -U_b \frac{\partial C_{ib}}{\partial x} + D_{ib} \frac{\partial^2 C_{ib}}{\partial x^2} - F_{be}(C_{ib} - C_{ie}) + R_{ib} \qquad (2)$$

(b) Emulsion phase: Similarly, a mass balance on gaseous species i over an elemental volume of $A_e \Delta x$ in the emulsion phase yields

$$\frac{\partial}{\partial t}(A_e \Delta x\, \varepsilon_{mf} C_{ie}) = U_e A_e C_{ie}\Big|_x - U_e A_e C_{ie}\Big|_{x+\Delta x}$$

$$- D_{ie} A_e \frac{\partial C_{ie}}{\partial x}\Big|_x + D_{ie} A_e \frac{\partial C_{ie}}{\partial x}\Big|_{x+\Delta x}$$

$$+ A_b \Delta x \Gamma_{be}(C_{ib} - C_{ie}) + A_e \Delta x\, R_{ie} \qquad (3)$$

Dividing both sides of this expression by $A_e \varepsilon_{mf} \Delta x$ and letting $\Delta x \to 0$, we obtain

$$\frac{\partial C_{ie}}{\partial t} = -\frac{U_e}{\varepsilon_{mf}} \frac{\partial C_{ie}}{\partial x} + \frac{D_{ie}}{\varepsilon_{mf}} \frac{\partial^2 C_{ie}}{\partial x^2} + \frac{A_b}{A_e} \frac{F_{be}}{\varepsilon_{mf}} (C_{ib} - C_{ie}) + \frac{R_{ie}}{\varepsilon_{mf}} \qquad (4)$$

Here, R_{ie} includes the rate of production of species i by the devolatization of the feed as well as by other chemical reactions in the emulsion phase.

For the solids in the emulsion phase, C_s is defined as the weight ratio of char with respect to the inert solids in the bed, and B is the total weight of the inerts in the bed. The solid concentration is defined in this manner because the gasification of coal is frequently conducted in a fluidized-bed reactor containing an inert matrix. Since the solids are assumed to be completely mixed in the emulsion phase, the material balance on the entire bed yields

$$B \frac{\partial C_s}{\partial t} = (W_{in} - W_{out}) + R_s$$

or

$$\frac{\partial C_s}{\partial t} = \left(\frac{W_{in} - W_{out}}{B}\right) + \frac{R_s}{B} \qquad (5)$$

The appropriate initial and boundary conditions (for gaseous species i in the bubble and emulsion phases, and char as the solid in the emulsion phase) are:

$$t = 0;\ 0 \leq x \leq H \qquad \begin{cases} C_{ib} = C_{io} \\ C_{ie} = C_{io} \\ C_s = 0 \end{cases} \tag{6}$$

$$t > 0;\ x = 0 \qquad \begin{cases} C_{ib} - \dfrac{D_{ib}}{U_b} \dfrac{\partial C_{ib}}{\partial x} = C_{io} \\ C_{ie} - \dfrac{D_{ie}}{U_e} \dfrac{\partial C_{ie}}{\partial x} = C_{io} \end{cases} \tag{7}$$

$$t > 0;\ x = H \qquad \begin{cases} \dfrac{\partial C_{ib}}{\partial x} = 0 \\ \dfrac{\partial C_{ie}}{\partial x} = 0 \end{cases} \tag{8}$$

Where, $i = 1, 2, \ldots, n$ with n representing the total number of gaseous species present in the reactor.

Note that the general governing equations; equations (1) through (4), with initial conditions, equation (6), and the boundary conditions, equations (7) and (8), may be used to describe various fluidization processes involving chemical reactions with their corresponding rate terms R_{ib}, R_{ie}, and R_s.

Chemical Reactions and Expressions of Rate Terms

In our previous studies (Howell, 1979; Raman et al., 1981; Chang et al., 1983), we have visualized that gasification of coal or any carbonaceous material takes place in three steps:

(1) Coal $\xrightarrow{\text{devolatization}}$ Heavy volatiles

+ Gas (CO_2, H_2, CO_2, CH_4, etc.) + Char

(2) Heavy volatiles $\xrightarrow{\text{cracking}}$ Liquid + Gas

(3) Char gasification reactions:

$$C + H_2O \xrightarrow{k_1} CO + H_2$$

$$C + CO_2 \xrightarrow{k_2} 2CO$$

$$C + 2H_2 \xrightarrow{k_3} CH_4$$

Water-gas shift reaction:

$$CO + H_2O \underset{k_5}{\overset{k_4}{\rightleftharpoons}} CO_2 + H_2$$

The first step in coal gasification, devolatization or pyrolysis, is a very rapid process, occurring almost instantaneously as small coal particles are fed to a fluidized bed and heated rapidly to the gasification temperature. Anthony and Howard (1976) have investigated this phenomenon in detail and have concluded that the devolatization of coal depends apparently on such operating conditions as the temperature, pressure, particle size, constituents of the carrier gas, type of coal and heating rate. The decomposition can be accelerated by elevating the temperature. When heated at a more or less conventional rate, coal begins to decompose at 350° to 400°C into a carbon rich residue and hydrogen rich volatile fraction. The decomposition continues until a temperature of about 950°C is reached. The volatiles are comprised of various gases and liquids, the relative proportions of which depend on the coal type, the manner and rate of heating and volatiles residence time. Peters et al. (1965) found that rapid heating techniques for small coal particles produces more volatiles than 'slow heating' methods.

The devolatization of coal has been examined by Anthony and Howard (1976) and Howell (1979); they have found that the kinetics can be described by the following equation;

$$1 - y = \frac{V^* - V}{V^*} = \int_0^{\alpha} \exp\left[-\int_0^t k_o e^{-E/RT} dt\right] f(E)\,dE \qquad (9)$$

where

$$f(E) = \frac{\exp\left[-(E-E_m)^2/2\sigma^2\right]}{\sigma(2\pi)^{1/2}} \tag{10}$$

and y is the fraction of coal devolatized.

A fluidized-bed reactor has an exceedingly high heat transfer rate, thus heating a small coal particle rapidly to the temperature of the reactor, which remains essentially constant. This fast response to temperature allows equation (9) to be integrated at isothermal conditions, thereby yielding

$$1-y = \int_0^{\alpha} \exp\left(-k_o t e^{-E/RT}\right) f(E)\,dE \tag{11}$$

According to Pitt (1962), the term $\exp(-k_o t e^{-E/RT})$ in the integrand changes from 0 to 1 as a steep S-shaped curve which can be approximated by a step function at

$$k_o t e^{-E/RT} = 1$$

Using this approximation, equation (11) can be integrated to give

$$y = F(\bar{z}) = \int_{-\infty}^{\bar{z}} \frac{e^{-z^2/2}}{(2\pi)^{\frac{1}{2}}}\,dz \tag{12}$$

where

$$\bar{z} = \frac{RT\,\ln(k_o t)-E_m}{\sigma} \tag{13}$$

Equation (12) is the standard normal distribution function. Anthony (1974) has determined average values of the kinetic parameters for Pittsburgh Seam Bituminous coal, whose properties are very similar to those of Kansas Bituminous coal, as

$$k_o = 2.91 \times 10^9 \text{ sec}^{-1}$$

E_m = 36.89 kcal/mole

σ = 4.18 kcal/mole

Equation (13) permits the evaluation of $\bar{z}$ as a function of the solid residence time, t, and temperature. Expressions for $\bar{z}$ for coal at selected residence times are presented in Table 1. The plot of y vs t at different temperatures is shown in Figure 2. Normally the gasification temperatures for coal are of the order of 900 K, and the residence time of the solids in a fluidized-bed reactor is relatively high, compared to that of the gas. In the light of this, it can be deduced from Figure 2 and Table 1 that the temperature is a dominant factor influencing the extent of devolatization in the reactor. We also see in Figure 2 that at temperatures above 900 K, ninety percent of the devolatization is complete in less than 1 second. This naturally gives rise to the assumption that the devolatization step is instantaneous in a fluidized-bed gasifier. This assumption simplifies the model substantially.

In the range of temperature (800K-1200K) and at atmospheric pressure under which coal is generally gasified, only eight species, CO, CO_2, H_2, H_2O, CH_4, C_2H_6, C_3H_6 (i = 1, 2, ..., 7, respectively) and char need be considered. Also, these species are the components that have significant concentrations in the gas produced during gasification. Therefore, the total number of differential equations to be solved are 15 (7 for C_{ib}, 7 for C_{ie}, and 1 for char). However, since the char gasification and water-gas shift reactions do not involve C_2H_6 and C_3H_6, the concentration of C_2H_6 and C_3H_6 predicted by the devolatization data can be added to the final gas concentration. This reduces the number of PDE to 11. It is to be noted that the boundary conditions of the model preclude any chemical reacitons taking place in the freeboard of the reactor, as stated in the initial assumptions for the model development.

The expressions for the rate terms are

$$R_{1b} = R_{4b} = -R_b \tag{14}$$

$$R_{2b} = R_{3b} = R_b \tag{15}$$

$$R_{5b} = 0 \tag{16}$$

$$R_{1e} = S(k_1 C_{4e} + \frac{k_2 C_{2e}}{2}) - R_{sr} \tag{17}$$

$$R_{2e} = -S(k_2 C_{2e}) + R_{sr} \tag{18}$$

$$R_{3e} = S(k_1 C_{4e} - k_3 C_{3e}) + R_{sr} \tag{19}$$

$$R_{4e} = -Sk_1 C_{4e} - R_{sr} \tag{20}$$

$$R_{5e} = \frac{1}{2} (Sk_3 C_{3e}) \tag{21}$$

$$R_s = -(k_1 C_{4e} + k_2 C_{2e} + \frac{k_3 C_{3e}}{2}) B\, A_c C_s M_c \tag{22}$$

where

$$R_b = k_4 C_{1b} C_{4b} - k_5 C_{2b} C_{3b} \tag{23}$$

$$C_g = \frac{F}{HA(1-\delta)} \tag{24}$$

$$S = \frac{B\, A_c C_s}{HA(1-\delta)} \tag{25}$$

$$R_{sr} = k_4 C_{1e} C_{4e} - k_5 C_{2e} C_{3e} \tag{26}$$

The bubble phase equations for each species can now be written as

$$\text{CO:} \quad \frac{\partial C_{1b}}{\partial t} = -U_b \frac{\partial C_{1b}}{\partial x} + D_b \frac{\partial^2 C_{1b}}{\partial x^2} - F_{be} (C_{1b} - C_{1e}) - R_b \tag{27}$$

$$CO_2: \quad \frac{\partial C_{2b}}{\partial t} = -U_b \frac{\partial C_{2b}}{\partial x} + D_b \frac{\partial^2 C_{2b}}{\partial x^2} - F_{be}(C_{2b} - C_{2e}) + R_b \tag{28}$$

$$H_2: \quad \frac{\partial C_{2b}}{\partial t} = -U_b \frac{\partial C_{3b}}{\partial x} + D_b \frac{\partial^2 C_{3b}}{\partial x^2} - F_{be}(C_{3b} - C_{3e}) + R_b \tag{29}$$

$$H_2O: \quad \frac{\partial C_{4b}}{\partial t} = -U_b \frac{\partial C_{4b}}{\partial x} + D_b \frac{\partial^2 C_{4b}}{\partial x^2} - F_{be}(C_{4b} - C_{4e}) - R_b \tag{30}$$

$$CH_4: \quad \frac{\partial C_{5b}}{\partial t} = -U_b \frac{\partial C_{5b}}{\partial x} + D_b \frac{\partial^2 C_{4b}}{\partial x^2} - F_{be}(C_{5b} - C_{5e}) \tag{31}$$

The emulsion phase equations are

$$CO: \quad \frac{\partial C_{1e}}{\partial t} = -\frac{U_e}{\varepsilon_{mf}} \frac{\partial C_{1e}}{\partial x} + \frac{D_e}{\varepsilon_{mf}} + \frac{\partial^2 C_{1e}}{\partial x^2} + \frac{F_{be}}{\varepsilon_{mf}} \frac{\delta}{(1-\delta)} (C_{1b} - C_{1e}) + \frac{R_{1e}}{\varepsilon_{mf}} + \frac{C_g C_2}{\varepsilon_{mf}} \tag{32}$$

$$CO_2: \quad \frac{\partial C_{2e}}{\partial t} = -\frac{U_e}{\varepsilon_{mf}} \frac{\partial C_{2e}}{\partial x} + \frac{D_e}{\varepsilon_{mf}} \frac{\partial^2 C_{2e}}{\partial x^2} + \frac{F_{be}}{\varepsilon_{mf}} \frac{\delta}{(1-\delta)} (C_{2b} - C_{2e}) + \frac{R_{2e}}{\varepsilon_{mf}} + \frac{C_g C_2}{\varepsilon_{mf}} \tag{33}$$

$$H_2: \quad \frac{\partial C_{3e}}{\partial t} = -\frac{U_e}{\varepsilon_{mf}} \frac{\partial C_{3e}}{\partial x} + \frac{D_e}{\varepsilon_{mf}} \frac{\partial^2 C_{3e}}{\partial x^2} + \frac{F_{be}}{\varepsilon_{mf}} \frac{\delta}{(1-\delta)} (C_{3b} - C_{3e}) + \frac{R_{3e}}{\varepsilon_{mf}} + \frac{C_g C_3}{\varepsilon_{mf}} \tag{34}$$

$$H_2O: \quad \frac{\partial C_{4e}}{\partial t} = -\frac{U_e}{\varepsilon_{mf}}\frac{\partial C_{4e}}{\partial x} + \frac{D_e}{\varepsilon_{mf}}\frac{\partial^2 C_{4e}}{\partial x^2} + \frac{F_{be}}{\varepsilon_{mf}}\frac{\delta}{(1-\delta)}(C_{4b} - C_{4e}) + \frac{R_{4e}}{\varepsilon_{mf}} + \frac{C_g C_4}{\varepsilon_{mf}} \tag{35}$$

$$CH_4: \quad \frac{\partial C_{5e}}{\partial t} = -\frac{U_e}{\varepsilon_{mf}}\frac{\partial C_{5e}}{\partial x} + \frac{D_e}{\varepsilon_{mf}}\frac{\partial^2 C_{5e}}{\partial x^2} + \frac{F_{be}}{\varepsilon_{mf}}\frac{\delta}{(1-\delta)}(C_{5b} - C_{5e}) + \frac{R_{5e}}{\varepsilon_{mf}} + \frac{C_g C_5}{\varepsilon_{mf}} \tag{36}$$

$$CHAR: \quad \frac{\partial C_s}{\partial t} = \frac{(W_{in} - W_{out})}{B} + \frac{R_s}{B} \tag{37}$$

Note that reactions involving the cracking of heavy volatiles are not included in the rate terms, however, an initial yield of heavy volatiles and its distribution are considered.

Hydrodynamic Relationships

Hydrodynamics of the bubbling phenomenon interrelates the variables involved in this model. Functional relationships among the parameters and variables that depend on the hydrodynamics of the fluid-bed are given below.

1. The bubble diameter, d_b, is estimated using Mori and Wen's (1975) correlation, i.e.,

$$d_b = D_{bm} - (D_{bm} - D_{bo}) \exp(-0.3\, x/D)$$

$$D_{bm} = 0.652\, \{A(U_o - U_{mf})\}^{0.4}$$

$$D_{bo} = 0.00376 (U_o - U_{mf})^2$$

where D_{bo} is the initial bubble diameter, and D_{bm} is the maximum bubble diameter. The equivalent bubble diameter, d_b, (Kunii and Levenspiel, 1969) is calculated at the middle of the total bed height, $x = H/2$.

2. The bubble velocity, U_b, is calculated by using the correlation proposed by Davidson and Harrison (1963).

$$U_b = (U_o - U_{mf}) + 0.711\, (g\, D_b)^{0.5}$$

3. The volume fraction of bubble phase, δ, is calculated from

$$\delta = (U_o - U_{mf})/U_b$$

4. The emulsion phase gas velocity, U_e, is calculated as

$$U_e = U_{mf}/(1-\delta)$$

5. The gas-exchange coefficient between bubble and emulsion phases, F_{be}, is calculated from the following correlation proposed by Kobayashi et al. (1967).

$$F_{be} = 0.11/D_b$$

6. The height of the expanded bed, H, is calculated iteratively from the material balance on the solid as

$$H = \frac{H_{mf}}{(1-\delta)}$$

Additional Assumptions Imposed in Simulation of Coal Gasification Process.

To illustrate the application of the present general model, the gasification of coal in our experimental fluidized-bed gasifer has been simulated. Additional assumptions made for simulating this particular process are:

1. The fraction of char and total volatiles generated in the devolatization step are the same as those obtained form thermogravimetric studies. Data obtained by Howell (1979) were used and are presented in Table 2.

2. The fractions of liquid and gas in the total volatiles generated as well as the initial composition of the gas, were taken from the results obtained by Yeboah et al. (1980). The initial product distribution and the initial gas composition are presented in Table 2.

3. Adjustments were made on the kinetic parameters, involving coal char, obtained by Biba et al. (1978). This was done to incorporate the fast rate of char-gasification. These

adjusted parameters, listed in Table 3, were used for simulation. The kinetic parameters of the gas phase shift reaction have the values reported by Biba et al. (1978) and by Yoon (1978).

Although, Yeboah et al. (1980) obtained the data by conducting atmospheric pressure pyrolysis of Illinois No. 6 Bituminous Coal in a fluidized-bed reactor using sand as the bed material, the second assumption is made because no devolatization data on Kansas Bituminous Coal is available. The proximate and ultimate analysis of both types of coal are very similar as shown in Table 4. Since pyrolysis was performed in an inert atmosphere in the temperature range of 540°C and 760°C, the secondary reactions involving the volatiles produced, and the char, are not significant because of the low temperature. It is, therefore, reasonable to assume that the product distribution reported by Yeboah et al. (1980) corresponds directly to the primary devolatization reaction.

METHOD OF NUMERICAL SOLUTION

There are eleven nonlinear partial differential equations that need be solved for simulation of the reactor. The simultaneous solution of these parabolic partial differential equations yields the transient concentration distributions of different species in the reactor. The numerical solution of these nonlinear PDEs is often complicated and time consuming. Sincovec and Madsen (1975) have developed a software interface that overcomes the difficulties associated with solving stiff and nonstiff nonlinear parabolic PDEs. It has been employed to numerically solve the governing equations of the model. The package uses the "Method of Lines" technique for spatial discretization to convert the nonlinear partial differential equations into a system of time-dependent, nonlinear, ordinary differential equations. Gear's backward difference formulas are then used for the time integration. A modified Newton's method with internally generated Jacobian matrix is used to solve the nonlinear equations. For each calculation, the subroutine automatically adjusts the time step size to achieve a specified error level.

A flow diagram of the computational procedure based on the present model is given in Figure 3. The relative error bound for the time integration process is set at 10^{-3} and the number of spatial meshes specified for this study is 11.

It should be noted that the dynamic solutions of the system include the steady-state solutions as the limit.

EXPERIMENTAL

Facilities

The fluidized-bed reactor used in this work was designed to study pyrolysis and gasification of various carbonaceous materials, e.g. coal, at atmospheric pressure and over a temperature range of 650 K to 1450K. The gasification system, as shown in Figure 4 consisted of three primary sections: the reactor section, the gas clean-up section, and the gas sampling and analysis section. Construction details for the the reactor are shown in Figure 5.

The inert matrix used for bed material was composed approximately of a mixture of 25% by weight of limestone and 75% by weight of silica sand. The limestone was used to prevent bed agglomeration which typically occurs in a bed composed only of sand (Walawender et al., 1981). The limestone particle size was -7 to +50 mesh (2.82 mm-0.287 mm); the sand particle size was -30 to + 50 mesh (0.595 mm-0.297 mm). The static bed height was 8-10 cm.

The reactor was heated by means of ten quarter cylindrical electrical resistance heaters, each capable of delivering up to 1200 watts of power with a maximum sustained operating temperature of 1500 K. Voltage to each of them was controlled by three-mode, PID controllers (Omega model 49K-814). There were five chromel alumel type thermocouples installed in the reactor. One of them, a sliding thermocouple, was used to measure the temperature profile inside the reactor. The others were located in the freeboard, fluidized bed section, preheating zone and the middle of the reactor inserted into the reactor from the side. controllers recorded the temperatures from these thermocouples and accordingly activated the heaters as required to maintain the temperature in the reactor at a preset value. A pressure probe, connected to a manometer, indicated the bed pressure and the state of

fluidization.

The feed was introduced into the reactor by gravity flow through a vertical feedpipe (3 cm I.D.) which discharged at a location about 8 cm above the static bed. A Vibra Screw Feeder (Model SCR-20) with a solid core flight screw was used to supply the feed at an uniform volumetric rate. A purge stream of N_2 aided solid flow through the feedpipe and prevented gas backflow and subsequent condensation of vapor in the feeder. The flow rate of nitrogen was measured by a wet test meter. To prevent the feed materials from prematurely devolatizing before reaching the bed (and possibly clogging the feedpipe in the process), the feedpipe was equipped with a water jacket which maintained the temperature inside the feedpipe below 400 K. Steam, as the sole fluidizing gas, was produced externally in a Sussman Hot Shot Electric Boiler (Model MB-6).

The gas exiting from the reactor was passed through a well-insulated cyclone which removed the elutriated fine solid particles, e.g. char, from the gas stream. After leaving the cyclone the gas stream passed through two water cooled, double pipe heat exchangers in series. This resulted in condensation of steam and tar, which was collected in a condensate receiver. Further gas cleaning was achieved by means of a dry scrubber packed with glass wool. This device was effective in removing the fine condensible mist suspended in the gas with little pressure drop. A wet test meter connected to a strip chart recorder measured the flow rate of the gas. A side draw of the off-gas was passed through a drying column packed with Drierite ($CaSO_4$) and then sent to an on-line process gas-chromatograph for analysis. The remaining gas was vented to the atmosphere. Nitrogen in the product gas, acting a tracer, allowed computation of the rate of product gas generation.

Procedure

For start-up of each experimental run, the reactor heaters and steam generators were turned on, and the controllers were set at the desired operating temperatures. During the heat-up period, air served as the fluidizing agent and as the feed pipe purge gas; the water flow to the jacketed feed pipe was turned on to maintain the feed pipe cool. The steam generator was set to supply steam at constant pressure. Once steam was available, the fluidizing air flow was gradually replaced by steam. The volumetric flow rate of steam required to maintain fluidization was measured by collecting condensate downstream from the heat-exchangers and controlled by a needle valve on the steam line.

When the bed and the freeboard reached the selected operating temperature, the axial temperature profile was measured, and if necessary minor corrections were made by adjusting the controllers to ensure a uniform temperature profile. The exit-gas from the system was analyzed to ensure that the system was free of air. At this point, the system was ready for feeding to begin. Total start-up time was about two hours from a cold start and about one hour from a warm start. Normally at the end of each run, the heaters were not turned off but just turned down so that the system stayed warm overnight.

A slight drop in the temperature of the reactor occurred when feeding was initiated, but was corrected automatically by the controllers. A gas sample was taken about 5 minutes after the initiation of feeding and every 11 minutes thereafter. Condensate and nitrogen flow rates were measured every 10 minutes throughout the run. A typical experiment at a given temperature lasted 100 to 120 minutes with the last 50 to 60 minutes yielding steady gas chromatograph readings. The feed rate of solids was

measured by disconnecting the lower section of the feed pipe and weighing the effluent collected over three 3-minute time intervals. This was carried out both at the start and end of the run.

Chemical Analyses

Analysis of the dry off-gas was conducted by an applied automation (Optichrom 2100) on-line process gas chromatograph. The components of interest were H_2, CO, CO_2, CH_4, C_2H_4, C_2H_6, C_3H_6, C_3H_8, O_2, and N_2. The chromatograph had a cycle time of 11 minutes. Moisture and ash analyses of feed material were performed according to standard ASTM procedures in a ventilated oven and muffle furnace, respectively. Elemental analysis of the feed was done using a Perkin-Elmer Model 240B Elemental Analyzer.

Operating Conditions

The operating conditions used in the experiment are summarized in Table 4. By adjusting the steam rate with the temperature of the run, an attempt was made to maintain a fairly constant mean residence time for the volatiles over all the runs. The gas phase mean residence time ranged from 4 to 7 seconds. The residence time was estimated on the basis of the reactor temperature, total dry gas flowrate, and steam rate. The steam rate was varied from 15.33 g/min. to 11.0 g/min. The average feed rate was 5.2 g/min. The principal experimental variable was the reactor temperature. All the experiments were performed with the temperature of the freeboard being same as in the fluidized bed section, resulting in an uniform axial temperature profile. The range of temperature studied was from 823 K to 1133 K.

Feed Material

The material used for the gasification experiments was bituminous coal from the Rowe coal bed in southeast Kansas. The particle size of the feed was -14 to +100 mesh with a mean particle size of 0.297 mm. The proximate and ultimate analyses of the coal are given in Table 4.

RESULTS AND DISCUSSION

The experimentally observed effect of temperature on the composition of the product gas is shown in Figures 6 and 7. Sixty-six data points for each component are shown in these figures. The total product gas mass yield as a function of temperature is plotted in Figure 8. The lines in each figure represent the simultaneous regression analysis of the data. Experimentally determined mass yields of the major components of the gas are presented in Table 6.

The concentration of H_2 increased with temperature and ranged from 51.1% at 873K to 60.0% at 1073K. Carbon dioxide increased from 25.0% at 873K to 30.5% at 923K and then decreased to 16.0% at 1073K. Methane decreased slightly with temperature ranging from 11.1% at 873K to 2.9% at 1073K. The minor components, C_2H_4, C_2H_6, C_3H_6 and C_3H_8, all decreased in concentration with an increase in temperature; their combined composition represented less than 3-4% of the total gas.

Mass yield of the product gas increased from 0.12 kg gas/kg DAF feed at 850 K to 1.88 kg gas/kg DAF feed at 1150 K. Mass yields greater than 1.0 kg gas/kg DAF feed were obtained at temperatures greater than 970 K (Figure 8). These high yields were simply due to steam becoming a part of the produced gas through water-gas shift and char gasification reactions. These reactions were enhanced because of the large excess steam in the experimental reactor system. Moreover, the small size of char particles made them highly reactive. The experimental data indicate that the water-gas shift and char-gasification reactions were the major factors influencing the gas composition and mass yield; the rate of these reactions increased as the temperature increased. It was also observed that tar cracking reactions were essentially complete below 970 K. The residence

time of the volatiles varied between 4 and 7 seconds, thereby ensuring that the cracking reactions were complete at a given temperature.

The experimentally determined product gas compositions approached steady-state within 15 to 20 minutes after the initiation of feeding in the reactor. The elutriation rate of char and the amount of char accumulated in the bed reached steady-state values within 20 to 30 minutes. The observed carbon conversion increased from 7% at 850 K to 82% at 1125 K. The carbon conversion was estimated to be 80% at 1050 K from the steady state char output. This over-estimated the conversion in light of the hold-up of char in the connecting pipes.

Figures 9 and 10 present the simulated transient dry product gas compositions for temperatures of 923 K and 1033 K, respectively. Since transient experimental data are not available, only the steady-state product gas compositions and mass yields predicted by the model are compared with the experimental data in Table 6. Note that the simulated gas compositions and mass yields are in good agreement with the experimental results at the two temperatures presented. At both temperatures, the molar concentrations as well as the mass yields of H_2 and CO predicted by the model are slightly higher than the experimental values, whereas the opposite is true for the molar concentrations of CO_2 and CH_4. This can be explained by the fact that the kinetic parameters chosen for simulating the char gasification reactions render the rates of these reactions slightly higher than the experimental rates. In fact, the model should predict low H_2 mass yields since tar cracking reactions, which produces additional H_2, are not included.

For the preliminary simulations, the rate constants given by Biba et al. (1978) for char gasification reactions were used since the corresponding

data were not available for Kansas bituminous coal. It was found that the model predicted negligible char gasification reactions for their condition. Since char gasification was extensive in our experiments, it was concluded that the kinetic parameters proposed by Biba et al. did not represent appropriate values for the coal under investigation. The experimentally determined frequency factors cited in the literature are strictly dependent on the type of coal, specific surface area, and corresponding values of the activation energy. It is necessary, therefore, to select a suitable set of parameters for the specific coal under investigation. Sensitivity studies of the model simulation results were conducted using different values of the frequency factor for the char gasification reactions. The resulting gas composition and mass yields were compared with the corresponding experimental values. This sensitivity analysis has yielded the frequency factors employed in the present simulation (Table 3). It should be noted that Biba et al. (1978) used coal with a particle size of the order of 2 cm, whereas the average coal particle size used in the present work was only 0.3 mm. Due to attrition in the bed the coal particles probably became even smaller resulting in an order of magnitude increase in their relativity.

The results predicted by the model are in good agreement with the experimental results, as shown in Table 6. It can be seen that the simulated mass yields of CO and H_2 are higher than the corresponding experimental observations; the opposite is true for CO_2. However, the rate constants used for the simulations predict trends that are quite consistent with the experimental observations, especially in view of the complexity of the overall system and the mathematical model.

Factors which are not taken into account in deriving the model include the effects of the residence time of the volatiles in the freeboard and tar

cracking. Recall that the residence time of the volatiles was found to be 4 to 7 seconds in the experimental system. The previous biomass gasification experiments in our pilot plant indicated that residence times of this order were sufficient to complete the cracking reactions at a given temperature (Walawender et al., 1978). Note that long gas phase residence times also increase the extent of water-gas shift reaction, thus producing additional CO_2 and H_2. A comprehensive simulation should include the cracking reactions involving the heavy volatiles and their time-temperature history in both the fluidized-bed and the freeboard. The experimental results suggest significant tar cracking at temperatures below 940 K. Since tar contributes 15 16 weight % of the initial feed, the tar cracking reactions should be incorporated in refining the model.

The simulated char content of the bed increases with time as shown in Figure 11. Notice that the amount of char accumulated in the bed approaches a steady value faster at a higher temperature (1033 K) than that at a lower temperature (923 K). Furthermore, a greater amount of char accumulates in the bed at the lower temperature. This is expected since the extent of the char gasification reactions increases with an increase in the temperature. As mentioned earlier, the weight of the char in the bed reached a steady value 20 to 30 minutes after the initiation of feeding in the experiments. The simulation has been carried out only for the first 16.7 min. after the initiation of feeding due to high computational costs. Even within the first 1000 seconds the weight of char in the bed tended towards a steady value, especially at the higher temperature. The foregoing discussion further substantiates that the proposed model simuluates the trend observed in the experimental system.

The axial concentration profiles predicted by the simulation are shown in Figure 12 for the major gas components (H_2, CO, and CO_2) in both the bubble and emulsion phases. It can be seen that the concentrations of H_2, CO, and CO_2 in the bubble phase increase with the bed height and that each component approaches its concentration in the emulsion phase before exiting from the top of the bed. This implies intensive interphase mixing between the emulsion and bubble phases under the operating conditions simulated. Also, inspection of the transient solutions (Figures 9 and 10) shows that the gas composition reaches steady state in about 800~900 seconds, thus agreeing well with the experimental observations.

To implement the present model in practice, several refinements need be made in three specific areas. The first involves the inclusion of the reactions of heavy volatiles. To do so requires the following information: (1) knowledge of the molecular species present in the heavy volatiles and their distribution, (2) kinetics of their cracking reactions, and (3) knowledge of the time-temperature history of the volatiles. The second entails improvement of the initial conditions of the model pertaining to the initial devolatization and of the rate constants for the gasification reactions. To achieve this, the initial product distribution and kinetic rate constants for the char formed from the coal of interest are needed. The third requires incorporation of the freeboard reactions in the model.

CONCLUSIONS

A mathematical model, incorporating the dominant mechanistic features, has been developed to describe the gasification of coal in a fluidized-bed reactor. The model does not include the initial devolatization because it is considered to proceed nearly instantaneously; it includes only the secondary reactions. The governing equations of the model, a set of partial differential equations, have been solved by an existing PDE software package for simlulation.

A series of gasification runs were conducted in a bench-scale fluidized-bed reactor to obtain experimental data for comparison with the model. The simulated steady-state gas compositions and mass yields compare favorably with the respective experimental observations. More specifically the model correctly predicts the trends in the gas composition, overall mass yield and mass yields of individual components, and char content in the bed. Among the model refinements suggested are inclusions of tar cracking reactions, and enhancement of the data base for the initial devolatization and char gasification reactions.

NOMENCLATURE

A_b = cross-sectional area of the reactor occupied by the bubble phase, m^2

A_e = cross-sectional area of the reactor occupied by the emulsion phase, m^2

A_c = surface area of char, m^2/kg

B = weight of the inert solids in the reactor, kg

C_i = yield of the i-th species by devolatization, kmol/kg of DAF feed

C_{ib} = concentration of the i-th species in the bubble phase, $kmol/m^3$

C_{ie} = concentration of the i-th species in the emulsion phase, $kmol/m^3$

C_{io} = initial or inlet concentration of the i-th species, $kmol/m^3$

C_s = concentration of char in the emulsion phase, kg char/kg inert solids

C_g = dry ash free feed rate per unit volume of the emulsion phase, kg/m^3

D = diameter of the reactor, m

D_{ib} = axial dispersion coefficient through the bubble phase, m^2/s

D_{ie} = axial dispersion coefficient through the emulsion phase, m^2/s

d_b = bubble diameter, m

D_{bm} = maximum bubble diameter, m

D_{bo} = initial bubble diameter, m

E = activation energy, kcal/gmol

E_m = mean activation energy, kcal/gmol

F = dry ash free feedrate of coal, kg/s

F_{be} = gas interchange coefficient between the bubble and emulsion phases based on the volume of bubbles, l/s

H = bed height, m

H_{mf} = bed height at minimum fluidization, m

k_o = frequency factor, l/sec

k_j = rate constant for the j-th reaction, 1/s

K_w = equilibrium constant for the water-gas shift reaction,-

M_c = atomic weight of carbon, 12 kg/kmol

R = gas constant = 1.987 kcal/kmol.K

R_{ib} = rate of generation of the i-th species in the bubble phase based on the volume of bubbles, kmol/m^3.s

R_{ie} = rate of generation of the i-th species in the emulsion phase based on the volume of the emulsion phase, kmol/m^3.s

R_s = rate of generation of char in the emulsion phase, kg/s

t = time, s

T = temperature, K

U_b = bubble rise velocity, m/s

U_e = superficial velocity of emulsion gas based on the emulsion phase cross sectional area, m/s

U_{mf} = superficial velocity of gas at minimum fluidization, m/s

W_{in} = rate of char into the reactor generated by the devolatization of coal, kg/s

W_{out} = rate of char out of the reactor, kg/s

x = axial distance from the distributor, m

y = weight fraction of coal devolatized,-

z = variable defined in the standard normal integral in eq. 12

$\bar{z}$ = variable defined by eq. 13

Subscripts

i = indices specifying species (1 = CO; 2 = CO_2; 3 = H_2; 4 = H_2O; 5 = CH_4; 6 = char)

j = indices indicating to the reactions

Greek Letters

δ = volume fraction of the bubble phase, -

ρ = density of the solids in the reactor, kg/m^3

σ = standard deviation from mean activation energy, kcal/g-mol

ε_{mf} = void fraction in the bed at minimum fluidization,-

REFERENCES CITED

Anthony, D.B., "Rapid Devolatilization and Hydrogasification of Pulverized Coal," Sc.D. thesis, Dept. of Chemical Engineering, M.I.T., Cambridge, 1974.

Anthony, D.B. and J.B. Howard, "Coal Devolatilization and Hydrogasification," AIChE Journal, 22, No. 4, 625-656 (1976).

Becker, H.A., J.M. Beer and B.M. Gibbs, "A model for Fluidized-Bed Combustion of Coal," Institute of Fuel Symposium Series No. 1: Fluidized Combustion, Proceedings Vol. 1, pp. A1-1 to A1-10, (1975).

Biba, V., J. Macak, E. Klose and J. Malecha, "Mathematical Model for the Gasification of Coal under Pressure," Ind. Eng. Chem. Process Des. Dev., 17, 92 (1978).

Chang, C.C., L.T. Fan and W.P. Walawender, "Dynamic Modeling of Biomass Gasification in a Fluidized Bed," Presented at 1983 AIChE Annual Meeting, Washington, D. C., Oct. 30-Nov. 4, 1983. Also in AIChE Symp. Series, 80(234), 80 (1984).

Davidson, J.F. and D. Harrison, "Fluidized Particles," Cambridge University Press, New York, 1963.

Howell, J.A., "Kansas Coal Gasification," M.S. Thesis, Kansas State University, 1979.

Kunii, D. and O. Levenspiel, "Fluidization Engineering", Chapter 4, Wiley, New York, 1969.

Kobayashi, H. and F. Arai, "Determination of Gas Cross-Flow Coefficient between the Bubble and Emulsion Phases by Measuring the Residence Time Distribution of Fluid in a Fluidized Bed," Kagaku Kogaku, 31, 239 (1967).

Mori, S. and C.Y. Wen, "Estimation of Bubble Diameter in Gaseous Fluidized Beds," AIChE Journal, 21, 109-115 (1975).

Peters, W., and H. Bertling, "Kinetics of the Rapid Degasification of Coals," Fuel, 44, 317 (1965).

Pitt, G.J., "The Kinetics of the Evolution of Volatile Products from Coal, "Fuel, 41, 267 (1962).

Raman, K.P., W.P. Walawender, L.T. Fan and C.C. Chang, "Mathematical Model for the Fluid-Bed Gasification of Biomass Materials. Application to Feedlot Manure," Ind. Eng. Chem. Process Des. Dev., 20, 686 (1981).

Sincovec, R.F. and N.K. Madsen, "Software for Nonlinear Partial Differential Equations," ACM Trans. Math. Software, 1, 232 (1975)

Uchida, S., H. Yamada and I. Tada, "Minimum Fluidization Velocity of Binary Mixture," Journal of the Chinese Institute of Chemical Engineers, 14, 257-264 (1983).

Walawender, W.P., S.Ganesan, and L.T. Fan, "Steam Gasification of Manure in a Fluid Bed: Influence of Limestone as a Bed Additive" Symposium Papers: Energy from Biomass and Wastes V., Institute of Gas Technology, pp. 517-527 (1981).

Walawender, W.P. and L.T. Fan, "Gasification of Dried Feedlot Manure in a Fluidized Bed -- Preliminary Pilot Plant Tests," Presented at 84th AIChE meeting, Atlanta, GA, Feb., 1978.

Yeboah, Y.D., J.P. Longwell, J.B. Howard and W.A. Peters, "Effect of Calcined Dolomite on the Fluidized Bed Pyrolysis of Coal," Ind. and Eng. Chem. Process Des. and Dev., 19, 646-653 (1980).

Yoon, H., J. Wei and M.M. Denn, "Modeling and Analysis of Moving Bed Coal Gasifiers," AF-590, Volume 1, Technical Planning Study 76-653, Research Project 986-1, Final Report, Nov., 1977.

Zeles, S.R., "Mathematical Model for Fluidized Bed Coal Gasifiation Reactors," M.S. Thesis, Massachusetts Institute of Technology, 1978.

Table 1. The Effects of Time and Temperature on Devolatization of Coal.

t, sec	$\bar{z}^a$
0.5	0.0101T - 8.825
1.0	0.0104T - 8.825
2.0	0.0107T - 8.825
5.0	0.0112T - 8.825
8.0	0.0114T - 8.825
10.0	0.0115T - 8.825
25.0	0.0119T - 8.825
50.0	0.0123T - 8.825

[a]Variable defined by equation 13 with E_m = 36.89 kcal/g-mol, σ = 4.18 kcal/g-mol, and $k_o = 2.91 \times 10^9$ sec^{-1}.

Table 2. Devolatization Product Distribution for Coal.

	Temperature		
	923 K	1033 K	Data Source
Char (wt% DAF)	62.6	65.1	TGA experiment
Volatiles (wt% DAF)	37.4	34.9	(Howell, 1979)
Volatiles composition			
Dry gas (wt% DAF)	14.2	15.0	
Tar (wt% DAF)	17.0	15.0	Yeboah et al. (1980)
Water (wt% DAF)	6.2	4.9	
Dry gas composition (Vol %)			
CO	14.1	17.0	
CO_2	13.7	12.9	
H_2	39.8	42.8	
CH_4	20.5	17.5	Yeboah et al. (1980)
C_2H_6	3.8	2.9	
C_3H_6	3.5	2.8	
Others	4.6	4.1	
Av. mol. wt.	18.7	17.9	

Table 3. Kinetic Parameters for the Reactions.

Reactions	Activation energy[b] (E_j) kJ/kmol	Adjusted frequency factor[a] (k_j^o), m/hr
$C + H_2O \xrightarrow{k_1} CO + H_2$	121,417	5.0×10^2
$C + CO_2 \xrightarrow{k_2} 2CO$	360,065	0.2×10^9
$C + 2H_2 \xrightarrow{k_3} CH_4$	230,274	0.75×10^3
$CO + H_2O \xrightarrow{k_4} CO_2 + H_2$	12,560	0.1×10^8 (m^3/kmol-hr)
$CO + H_2O \underset{k_5}{\overset{k_4}{\rightleftharpoons}} CO_2 + H_2$	$K_w = \frac{k_4}{k_5} = 0.0265 \exp(3955.7/T)$ [b]	

[a] $k_j = k_j^o \exp(-E_j/RT)$.

[b] Yoon (1977).

Table 4. Analysis of Kansas Bituminous and Illinois No. 6 Coal.

	Kansas Bituminous	Illinois No. 6 Coal
Proximate Analysis (%)		
Fixed Carbon (DAF)	55.4	55.47
V.M. (DAF)	44.6	44.53
Ash (Dry)	8.4	2.69
Moisture	7.8	8.40
Ultimate Analysis (% DAF)		
C	75.0	76.91
H	5.3	5.95
N	1.4	1.2
O (by diff.)	10.9	11.71
S	7.5	4.43

Table 5. Operating Conditions of the Experiment.

ε_{mf} = 0.43

U_{mf} = 0.12 - 0.09 m/s

B = 0.973 kg

ρ = 2608 kg/m^3

A_c = 1313 m^2/kg

Feed Rate = 0.00007289 (DAF kg/s)

U_o = 0.165 - 0.14 m/s

D_{ib} = 0.001 m^2/s

D_{ie} = 1000 m^2/s

T = 873 - 1073 K

Mean coal particle size = 0.297 mm

Composition of fluidizing gas = H_2O (steam): 100%

Steam rate = 15.33 - 11.0 g/min

Table 6. Comparison of Experimental and Simulated Steady-State Results.

Temp.	923 K		1033 K	
	Experimental	Simulated	Experimental	Simulation
CO mole %	6.0	11.50	12.4	16.42
CO_2 mole %	30.5	24.03	24.0	21.60
H_2 mole %	55.1	59.40	59.4	59.73
CH_4 mole%	6.2	3.05	3.1	1.44
C_2H_6 mole%	0.4	0.62	0.1	0.26
C_3H_6 mole%	0.42	0.57	0.1	0.25
Others[a] mole%	1.4	0.75	0.6	0.37
Mass Yield of Gas (kg gas/kg DAF feed)	0.65	0.75	1.50	1.51

[a]Others include C_2H_4 and C_3H_8

Table 6. continued

Temp.	923 K		1033 K	
	Experimental	Simulated	Experimental	Simulated
Mass yields of individual gas components (kg gas/kg DAF feed)				
CO	0.05	0.16	0.36	0.44
CO_2	0.52	0.51	0.94	0.92
H_2	0.05	0.06	0.11	0.12
CH_4	0.03	0.02	0.04	0.02

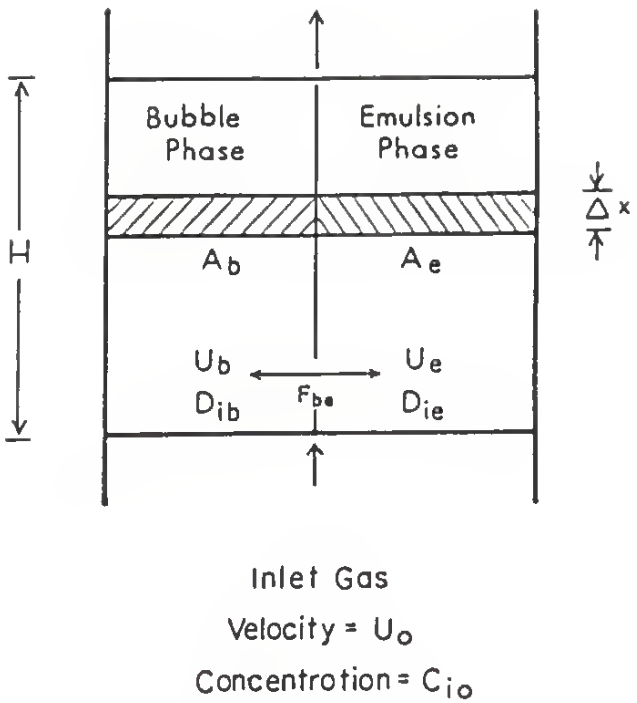

Fig. 1. Schematic representation of the model.

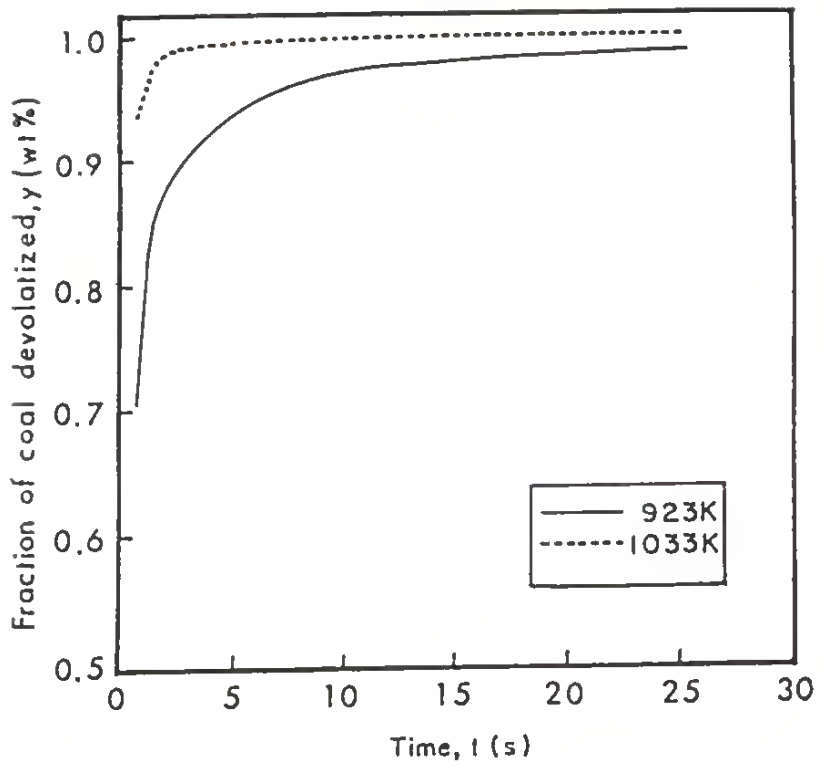

Fig. 2. Temperature effect on the rate of devolatization of coal E_m = 36.89 kcal/mole, σ = 4.18 kcal/mole, k_o = 2.91 x 10 sec^{-1}.

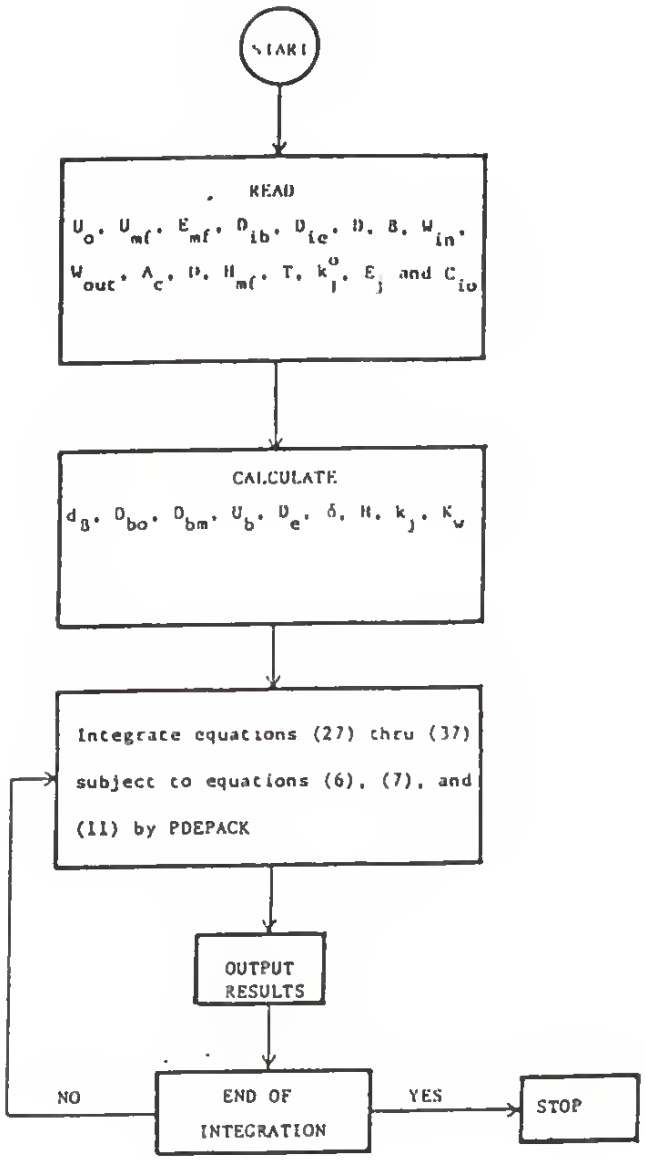

Fig. 3. Flow diagram of the computation.

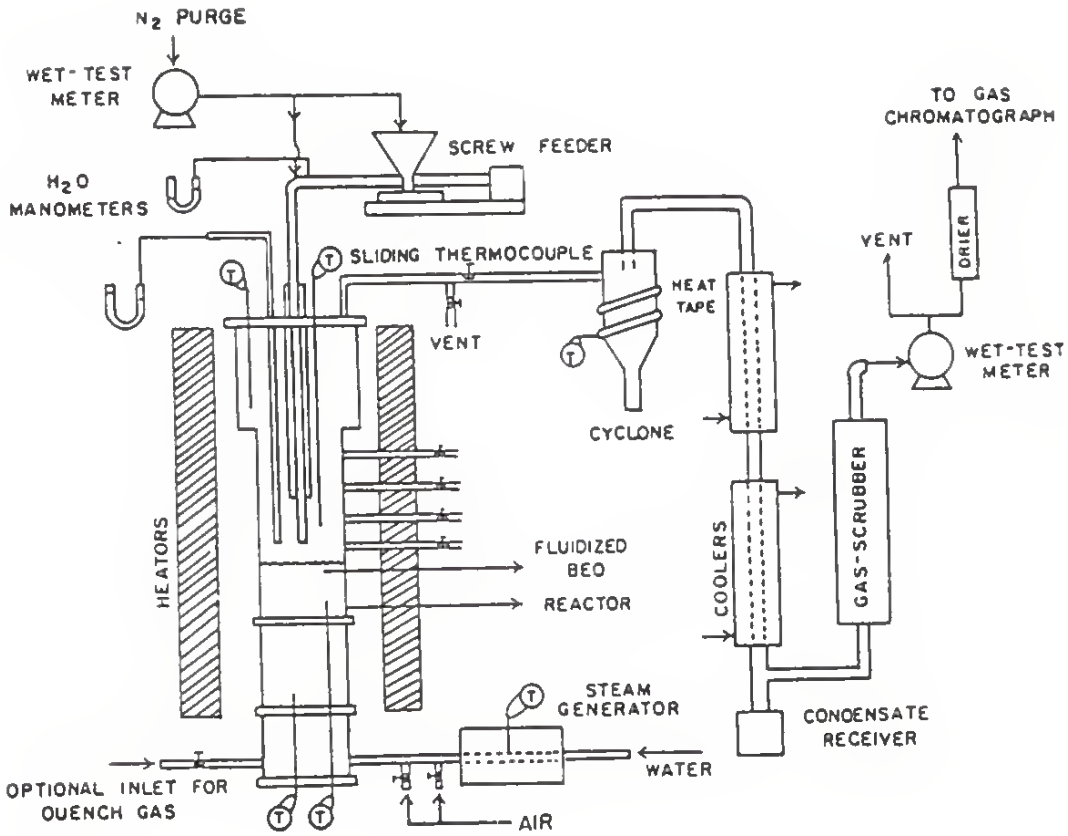

Fig. 4. Bench scale fluidized bed coal gasification system.

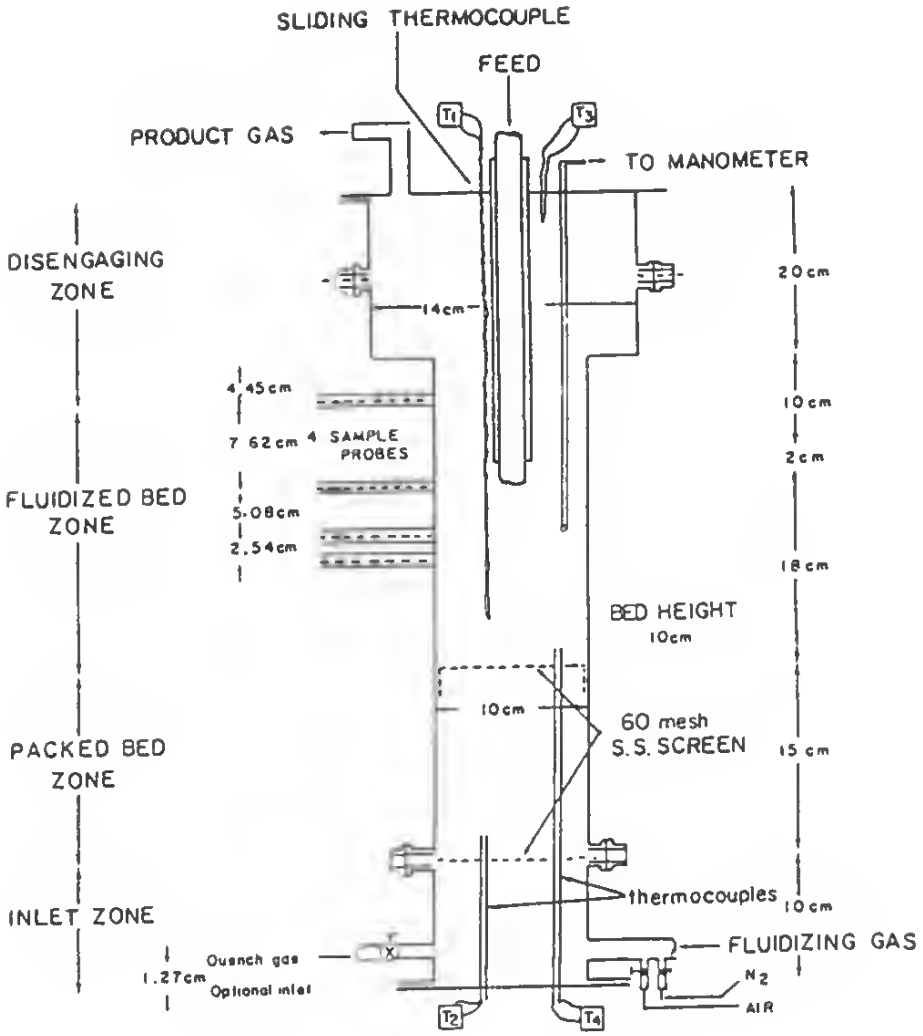

Fig. 5. Fluidized bed reactor.

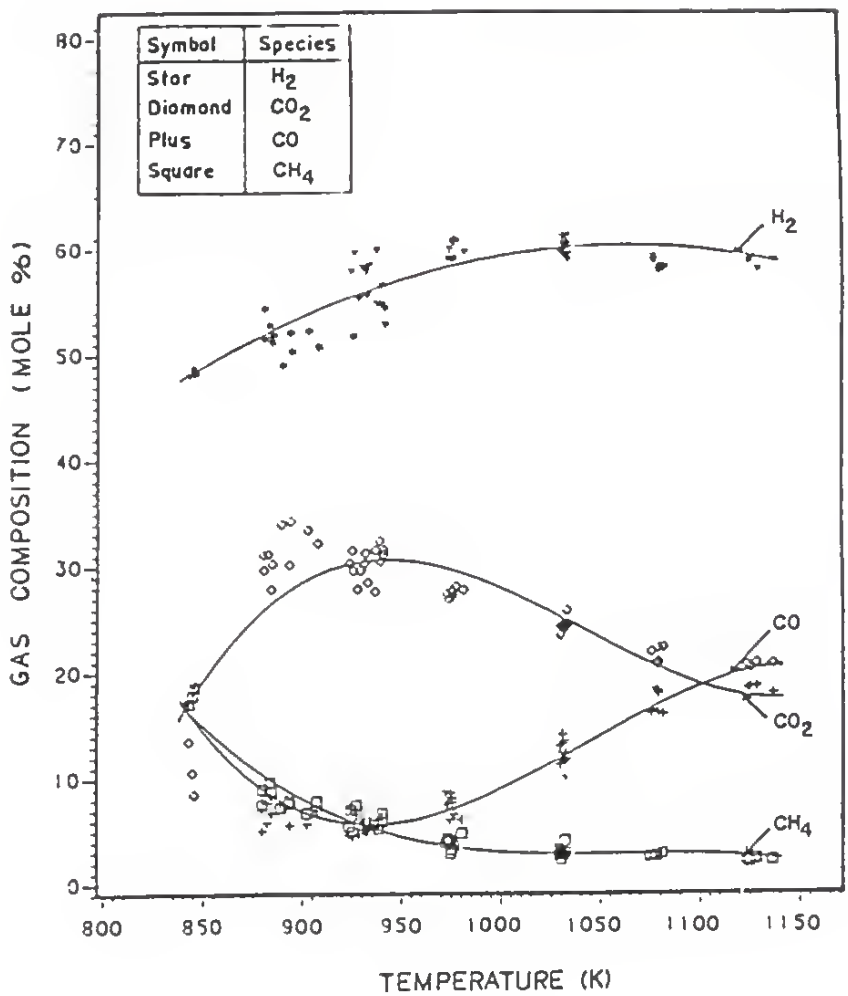

Fig. 6. Experimental result: Effect of temperature on the product gas composition (major components).

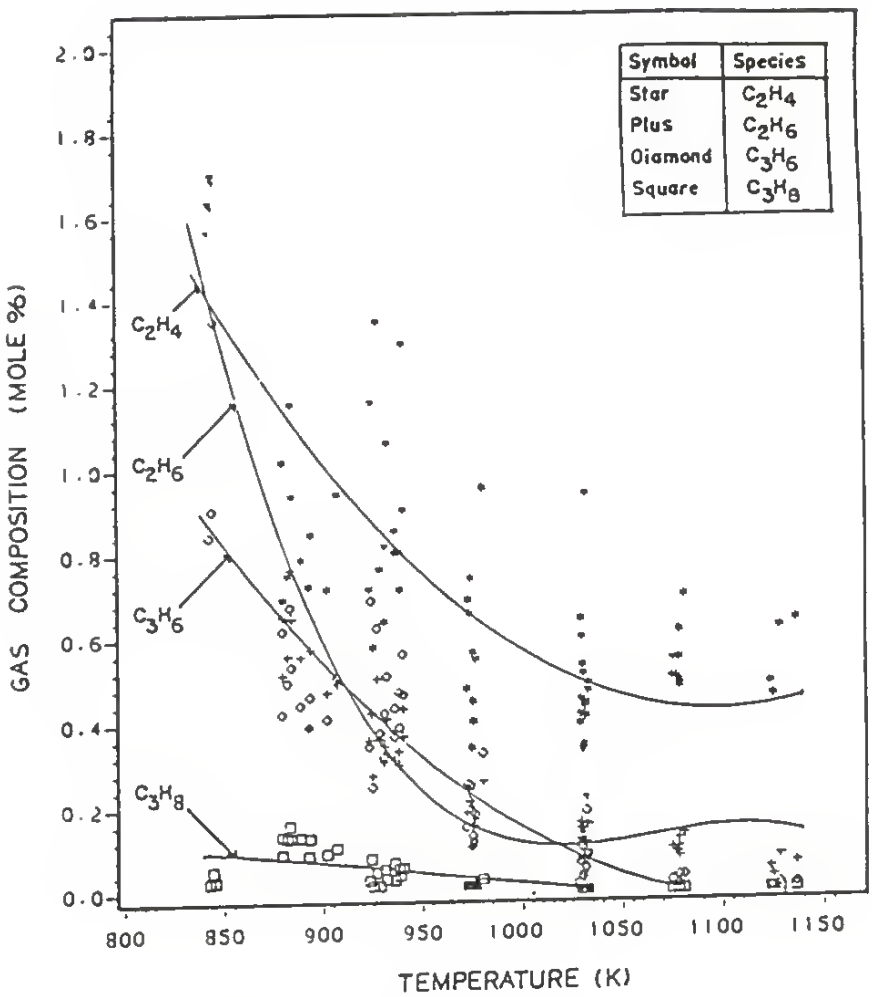

Fig. 7. Experimental result: Effect of temperature on the product gas composition (minor components).

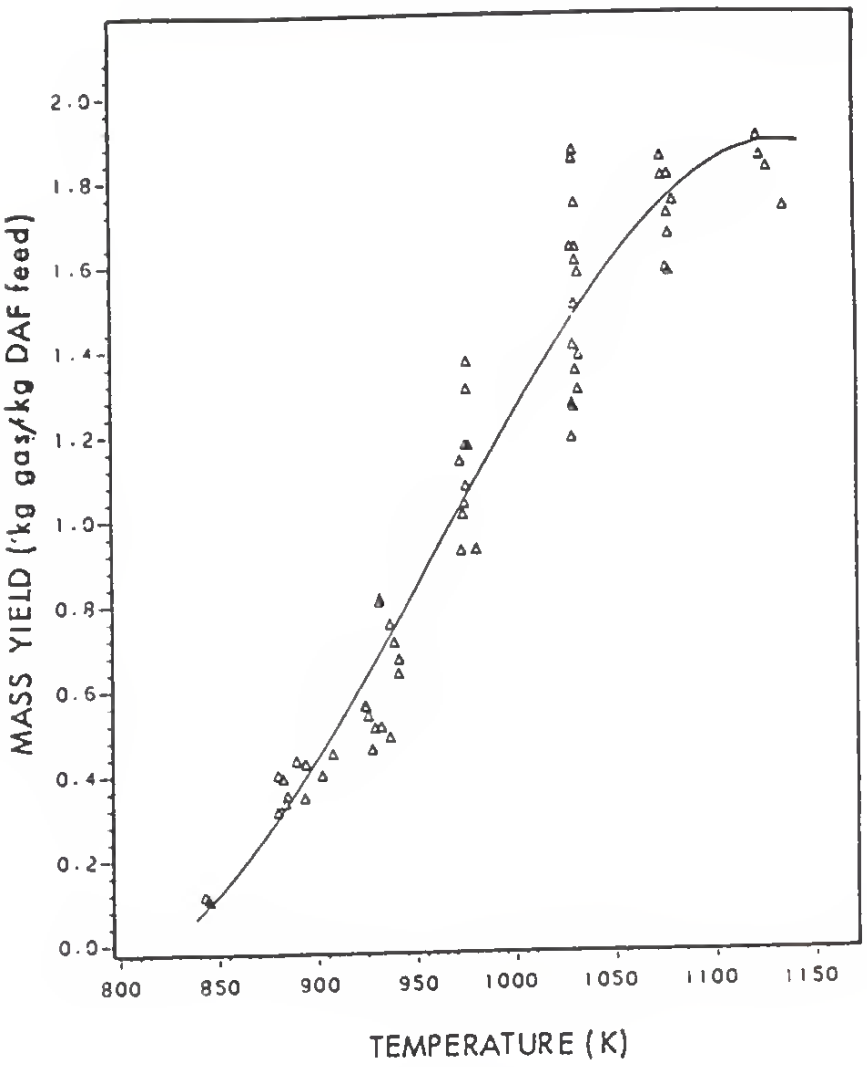

Fig. 8. Experimental result: Effect of temperature on the product gas mass yield.

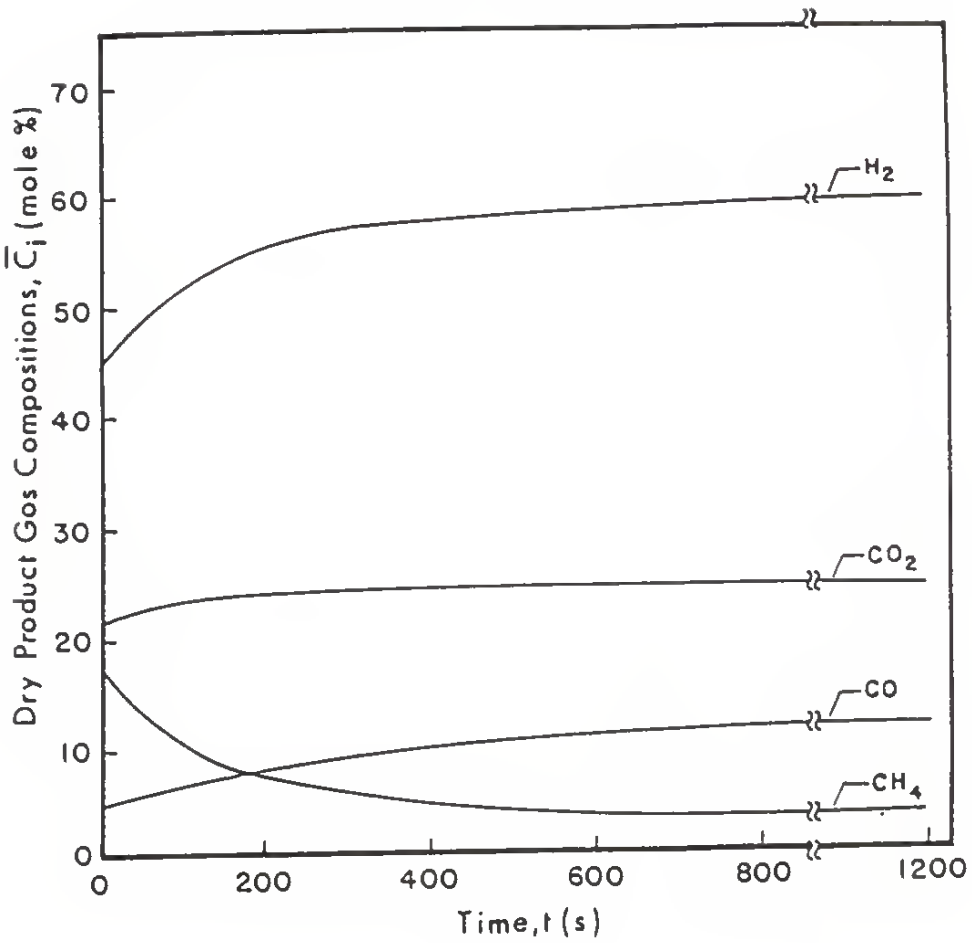

Fig. 9. Simulated result: Transient dry product gas composition at T = 923 K.

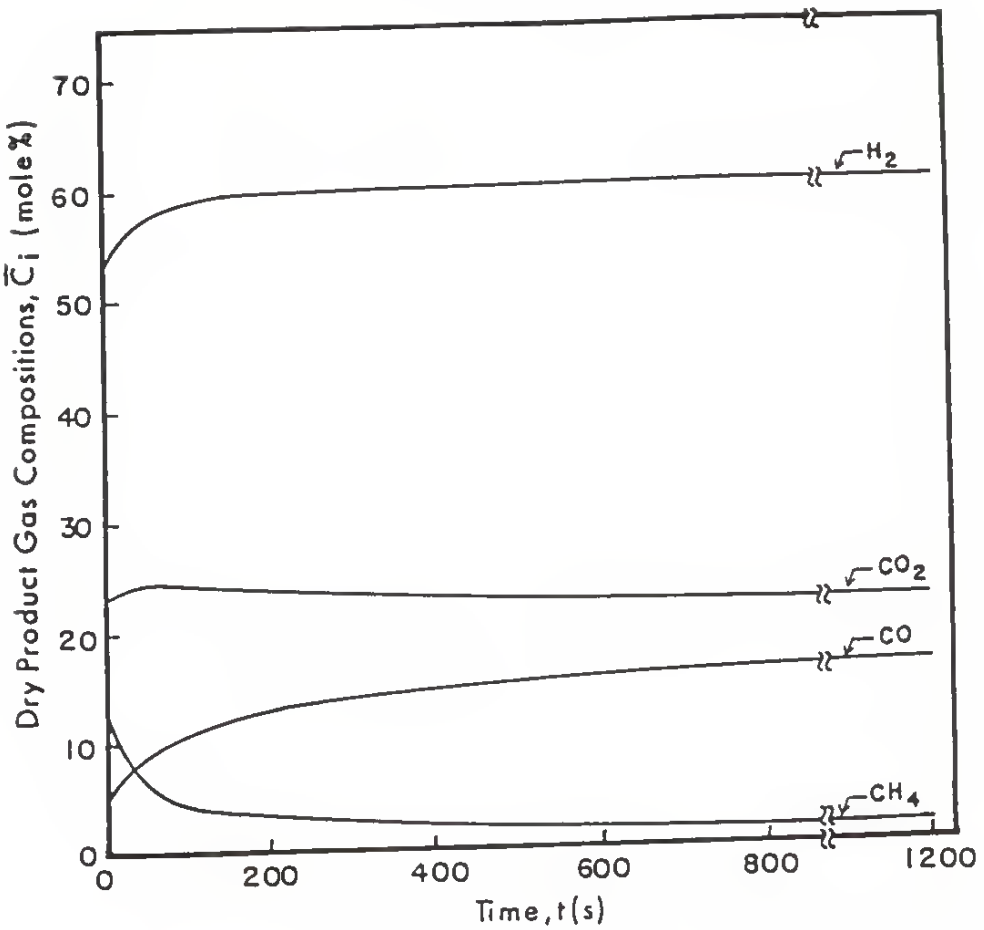

Fig. 10. Simulated result: Transient dry product gas composition at T = 1033 K.

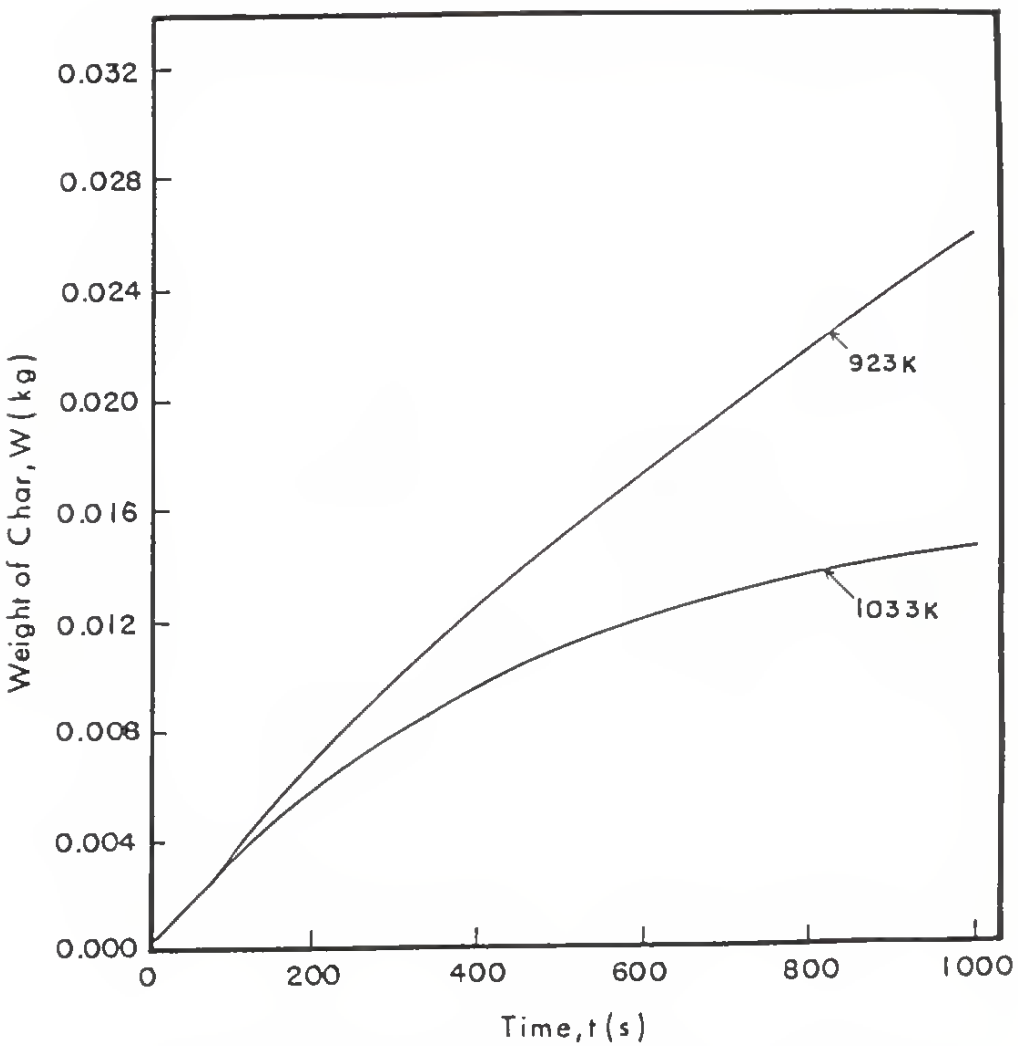

Fig. 11. Simulated result: Weight of char in the reactor as a function of time.

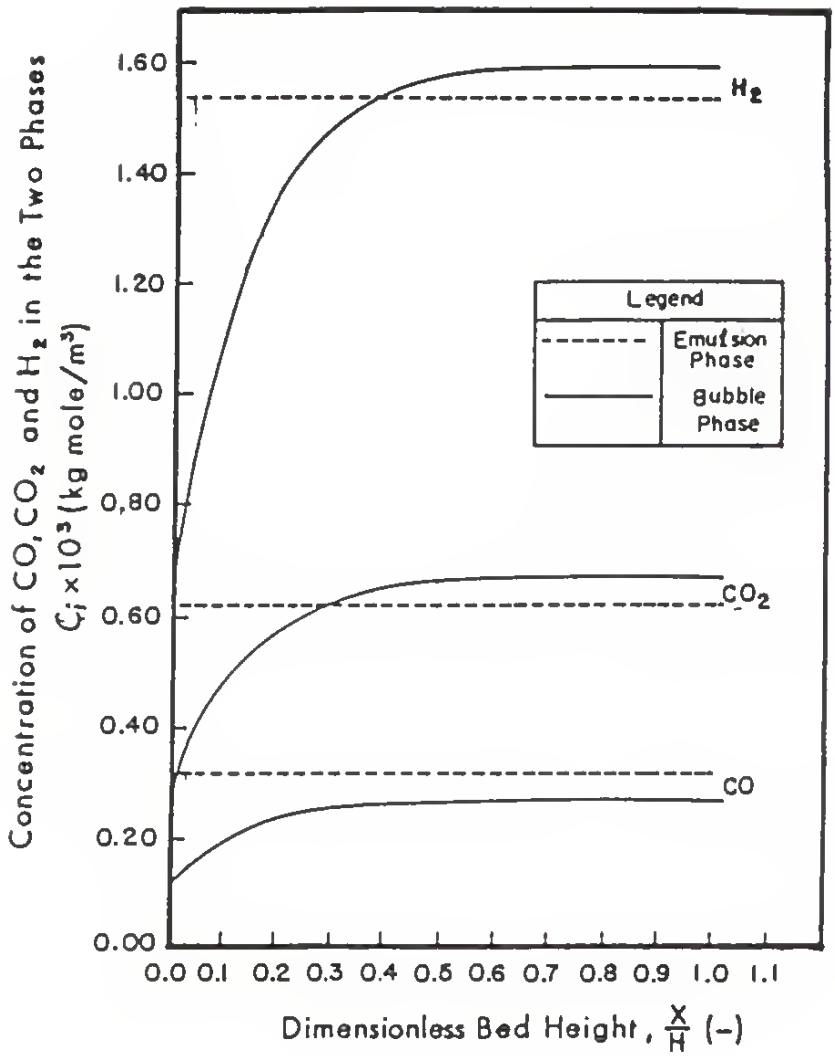

Fig. 12. Simulated result: Steady-state axial concentration profiles of CO, CO_2, and H_2 at T = 923 K.

CHAPTER V

CONCLUSIONS AND RECOMMENDATIONS

Gasification experiments were conducted on Kansas coal in a 0.1016 m I.D. fluidized bed reactor. Steam was used as the fluidizing and gasification agent. The objective was to examine the steam gasification of coal under steady-state conditions. The produced gas characteristics were examined as functions of temperature, in the range 833 - 1125 K with the gas residence time being held fairly constant. The major components of the produced gas were CO, CO_2, H_2, and CH_4, which comprised over 95% of the gas. The volumetric gas yield, mass yield, energy recovery, and carbon conversion increased with temperature from 0.15 to 2.82 m/kg DAF feed, 0.12 to 1.88 kg gas/kg DAF feed, 8 to 94%, and 7 to 82%, respectively. The heating value of the gas decreased from 16.5 to 11.2 MJ/m.

The behavior of the produced characteristics indicated the existence of two regimes in the coal gasification process. The first regime ($T < 940$ K) was dominated by tar cracking and water-gas shift reaction. Char gasification and water-gas shift reactions were the major reactions taking place in the second regime ($T > 940$ K). Steam, in large excess, was found to be an active gasification agent and participated in the gasification process through the water-gas shift and char gasification reactions.

The steam-to-feed ratio was found to have a significant effect on the gasification process. This decision was based on the statistical analysis performed on the experimental data.

A mathematical model was developed to describe the fluidized-bed coal gasification process. The model assumed a reaction mechanism which took into account the devolatization of coal, char gasification, and water-gas shift reaction. Both the dynamic and steady-state performance of the gasifier were simulated based on the model. The model predicted steady-state gas compositions and mass yields which compared favorably with the experimental observations. Thus future use of this model seems justifiable.

Based on the experimental observations and modeling studies certain modifications are recommended. Further modifications may be required on the reactor system to provide a more uniform feed rate. A better method of estimating feed rate is also needed. This will reduce some of the experimental data scatter and make it more suitable for analysis. At present two layers of heaters, each consisting of five quarter cylindrical heaters, are used. If four layers of heaters, each consisting of two semi-cylindrical heaters are used instead, then temperature control will be easier and more accurate. Computer control of temperature in the reactor is highly recommended. Investigations are already underway, and preliminary experiments show that temperatures can be controlled to an accuracy of ± 2 K by the use of computer as compared to 10-20 K when conventional PID controllers are used. Modifications are also needed to conduct mass balances on the system. For this purpose, improved steam and condensate rate estimation techniques are needed. Char estimation will have to be done by indirect methods like elemental balance or ash balance unless char hold-up can be estimated. Analysis of the tar will help in confirming the bounds on the tar cracking regime and may show the possibility of extracting a range of useful products from it.

Future experiments with coal may be done at lower temperatures which will produce more liquid products. This will help in investigating the possibility of coal liquefraction by using a fluidized-bed reactor. Coal pyrolysis in an inert atmosphere is recommended in order to gain insights to the phenomenon of devolatization. Statistical design of experiments are recommended in future. Analysis using statistical methods are done on the data available from the past experiments. Based on this analysis variables

which affects the outcome of the experiment are determined, which are used as the independent variables in the future experiments. For example, in the present investigation of the gasification of coal it was found that apart from temperature, steam-to-feed ratio also had a significant effect on the product characteristics. This decision was based on the statistical analysis done on the experimentally obtained data. For future experiments it is recommended to use different steam-to-feed ratio at each temperatures.

The work on fluidized bed can be extended by gasifying lignin in the same system. Difficulty in gasifying lignin is due to the fact that lignin becomes plastic at a very low temperature, thus causing the feed pipe to clog. In the present system this problem will be eliminated because of the water cooled feed pipe. Cold water flows through the jacket of the feed pipe, keeping the temperature in the feed pipe relatively low. The other materials, which are suggested from gasification studies, are oilshale, woodchips, manure, etc.

In order to implement the present mathematical model in practice several refinements are suggested. They are inclusion of the reactions of heavy volatiles, improvement of the initial conditions of the model pertaining to the initial devolatization and of the rate constants for the gasification reactions, and lastly incorporation for a longer period of time will help us in finding the steady-state mass of char in the bed as predicted by the model.

COAL GASIFICATION IN AN EXPERIMENTAL FLUIDIZED-BED REACTOR

by

DEBASHIS NEOGI

B. Tech. ChE. Indian Institute of Technology, Kharagpur, India, 1981

AN ABSTRACT OF A MASTER'S THESIS

submitted in partial fulfillment of the

requirements for the degree

MASTER OF SCIENCE

Department of Chemical Engineering

KANSAS STATE UNIVERSITY
Manhattan, Kansas

1984

The gasification of coal was studied in a 0.1016 m I.D. bench scale fluidized-bed reactor. The overall objective of this work was to investigate the effect of the reactor temperature on the produced gas composition, mass and volumetric yields, and heating value. The energy recovery and carbon conversion were also determined.

Kansas bituminous coal was gasified over a temperature range of 833-1133 K. The major components of the produced gas were CO, CO_2, H_2, and CH_4, which comprised over 95% of the gas. The remainder of the 5% consisted of C_2H_4, C_2H_6, C_3H_6, and C_3H_8. The volumetric gas yield, mass yield, energy recovery, and carbon conversion increased with temperature from 0.15 to 2.82 m^3/kg DAF feed, 0.12 to 1.88 kg gas/kg DAF feed, 8 to 94%, and 7 to 82% respectively. The heating value of the gas decreased from 16.5 to 11.2 MJ/m^3.

The behavior of the gas composition data indicated the existence of two regimes in the coal gasification process. The first regime ($T < 940$ K) was dominated by tar cracking and the water-gas shift reaction. Char gasification and the water-gas shift reactions were the major reactions taking place in the second regime ($T > 940$ K). The char gasification reactions were found to control the product characteristics at higher temperature. Steam, in large excess, was found to be an active gasification agent and participated in the gasification process through the water-gas shift and char gasification reactions. The proposed hypothesis indicating the existence of the two regimes was supported by the mass and volumetric yields, HHV, carbon conversion, and energy recovery data obtained from the experiments.

The steam/feed ratio was found to have a significant effect on the gasification process. This decision was based on the statistical analysis performed on the experimental data.

To study the heterogeneous reactions taking place in the reactor and also the transient behavior of the system, a mathematical model was developed. The model assumed a reaction mechanism which took into account the devolatization of coal, char gasification, and the water-gas shift reaction. Both the dynamic behavior and steady-state performance of the gasifier were simulated based on the model. The results of the simulations were compared with the experimental data. This comparison enabled us to ascertain the validity of the proposed reaction mechanism and dynamic model.